AD-A128 844 VIBRATION TEST OF RICHARD B RUSSELL CONCRETE DAM BEFORE RESERVOIR IMPOUND..(U) ARMY ENGINEER WATERWAYS EXPERIMENT STATION VICKSBURG MS STRUC..

1/1

UNCLASSIFIED V P CHIARITO ET AL. MAY 83 WES/TR/SL-83-2 F/G 13/13 NL

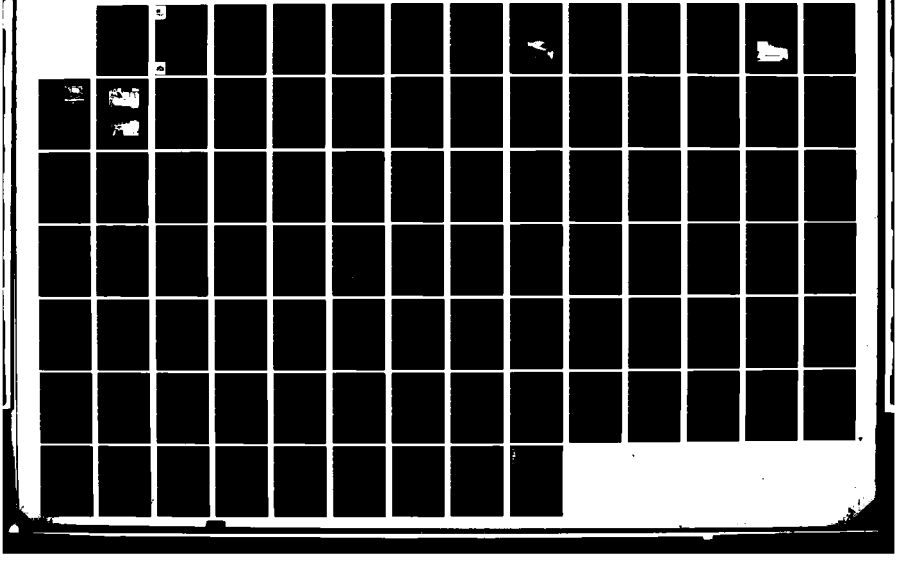

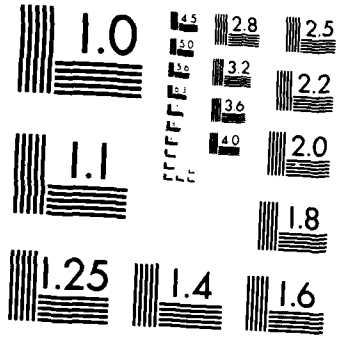

TECHNICAL REPORT SL-83-2

US Army Corps of Engineers

VIBRATION TEST OF RICHARD B. RUSSELL CONCRETE DAM BEFORE RESERVOIR IMPOUNDMENT

by

Vincent P. Chiarito, Paul F. Mlakar

Structures Laboratory
U. S. Army Engineer Waterways Experiment Station
P. O. Box 631, Vicksburg, Miss. 39180

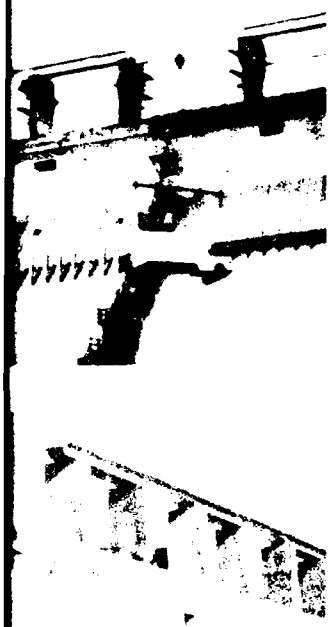

May 1983
Final Report

Prepared for Office, Chief of Engineers, U. S. Army
Washington, D. C. 20314

and

U. S. Army Engineer District, Savannah
Savannah, Ga. 31402

STRUCTURES LABORATORY

Destroy this report when no longer needed. Do not return it to the originator.

The findings in this report are not to be construed as an official Department of the Army position unless so designated by other authorized documents.

The contents of this report are not to be used for advertising, publication, or promotional purposes. Citation of trade names does not constitute an official endorsement or approval of the use of such commercial products.

The covers of U. S. Army Engineer Waterways Experiment Station (WES) engineering and scientific reports have been redesigned. Each WES Laboratory and support organization will have its own distinctive color imprinted on white coverstock. This standardizes WES publications and enhances their professional appearance.

Unclassified

SECURITY CLASSIFICATION OF THIS PAGE *(When Data Entered)*

REPORT DOCUMENTATION PAGE

READ INSTRUCTIONS BEFORE COMPLETING FORM

1. REPORT NUMBER: Technical Report SL-83-2	2. GOVT ACCESSION NO.
3. RECIPIENT'S CATALOG NUMBER	
4. TITLE *(and Subtitle)*: VIBRATION TEST OF RICHARD B. RUSSELL CONCRETE DAM BEFORE RESERVOIR IMPOUNDMENT	5. TYPE OF REPORT & PERIOD COVERED: Final Report
	6. PERFORMING ORG. REPORT NUMBER
7. AUTHOR(s): Vincent P. Chiarito, Paul F. Mlakar	8. CONTRACT OR GRANT NUMBER(s)
9. PERFORMING ORGANIZATION NAME AND ADDRESS: U. S. Army Engineer Waterways Experiment Station, Structures Laboratory, P.O. Box 631, Vicksburg, Miss. 39180	10. PROGRAM ELEMENT, PROJECT, TASK AREA & WORK UNIT NUMBERS
11. CONTROLLING OFFICE NAME AND ADDRESS: Office, Chief of Engineers, U. S. Army, Washington, D. C. 20314 and U. S. Army Engineer District, Savannah, Savannah, Ga. 31402	12. REPORT DATE: May 1983
	13. NUMBER OF PAGES: 84
	15. SECURITY CLASS. *(of this report)*: Unclassified
14. MONITORING AGENCY NAME & ADDRESS *(if different from Controlling Office)*	15a. DECLASSIFICATION/DOWNGRADING SCHEDULE

16. DISTRIBUTION STATEMENT *(of this Report)*

Approved for public release; distribution unlimited.

17. DISTRIBUTION STATEMENT *(of the abstract entered in Block 20, if different from Report)*

18. SUPPLEMENTARY NOTES

Available from National Technical Information Service, 5285 Port Royal Road, Springfield, Va. 22151.

19. KEY WORDS *(Continue on reverse side if necessary and identify by block number)*

Concrete dams
Vibration response tests

20. ABSTRACT *(Continue on reverse side if necessary and identify by block number)*

This forced vibration test of Richard B. Russell Dam was conducted before an appreciable reservoir is impounded. Hence a rare opportunity was seized to experimentally measure the dynamic properties of a concrete gravity dam without hydrodynamic interaction. Richard B. Russell Dam has recently been built by the Corps of Engineers approximately 170 miles from the mouth of the Savannah River between the States of Georgia and South Carolina. The crest

(Continued)

DD FORM 1 JAN 73 1473 EDITION OF 1 NOV 65 IS OBSOLETE

Unclassified

SECURITY CLASSIFICATION OF THIS PAGE *(When Data Entered)*

20. ABSTRACT (Continued).

of the concrete gravity part of the dam is 1884 feet long and is composed of 13 nonoverflow, 8 intake, and 11 spillway monoliths, the tallest of which is approximately 200 feet high. In conjunction with a second test, planned after reservoir impoundment in 1984, an experimental measure of prototype hydrodynamic interaction will also be obtained.

The structure was excited at three locations by a crest mounted 17,000-pound inertial mass which was driven by an electrohydraulic servo-controlled actuator. The force input to the dam was computed as the product of the measured acceleration and the 17,000-pound mass. Servo accelerometers with a sensitivity of 0.25 volts/g measured the horizontal crest accelerations of the tallest 31 monoliths and the distribution of horizontal acceleration with elevation in the three drive point monoliths. All tests were 1/2 decade/minute sine sweeps from 25 to 1 Hz. Analog signals were recorded on magnetic tapes and later digitized and processed by a Structural Dynamics Analyzer.

The results reveal the linear and the nonlinear characteristics of the complex structure. The natural frequencies and mode shapes are consistent with the results of two- and three-dimensional finite element analyses when foundation flexibility is considered. Modal damping ratios were greater than independently measured concrete specimen values but were scattered between 1.4 and 5.2 percent. Relative joint motion was observed above a low response threshold.

PREFACE

This study was conducted during the period September 1981 through September 1982 by the U. S. Army Engineer Waterways Experiment Station (WES) under the sponsorship of the Office, Chief of Engineers, and the U. S. Army Engineer District, Savannah. The Technical Monitor was Mr. Lucian Guthrie, OCE.

This work was conducted under the supervision of Messrs. Bryant Mather, Chief, Structures Laboratory (SL), W. J. Flathau, Assistant Chief, SL, and J. T. Ballard, Chief of the Structural Mechanics Division (SMD). Dr. Paul F. Mlakar and CPT Robert Volz were involved in the planning and directing phases of the work. Acknowledgment is made to Messrs. James L. Pickens and Rick Floyd, Instrumentation Services Division, for instrumentation support, and to Messrs. Stafford S. Cooper and Donald Douglas, Geotechnical Laboratory (GL), for their efforts in conducting the field tests and to Mr. Alton M. Alexander for the concrete material property testing and help with the data analysis. Also acknowledgment is made to personnel of the Richard B. Russell Area Office for their support. This report was prepared by Mr. Vincent P. Chiarito and Dr. Mlakar.

The Commander and Director of WES during the course of the study and the publication of this report was COL Tilford C. Creel, CE. Technical Director was Mr. F. R. Brown.

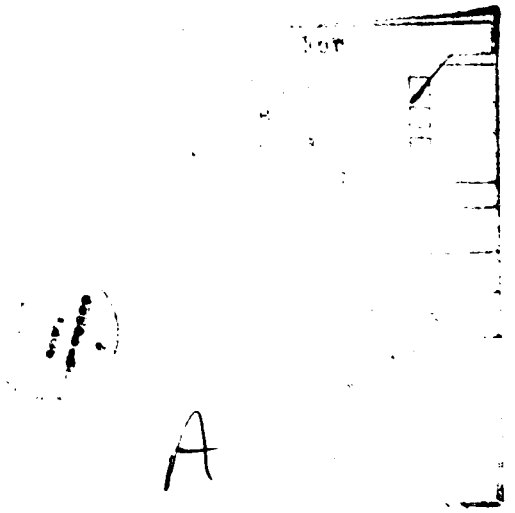

CONTENTS

VIBRATION TEST OF RICHARD B. RUSSELL CONCRETE DAM BEFORE RESERVOIR IMPOUNDMENT

PART I: INTRODUCTION

1. Information from forced vibration tests of Richard B. Russell Dam before impoundment of the reservoir was used to determine the natural frequencies, mode shapes, modal damping ratios, and relative joint motions. This low-level forced vibration test conducted in January and February 1982 seized a rare opportunity to experimentally measure the dynamic properties of a concrete gravity dam without hydrodynamic interaction. The experimentally measured dynamic properties can be compared to 2-D and 3-D finite element dynamic modeling to check the validity of these analyses. A forced vibration test planned in 1984 after impoundment of the reservoir will provide an experimental measure of the prototype hydrodynamic interaction and a comparison of the changes of the dynamic properties.

2. Richard B. Russell Dam has recently been built by the Corps of Engineers approximately 170 miles (274 km) from the mouth of the Savannah River between the States of Georgia and South Carolina. A view of the dam from the downstream Georgia side is shown in Figure 1. As shown in

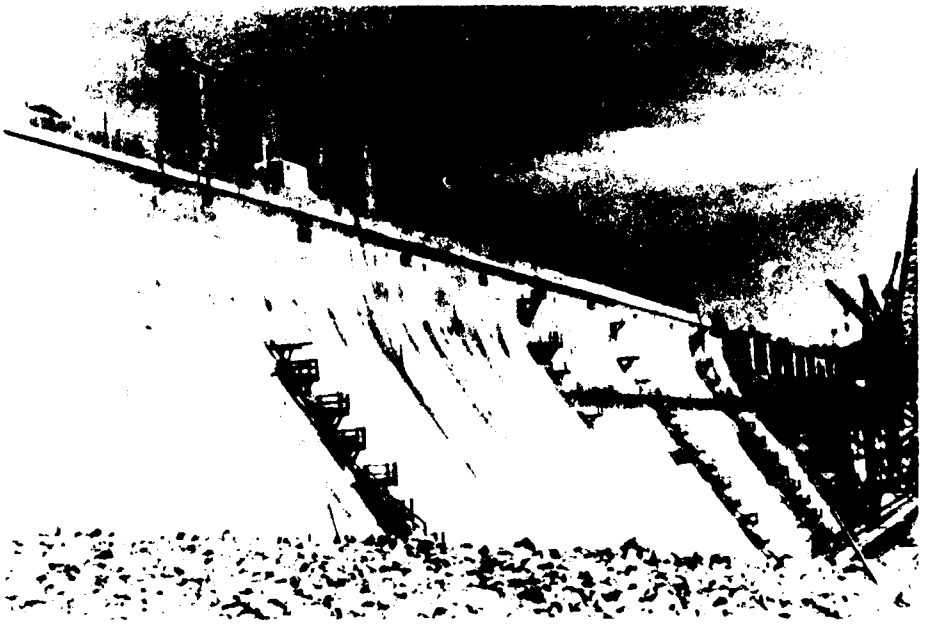

Figure 1. View of Richard B. Russell Dam from downstream Georgia side

Figures 2 and 3, the crest of the concrete gravity part of Richard B. Russell Dam is 1884 ft (574 m) long and is composed of 13 nonoverflow, 8 intake, and 11 spillway monoliths, the tallest of which is approximately 200 ft (61 m) high.

3. Another role of measuring the dynamic properties of the dam is to provide a record of the dam's structural condition as built. If the dam's structural integrity is suspect, following damage sustained from an earthquake or other sources, the results of test data before and after the damage would be useful in determining the significance of the damage (Richardson 1980). Finally, the results from the first vibration test also can be used to evaluate dynamic analyses previously conducted to assure the safe seismic design of the project (Norman and Stone 1979; Norman 1979).

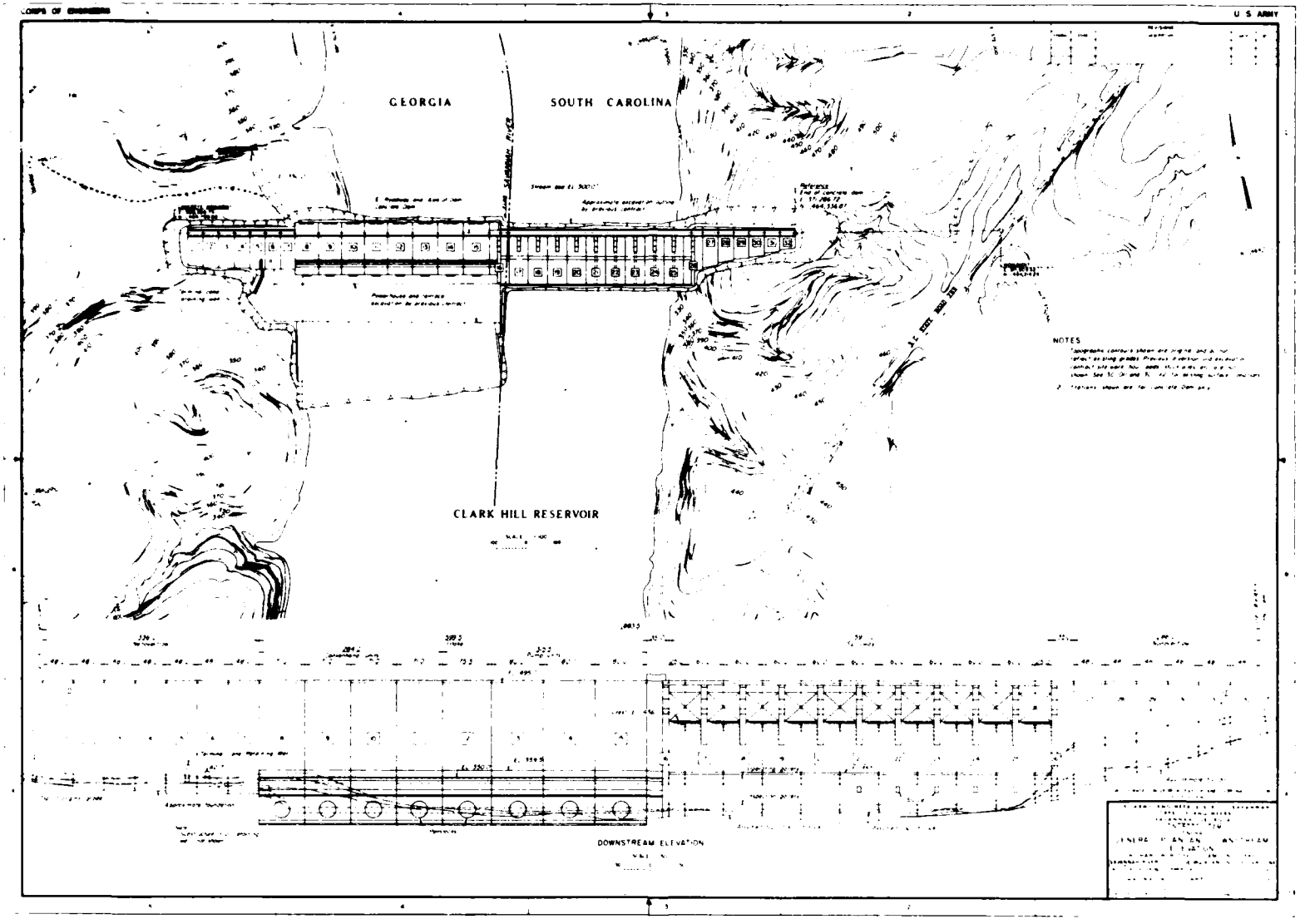

Figure 2. Plan and elevation views of Richard B. Russell Dam

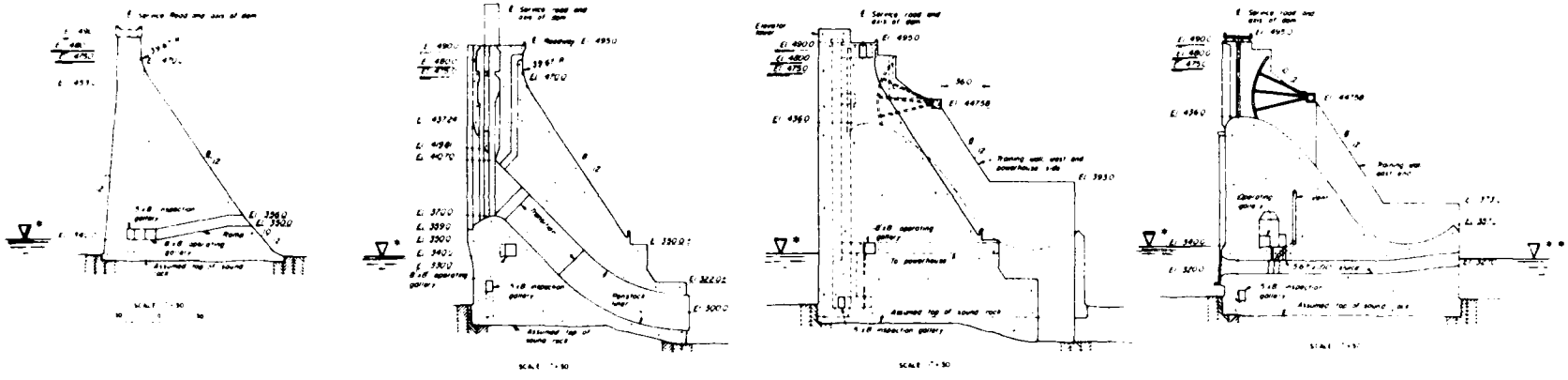

TYPICAL NONOVERFLOW | TYPICAL POWER INTAKE | SPILLWAY TRANSITION | TYPICAL SPILLWAY

* AVERAGE HEADWATER ELEVATION-EL 342.0
** AVERAGE TAILWATER ELEVATION-EL 331.9 (FROM MONOLITHS 17 TO 25 ONLY)

Figure 3. Elevation views of monolithic sections

PART II: EXPERIMENTAL PROCEDURE

Experimental Equipment

4. Richard B. Russell Dam was excited by the device shown in Figure 4. It consists of a 17,000-lb (7,711-kg) inertial mass, which was driven by a Zonic ZTL electrohydraulic serve-controlled actuator. The shaker was welded to a 4-ft by 5-ft by 2-in.-thick (1.22 by 1.52 by 0.0508 m) steel plate which was epoxied to the mass concrete of the dam. The epoxy used w[illegible]ika's Sikastix 370 Sikadur HiMod and it performed very well at the c[illegible] temperatures encountered during the curing process. Three plates were affi[illegible] at the exciter locations. The force input to the dam was computed as [illegible]roduct of the measured acceleration and the 17,000-lb mass. A typical fo[illegible] spectrum of the shaker for the tests is shown in Figure 5. The maximum stroke of the actuator is limited to 1 in. (0.0254 m). From 25 to 6 Hz (1 Hz = 1 Hertz = 1 cycle/second), the force spectrum is flat (for a peak force output of 20 kips (89 kN)). The rolloff from 6 to 1 Hz is due to the stroke limitation.

5. Q-Flex Model No. QA1000 servo-accelerometers, as shown in Figure 6, with a sensitivity of 0.25 volts/g were used to measure the horizontal accelerations of the concrete dam. The accelerometers have a frequency response

Figure 4. Inertial mass vibrator - located on monolith 7

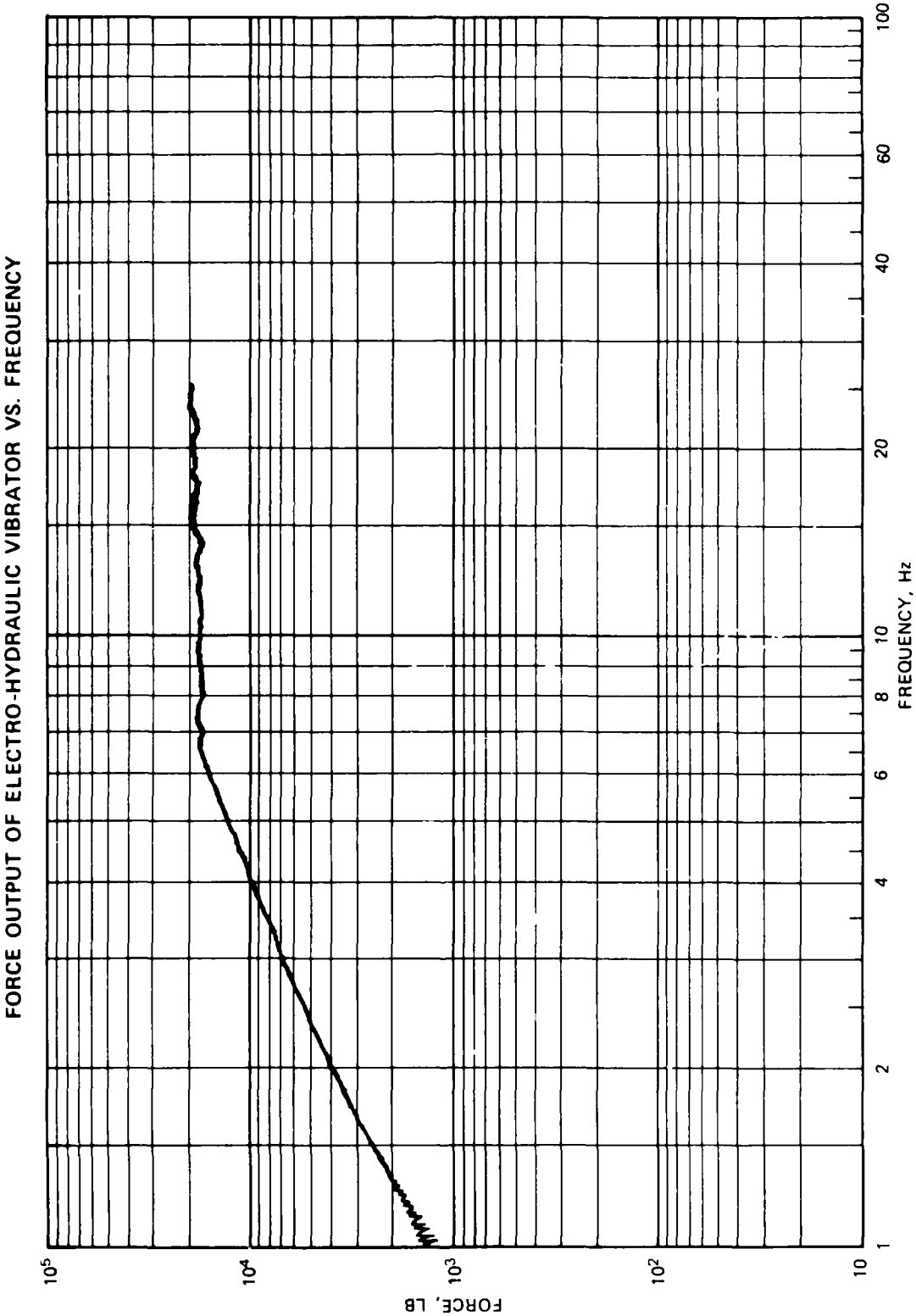

Figure 5. Typical force spectrum

range from 0 to 500 Hz. Analog signals were recorded by a Sangamo Sabre V tape recorder on 32-track magnetic tapes. The tape recorder has a frequency response range from 0 to 2,500 Hz. A Structural Dynamics Analyzer HP5423A manufactured by the Hewlett-Packard Company was used to later digitize and process the analog signals.

6. All the recording instrumentation was housed in a closed van positioned on the crest of the monolith adjacent to the drive point as shown in Figure 7a. The generator and the hydraulic power supply for the shaker are seen to be located on the same monolith with the van. The contractor's gantry crane was required to place all the experimental equipment. In Figure 7b the van is seen being lifted to the crest of the dam. All the equipment is listed in Table 1. A schematic of the excitation setup is shown in Figure 8.

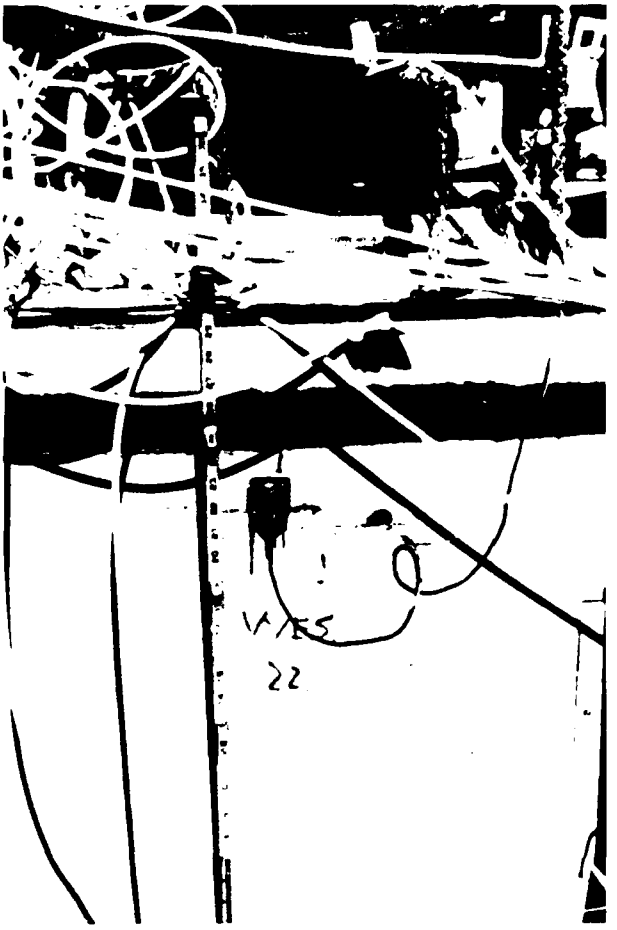

Figure 6. Accelerometer mounted on monolith 22

Vibration Tests

7. The three exciter locations were chosen at monoliths 7, 16, and 22. These positions roughly correlate to the sixth, half, and quarter points of the dam, respectively. Monolith 7 is the tallest nonoverflow section and the existence of vertical shafts in monoliths 16 and 22 made it convenient for placing instrumentation for monitoring the cross section's horizontal response. In Figures 3 and 9 the cross sections and the locations of the drive point monoliths are shown. The force input in the downstream-upstream

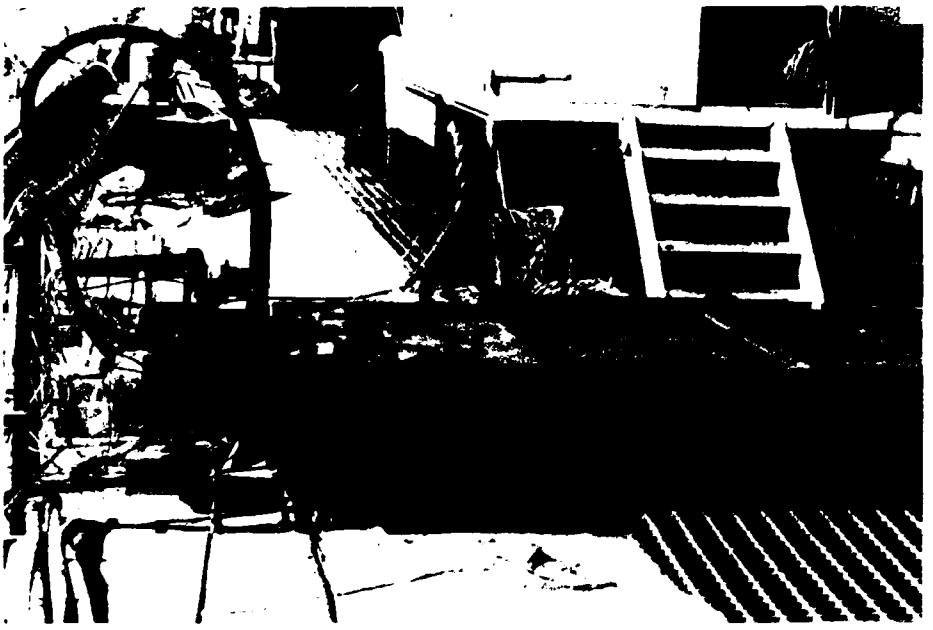

a. Instrumentation van (white, upper right corner) and setup at monolith 22

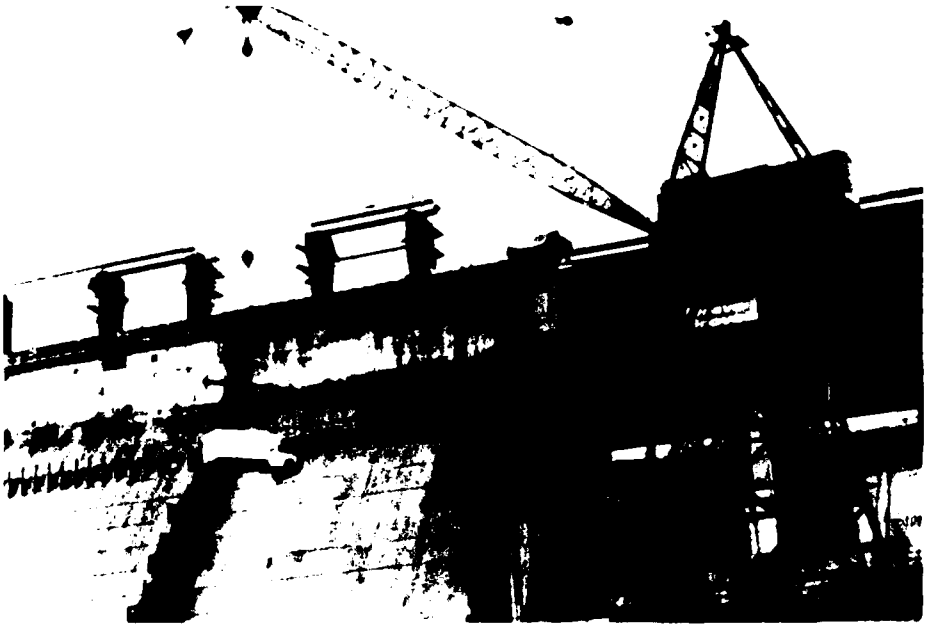

b. Lifting of van to crest

Figure 7

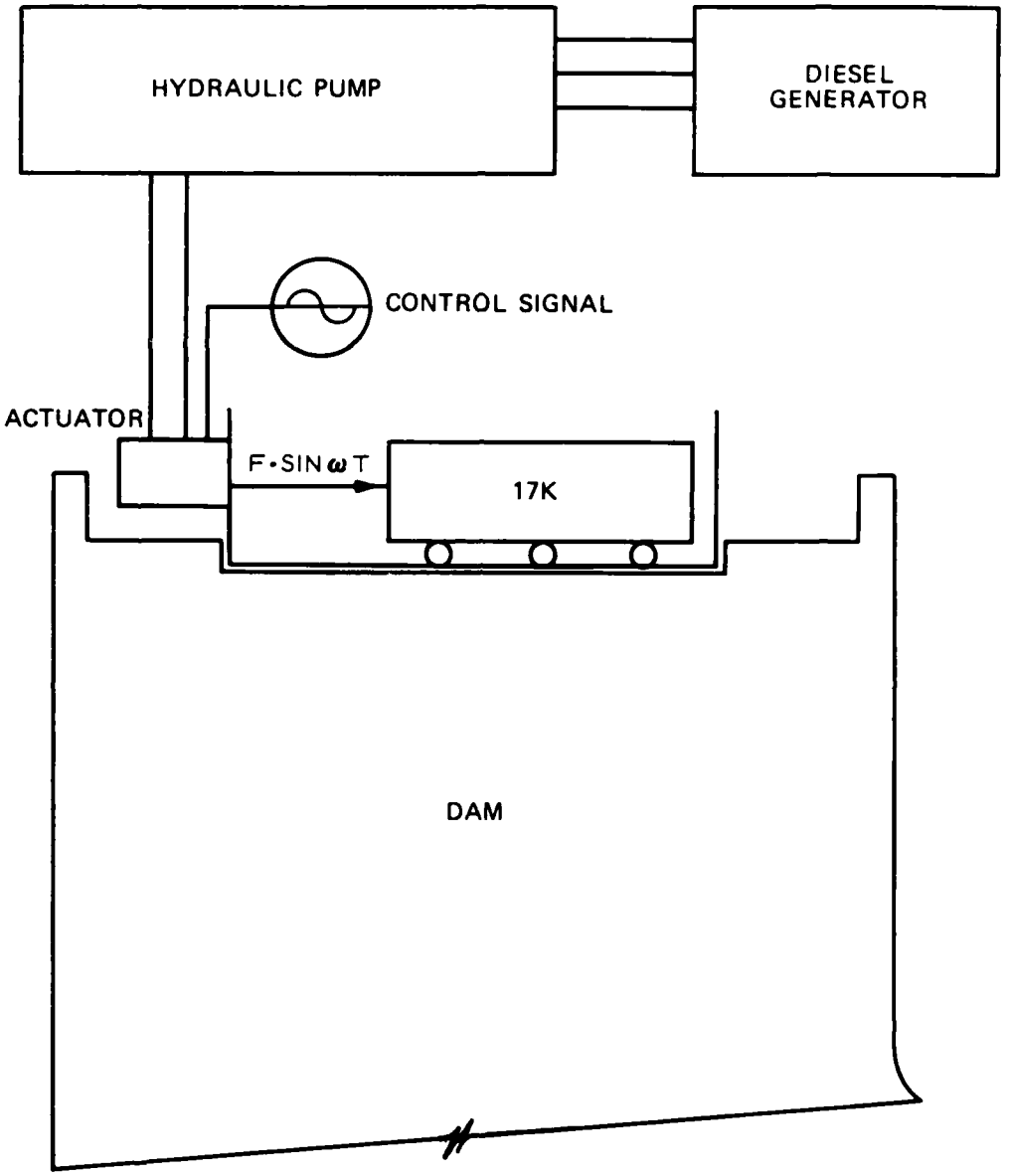

Figure 8. Schematic of excitation setup

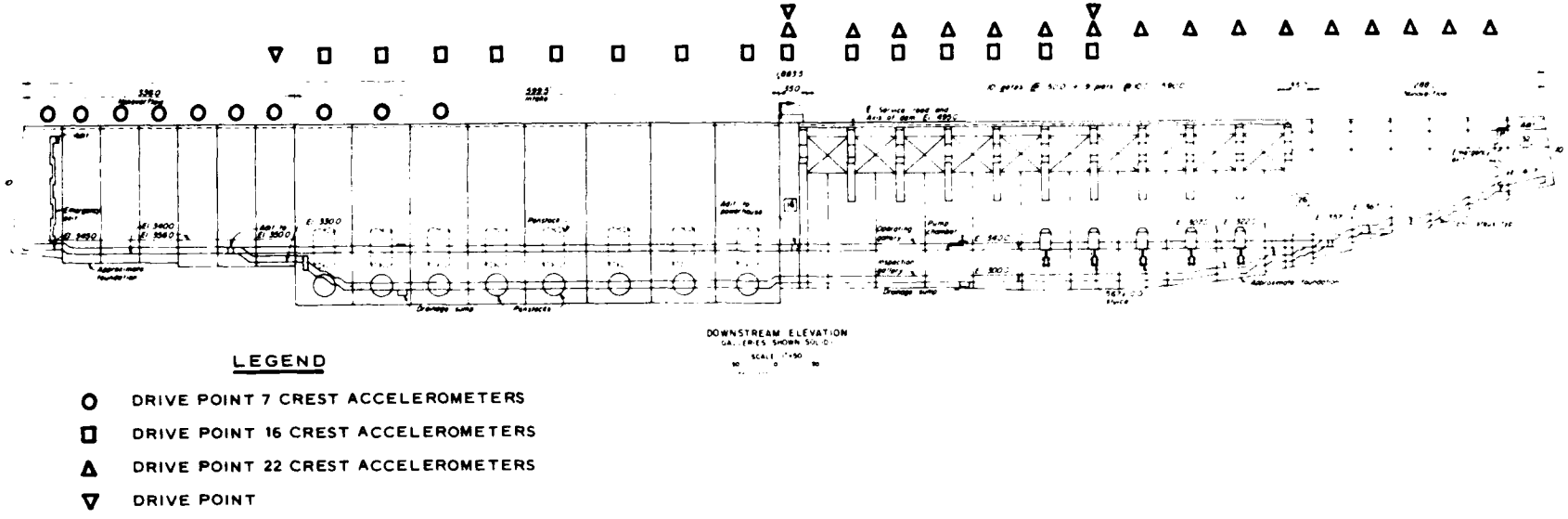

Figure 9. Crest accelerometer locations

direction to the dam was computed as the product of the measured acceleration and the 17,000-lb mass (7,711 kg). The three exciter locations were at monoliths 7 (elevation 494), 16 (elevation 483), and 22 (elevation 494).

8. Ideally it would be desirable to excite a structure at one location and mount enough transducers at all points of interest to measure the response of the structure. However, on a structure as large as Richard B. Russell Dam this was not possible because of the number of available transducers and the construction on portions of the dam. The first series of tests to measure horizontal accelerations of the dam in plan and cross section began with drive point 7 (monolith 7). The first array of accelerometers was placed along the crest at the center line of monoliths 1 to 11 to monitor the horizontal upstream-downstream motion. The accelerometer locations are shown in Figure 9 for all the crest tests. The second and third arrays of crest accelerometers were placed, respectively, at the center line of monoliths 8 to 16 and 16 to 22 for drive point 16. The final two arrays of crest accelerometers were placed at the center line of monoliths 16-22 (complete overlap of the third crest array) and 22 to 31 for drive point 22.

9. At each drive point the corresponding monoliths' accelerometers were placed to measure the distribution of horizontal acceleration with elevation. The location of accelerometers with respect to elevation of the monoliths' cross sections is shown in Figure 10.

10. Relative joint motion arrays were positioned at three locations and consisted of two accelerometers closely spaced on each side of the monoliths' joint being monitored. The joint arrays were at elevation 483 joint 15-16 and elevation 436 spillway crest joints 21-22 and 22-23. The joint accelerometer locations are shown in Figure 11.

11. There were eight distinctive test arrays and sixteen separate tests were conducted. All the tests were 1/2* decade/minute sine sweeps from 25 Hz to 1 Hz. This rate was found to be slow enough for a required quasi-steady state condition to provide enough data in a given time interval for adequate digital time resolution. Each test lasted about 2.8 minutes; but there were many hours of preparation required to conduct a test for a given array. The electrical signals output from the accelerometers and the shaker were recorded as analog signals on the 32-track tape recorder.

---

* For example (refer to Figure 5), to sweep from 20 Hz to 2 Hz (1 decade) took 2 minutes.

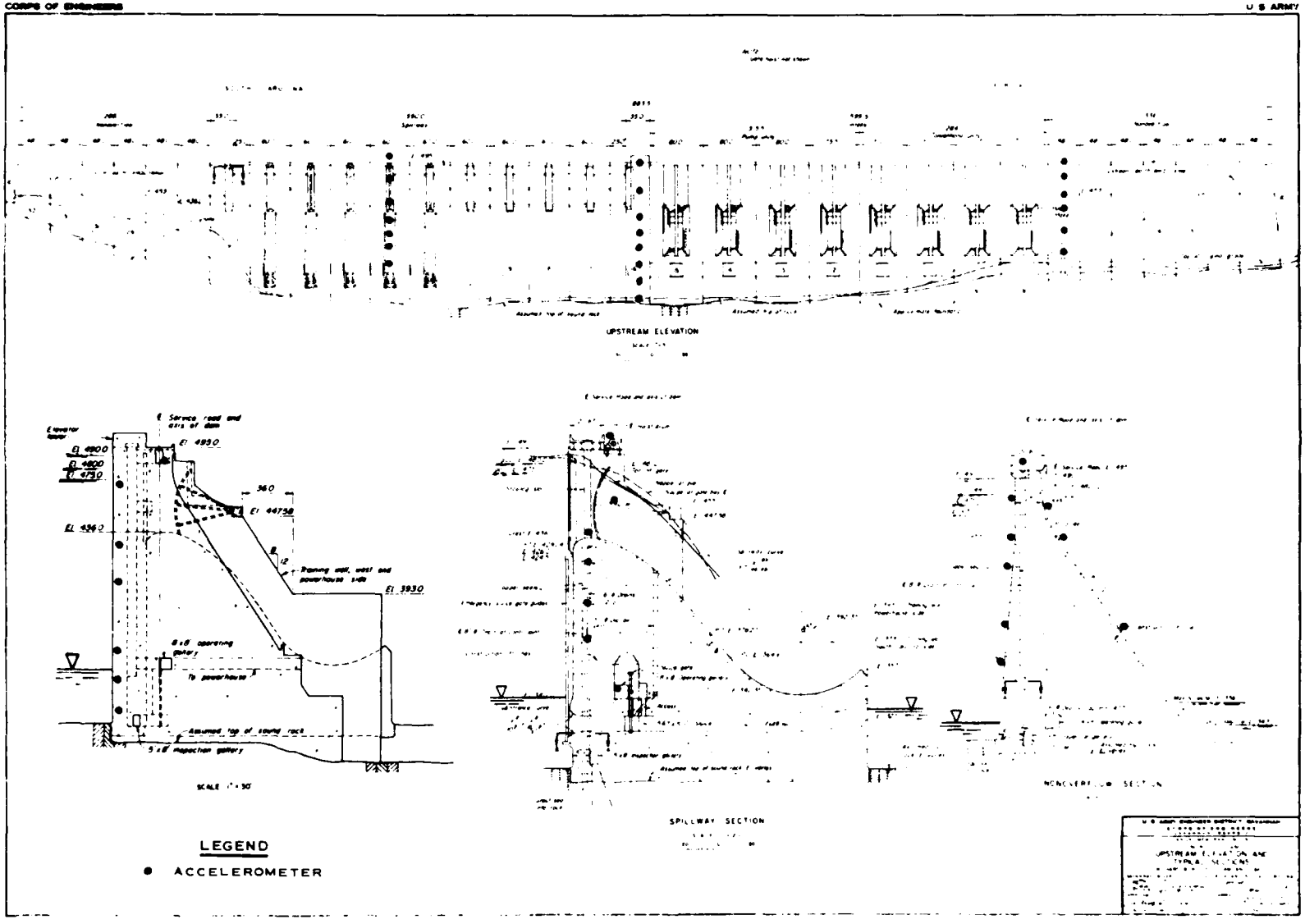

Figure 10. Cross sectional accelerometer locations

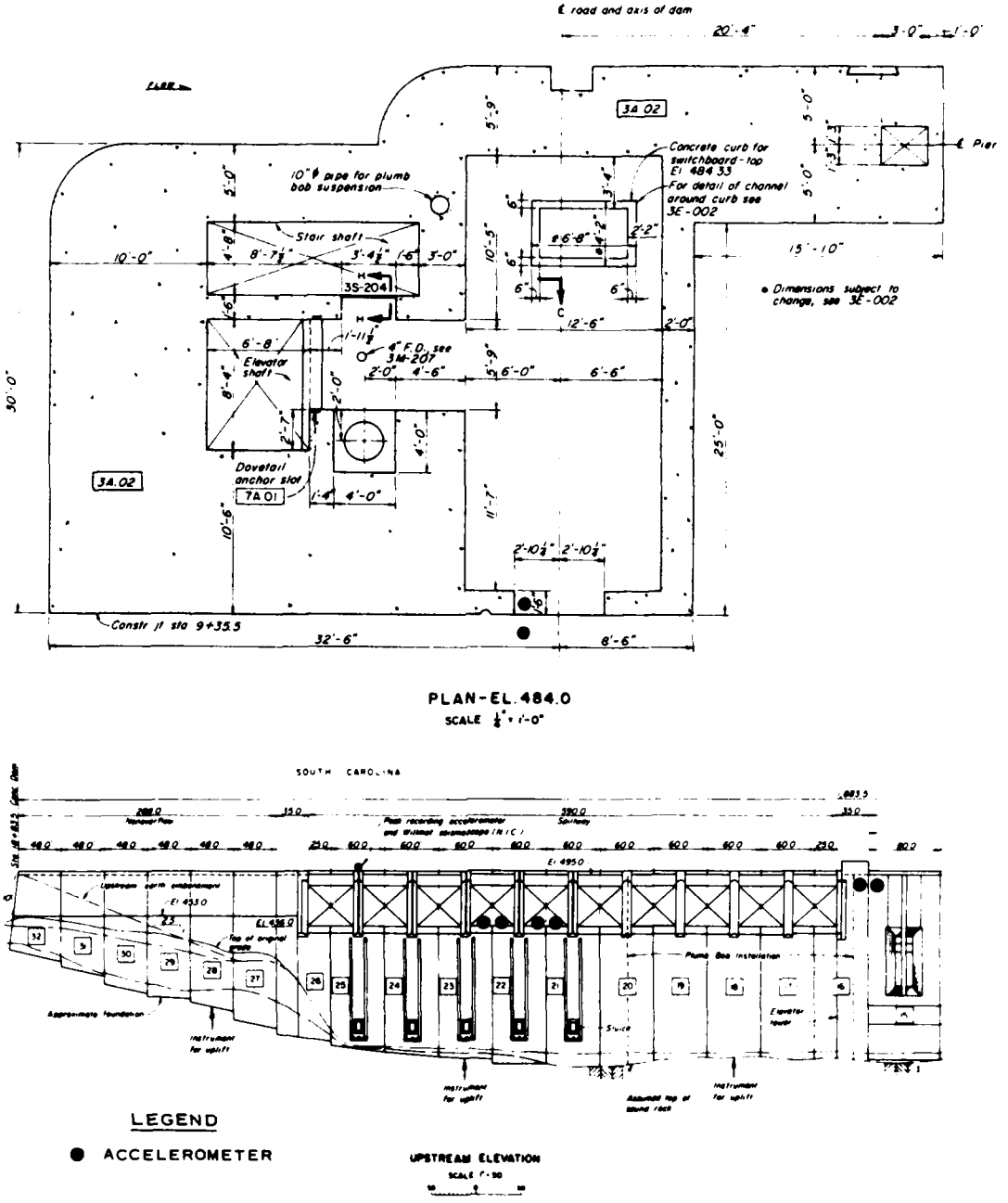

Figure 11. Relative joint accelerometer locations

Dynamic Cylinder Tests

12. Dynamic tests were conducted on 5 of 22 standard 6- by 12-in. (152- by 305-mm) cylinders cast from concrete mixtures used in the construction of the dam. The cylinders were placed in a fog room within 48 hours of casting. Before being transported to WES the cylinders were removed from the fog room. Once at WES the cylinders remained in the testing room up to test time.

13. For the dynamic tests the cylinders were supported horizontally at the node points (corresponding to the fundamental flexural mode of vibration of a free-free beam, see Figure 12). With an accelerometer mounted on a test

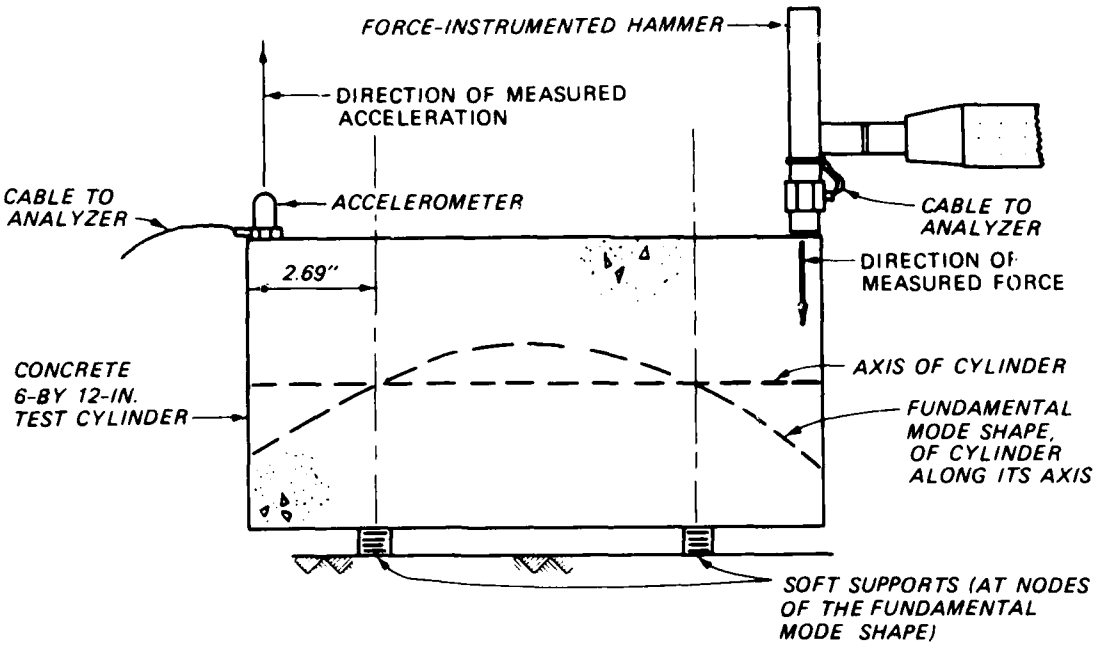

Figure 12. Schematic of dynamic cylinder test setup

cylinder a force-instrumented hammer was used to strike the cylinder with the applied force parallel to the measured acceleration. This method of testing has provided reasonable results in a number of similar applications (Alexander, A. Michel, 1981).

PART III: DATA REDUCTION AND EXPERIMENTAL RESULTS

14. To obtain the necessary data form for the modal analysis the HP5423A Structural Dynamics Analyzer was used. The HP5423A has a two-channel digital processor with 12-bit resolution per channel. All the analog signals were played back by using the force input and one of the accelerometer's output for that test to digitize an input/output (I/O) pair. A total of 70 I/O pairs were digitized representing the transfer functions (or frequency response functions) at the 58 accelerometer locations on the dam. A transfer function is the complex (i.e., composed of real and imaginary parts) ratio of the measured output acceleration to the measured input force. The data were stored on HP data cartridges compatible with the HP5423A. Besides the frequency response functions (or transfer functions) the coherence functions from strategic points were also computed and saved. The coherence function for an I/O pair measures what ratio of the output acceleration is linearly caused by a measured input force; thus each I/O pair represents a single input/single output model. For a more detailed description of spectral functions an excellent reference is Engineering Applications of Correlation and Spectral Analysis (Bendat and Piersol 1980).

15. Transfer and coherence functions are shown in Appendix A which are representative of the overall response of the dam. The coherence function is nondimensional and has values from 0 to 1 (0 to 100% coherent signal). The natural frequencies were determined by a quadrature peak picking method (called a line cursor fit in the HP users guide (Hewlett-Packard Co. 1981 and Hewlett-Packard Co. 1982)). This involves observing the peaks in the imaginary part and the zero crossings in the real part of the transfer function for a particular frequency. The HP5423A fits a curve through 11 data points of the peak in the imaginary plot of the transfer function and computes the modal damping ratios and shape parameters. Therefore, one transfer function is representative of the overall structural damping for a particular resonant frequency and mode shape. Ten mode shapes were investigated and the modal parameters are tabulated in Table 4. For an explanation and example of the modal parameter extraction method see Appendix B.

16. Before the modal analysis was performed a geometry of the dam represented by the accelerometer locations was described and the coordinates were entered into structural component tables in the HP5423A. Using the

estimates of natural frequencies and damping ratios residue values are computed from each transfer function of the response points. The residues are used to compute shape vectors for each response point. Then the shape vectors combined from each response point define the mode shapes of the dam for each resonant frequency investigated. The 10 identified mode shapes are shown in crest plan, three cross sections, and isometric views in Figures 13-22.

17. The relative joint motions are determined by taking the ratio of one transfer function to the transfer function across the joint. Thus the input term cancels out resulting in the ratio of accelerations across the joint. The relative joint motions are shown for joints 15-16, 21-22, and 22-23 in Figures 23-28.

Dynamic Cylinder Tests

18. The dynamic cylinder test results were used to independently measure material damping and the dynamic modulus of the concrete used in constructing the dam. The values of damping obtained from the dynamic cylinder tests are a lower bound that could be expected in the dam structural system. Using the HP5423A the electrical signals from the accelerometer and the load cell (force instrumentation) were processed and a transfer function was computed. From the transfer function the fundamental resonant frequency was determined, and using an appropriate frequency bandwidth a damping ratio was computed. The results are listed in Table 3.

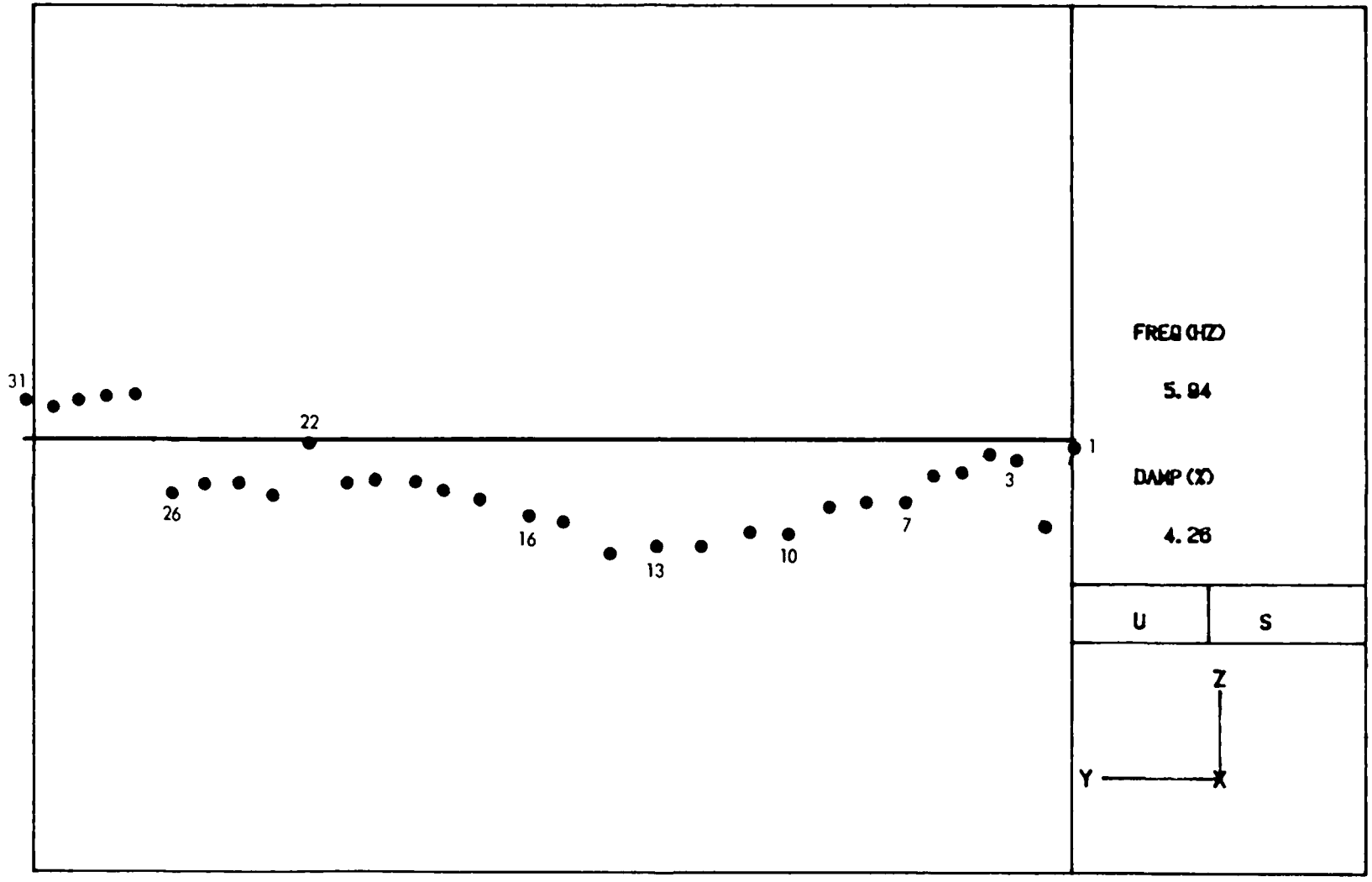

a. Plan view of crest

Figure 13. Mode shape 1 (all dots on following figures indicate measured response) (Sheet 1 of 3)

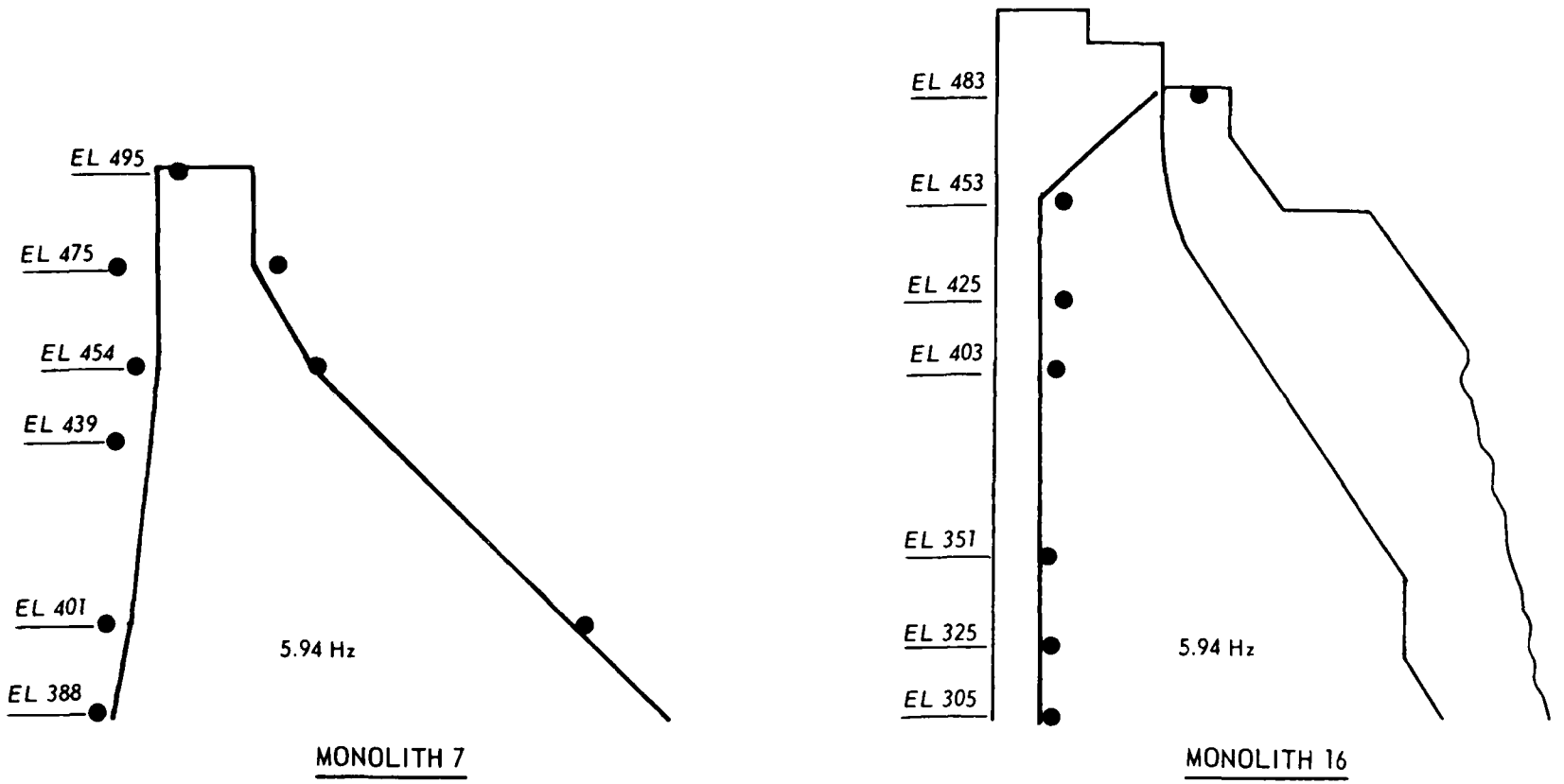

b. Cross sectional views

Figure 13. (Sheet 2 of 3)

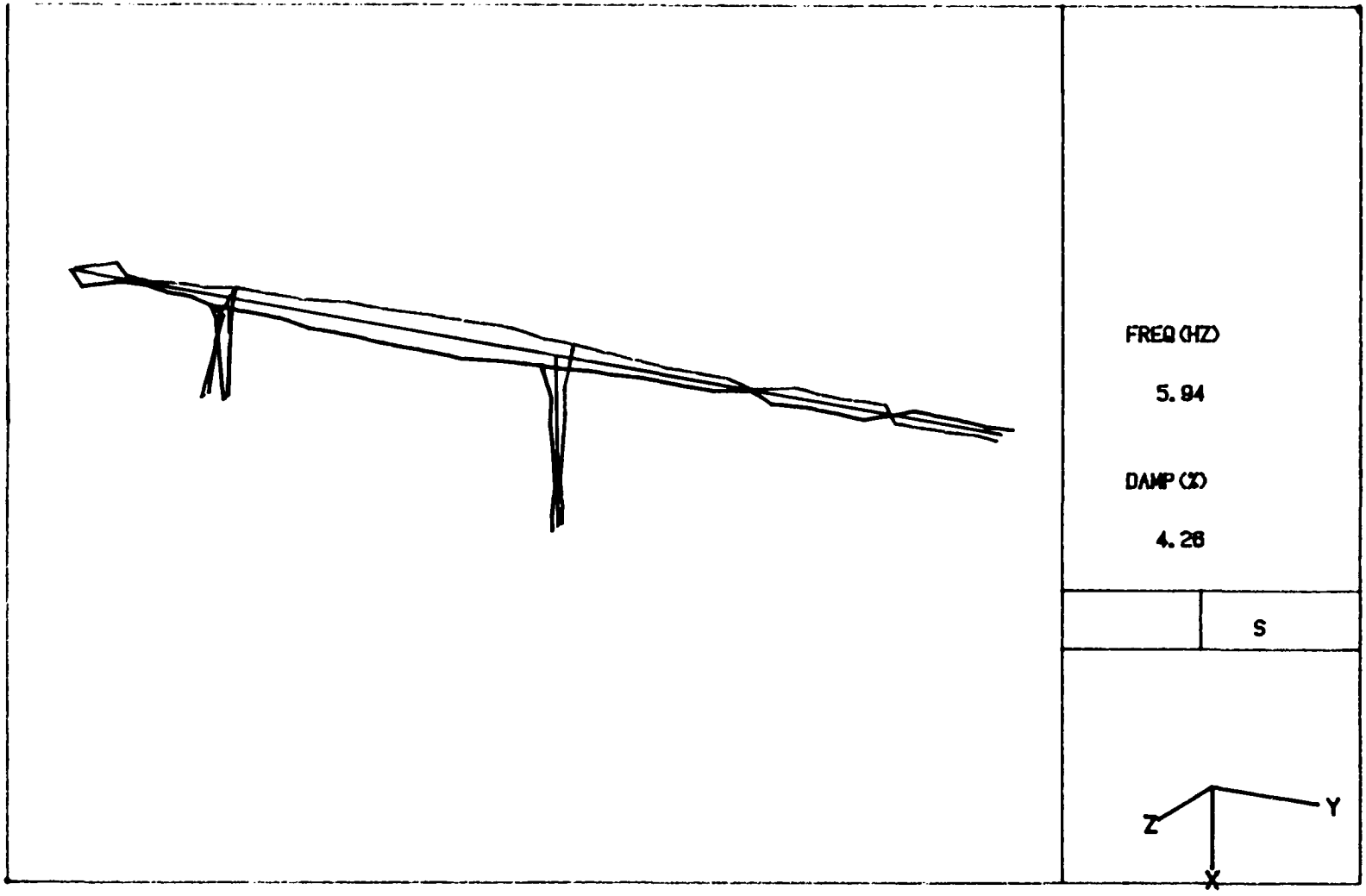

c. 3-D view

Figure 13. (Sheet 3 of 3)

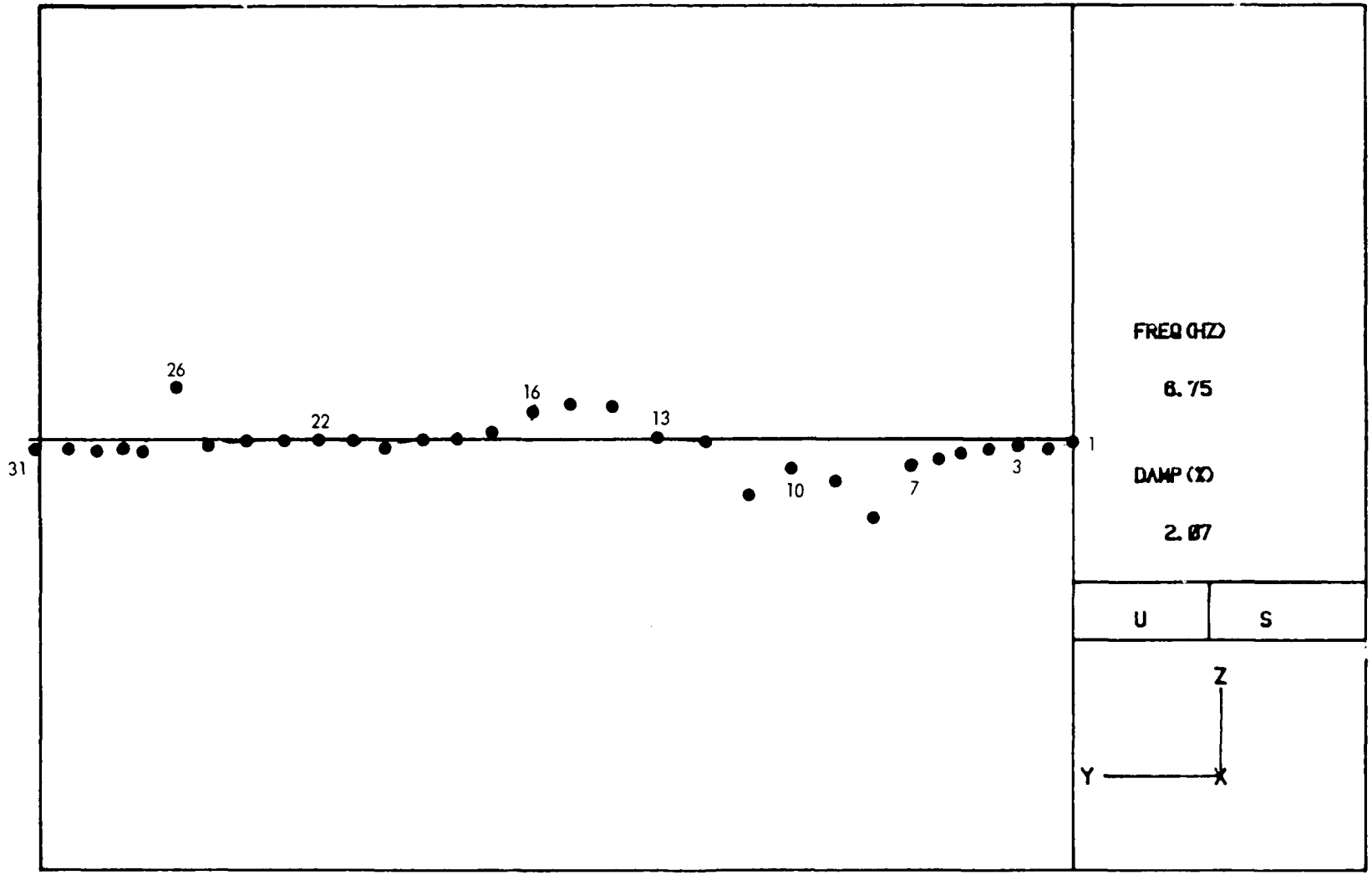

a. Plan view of crest

Figure 14. Mode shape 2 (Sheet 1 of 3)

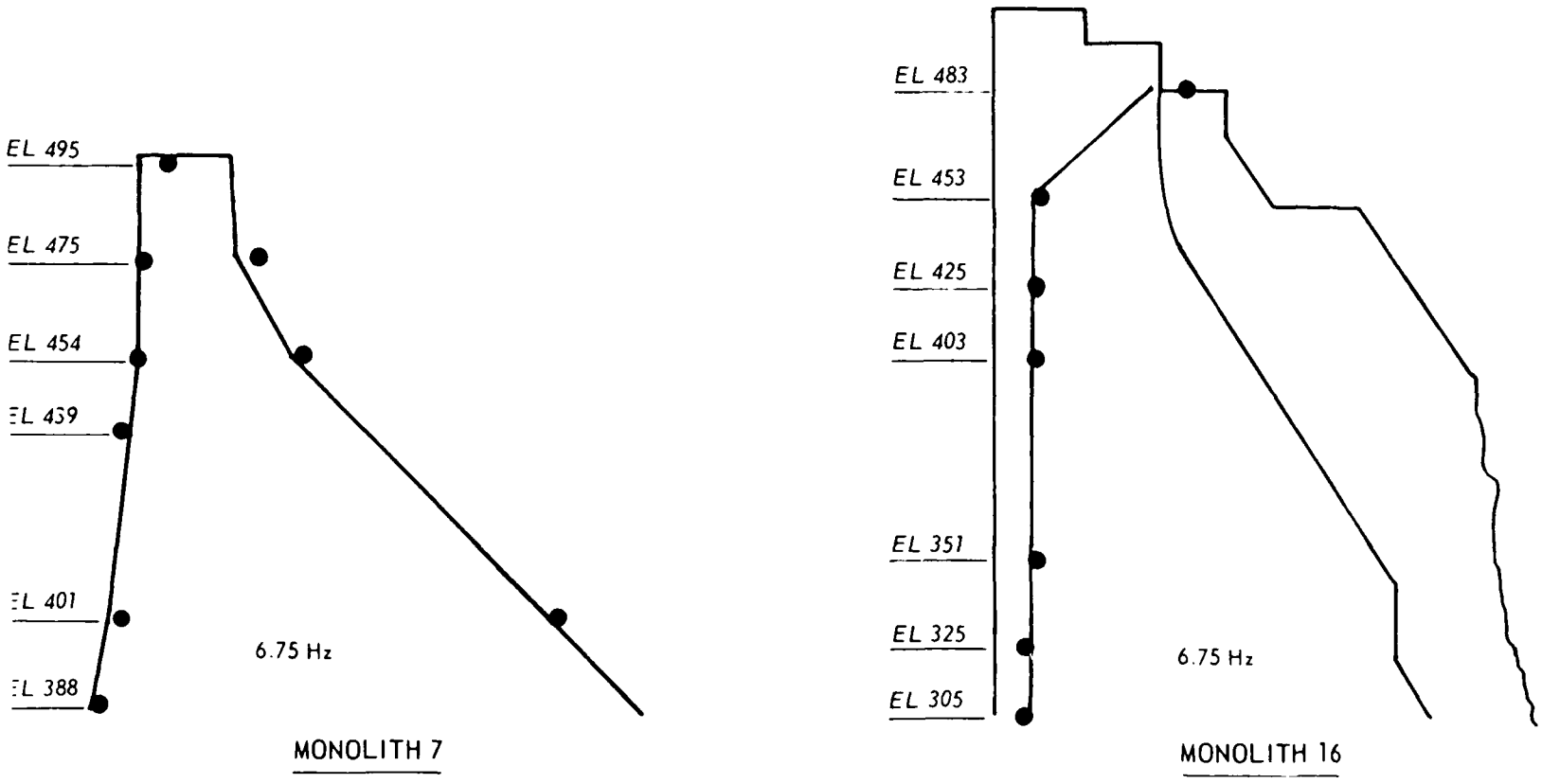

b. Cross sectional views

Figure 14. (Sheet 2 of 3)

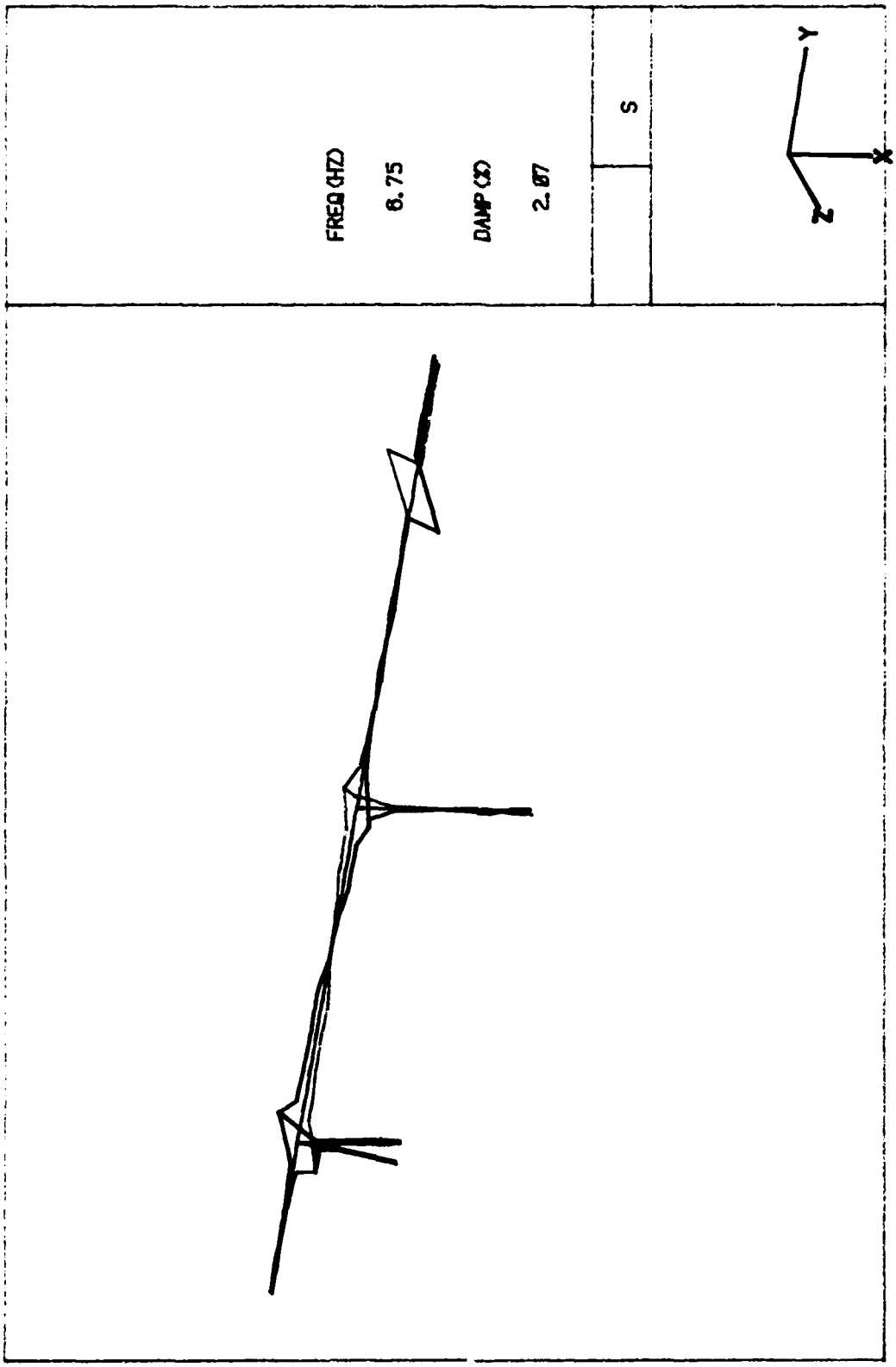

c. 3-D view

Figure 14. (Sheet 3 of 3)

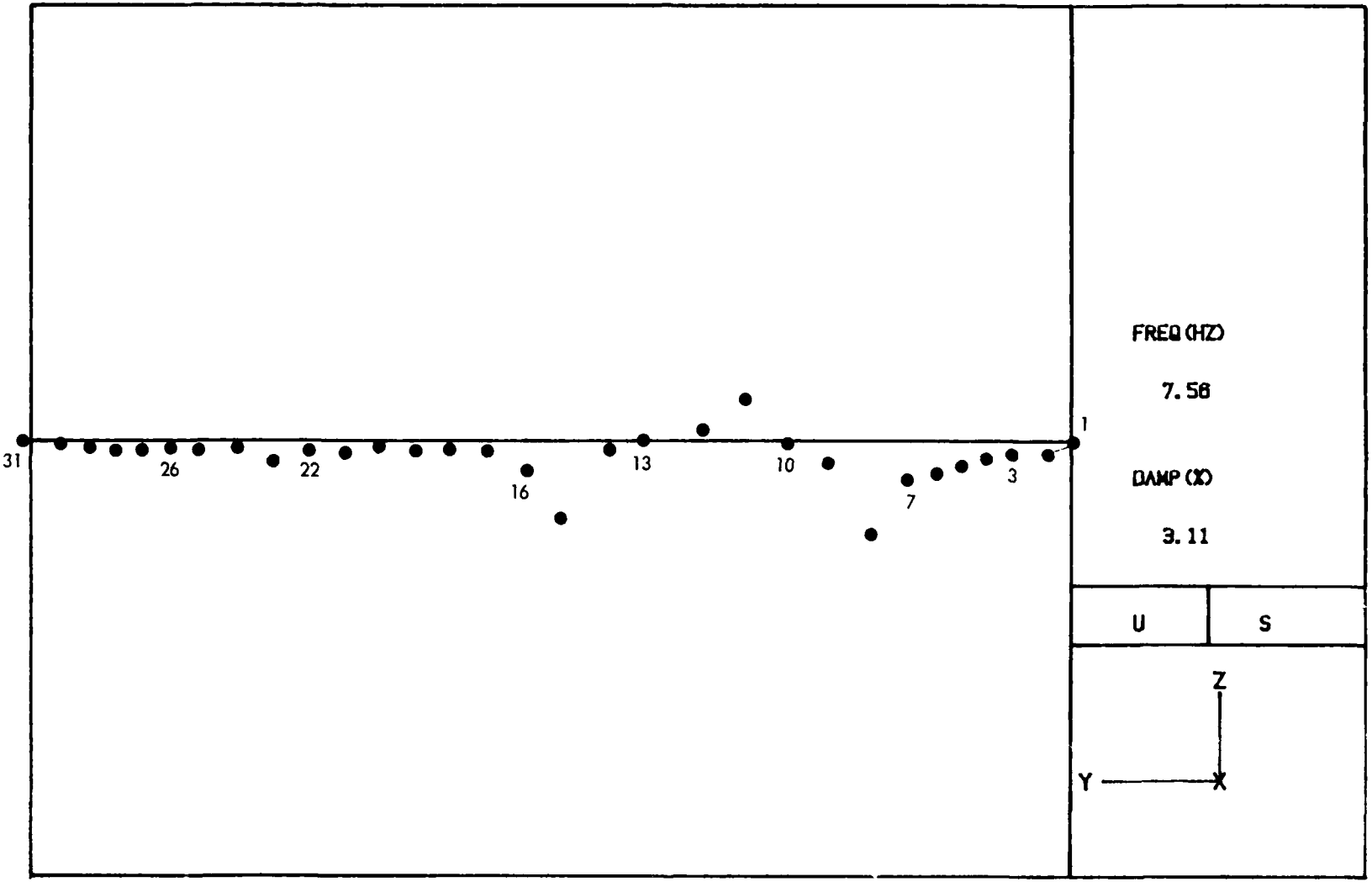

a. Plan view of crest

Figure 15. Mode shape 3 (Sheet 1 of 3)

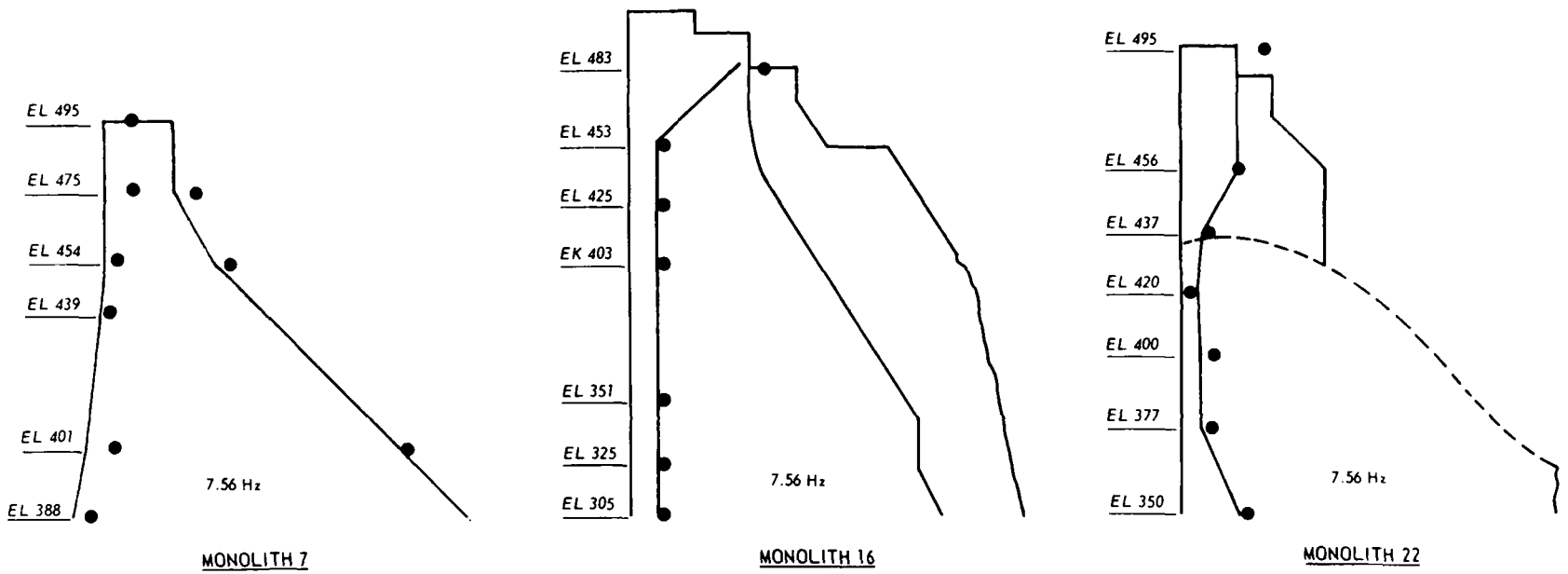

b. Cross sectional views

Figure 15. (Sheet 2 of 3)

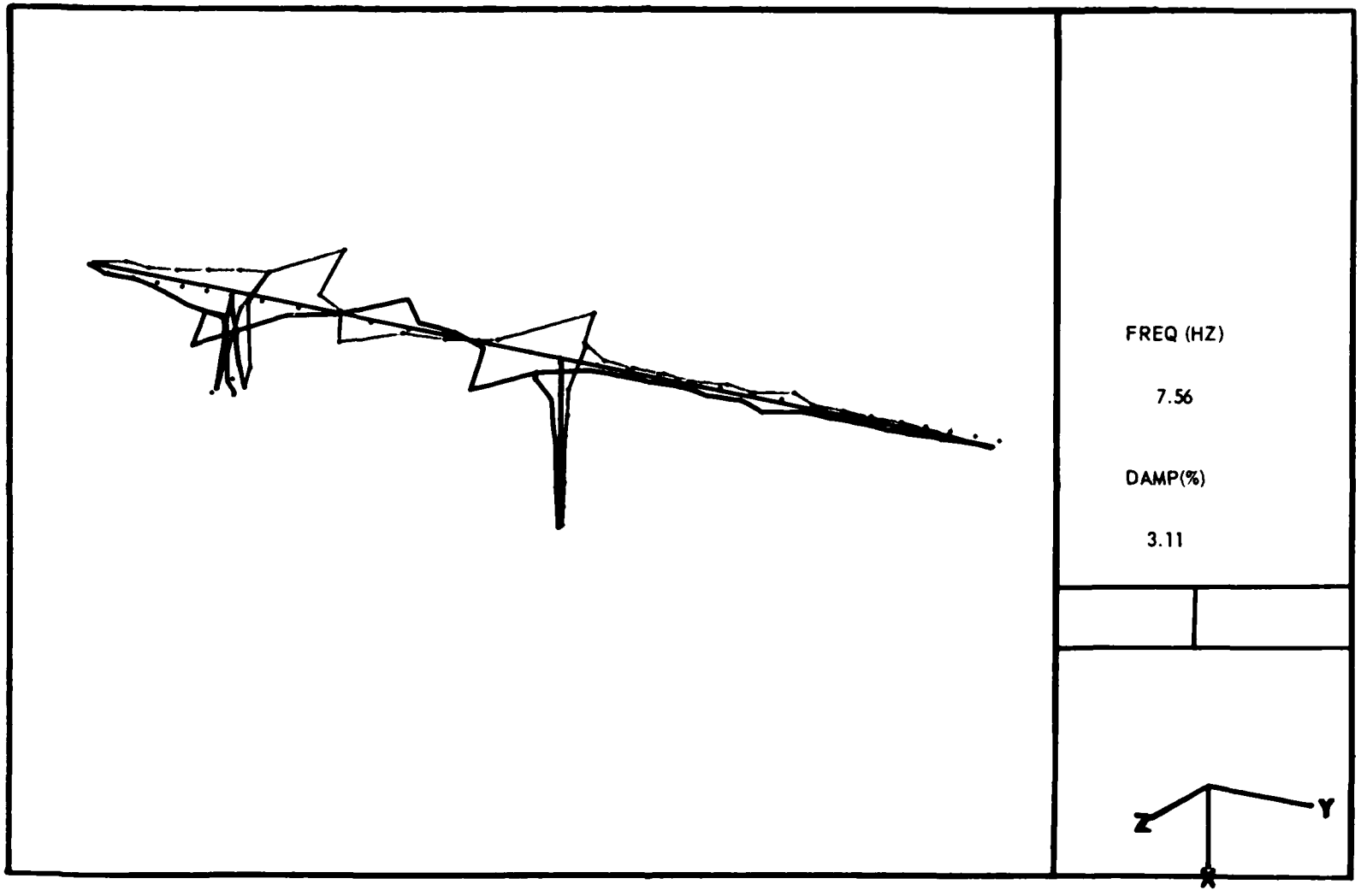

c. 3-D view

Figure 15. (Sheet 3 of 3)

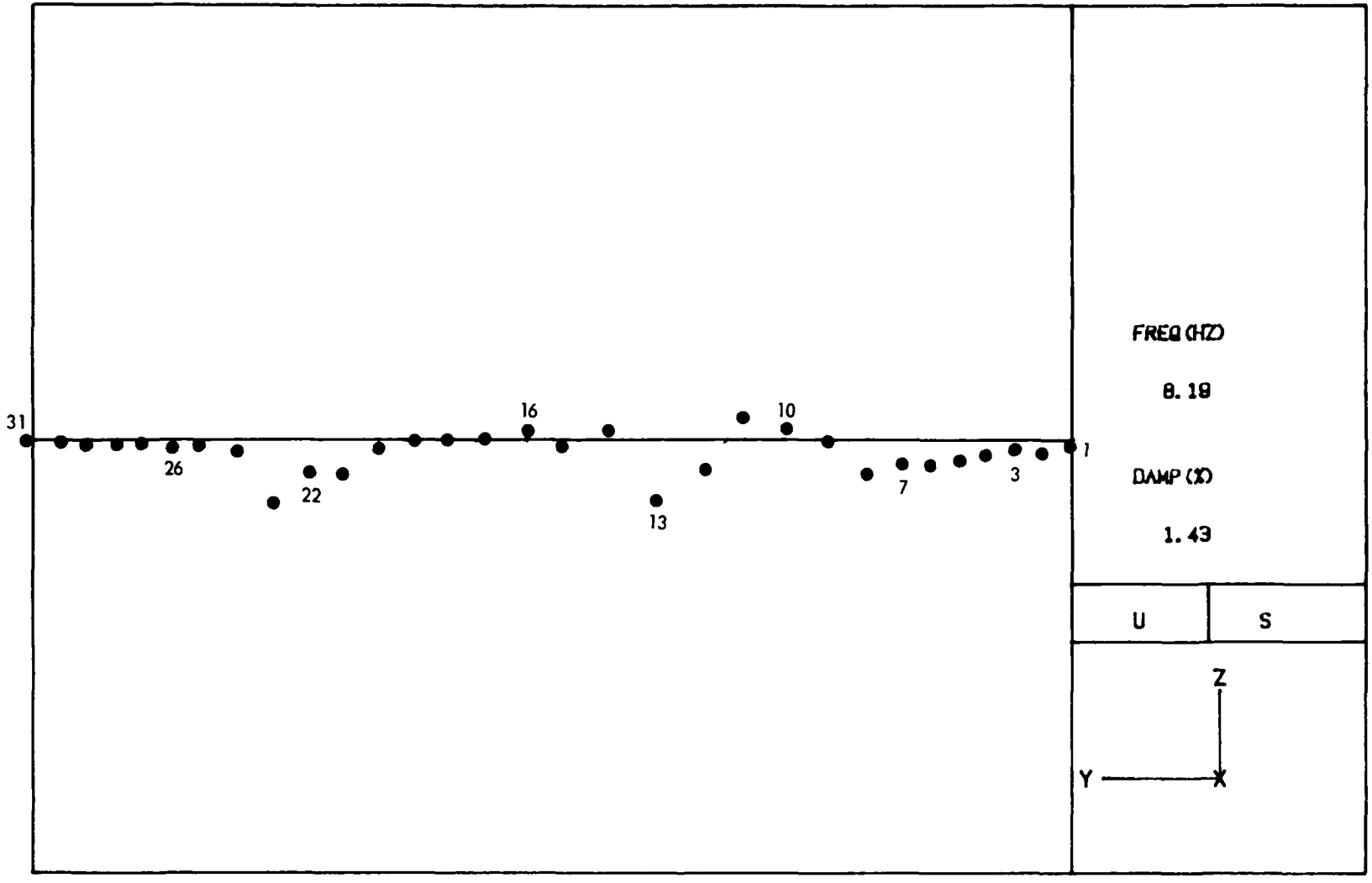

a. Plan view of crest

Figure 16. Mode shape 4 (Sheet 1 of 3)

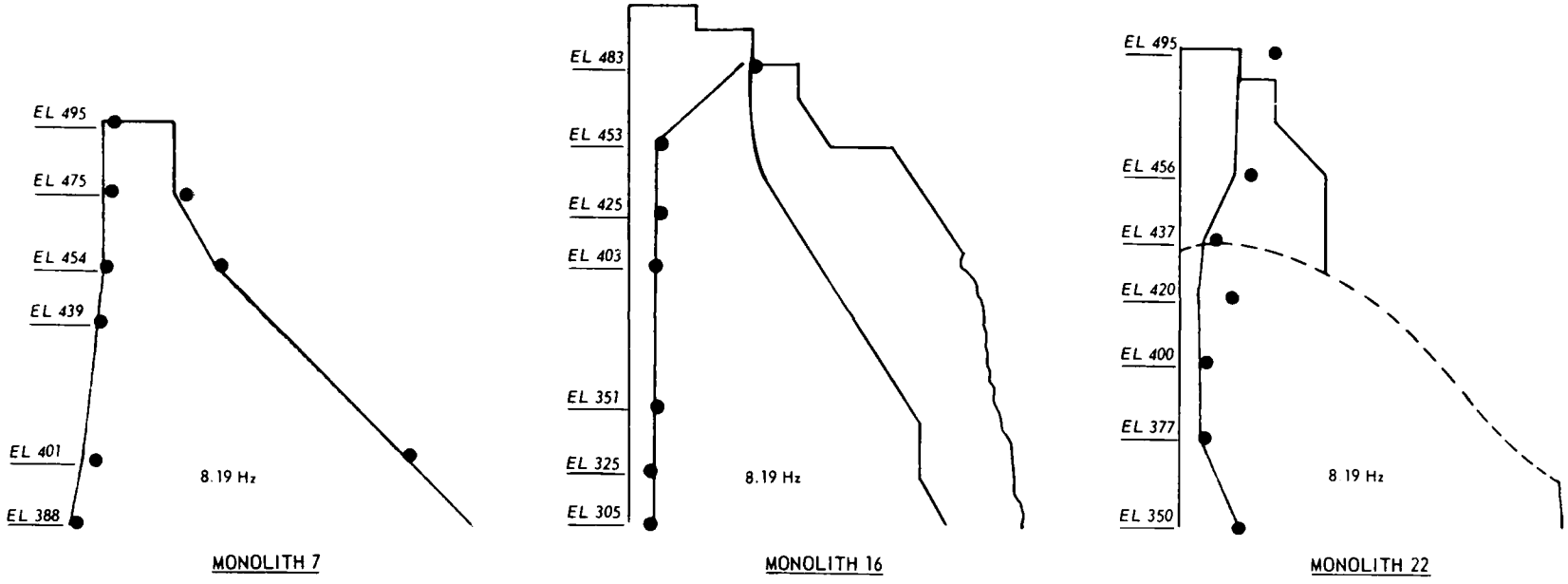

b. Cross sectional views

Figure 16. (Sheet 2 of 3)

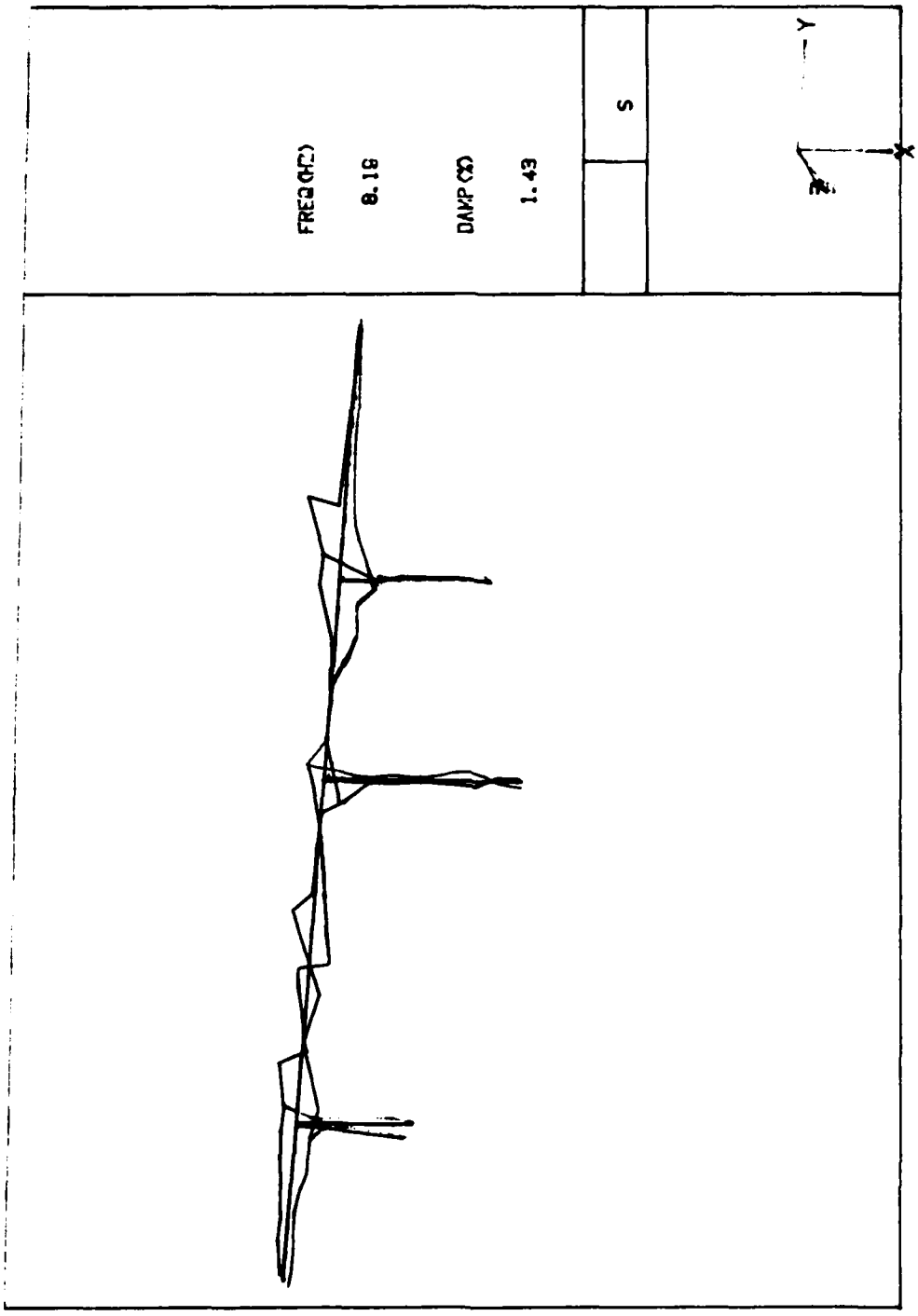

c. 3-D view

Figure 16. (Sheet 3 of 3)

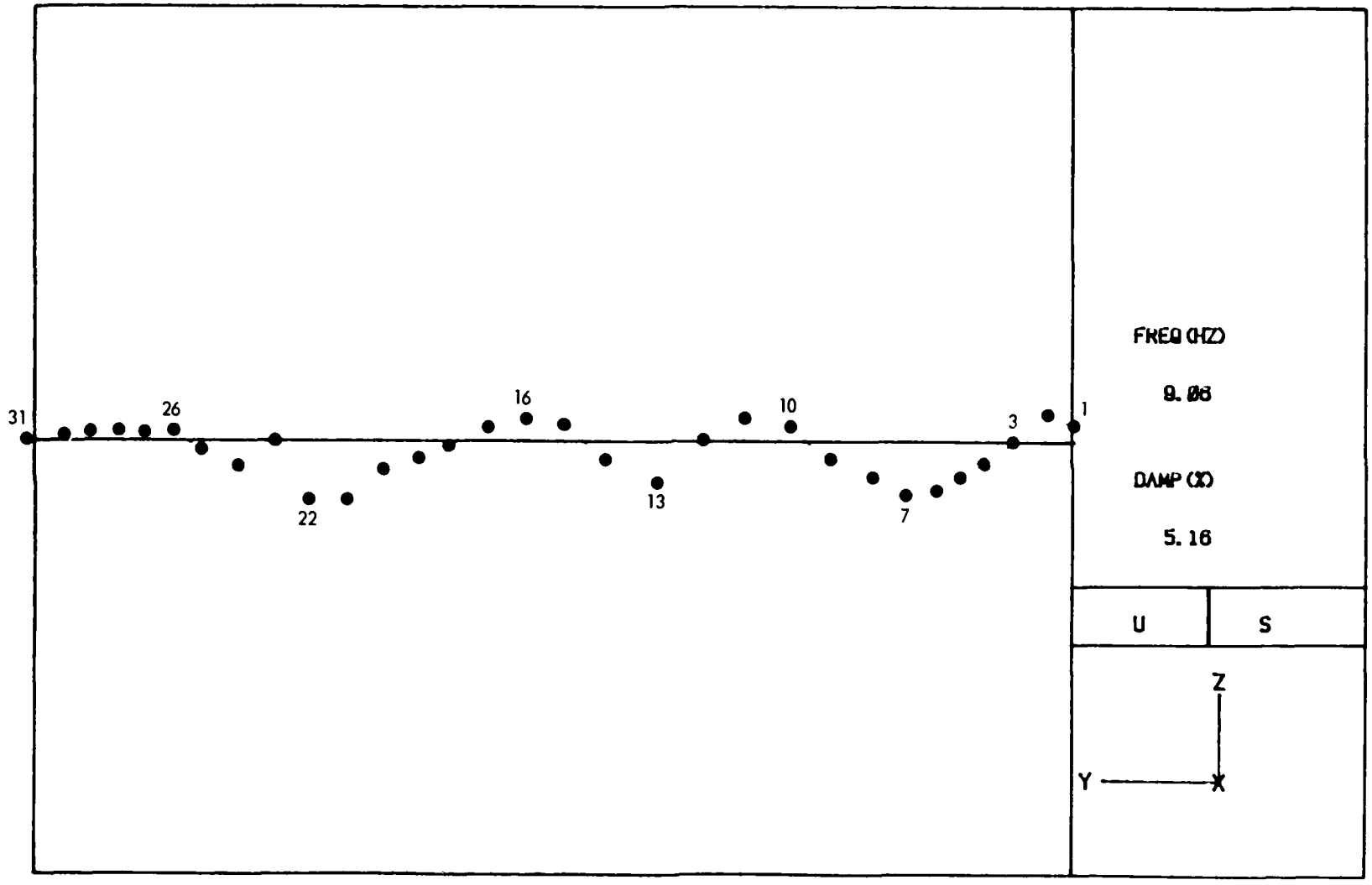

a. Plan view of crest

Figure 17. Mode shape 5 (Sheet 1 of 3)

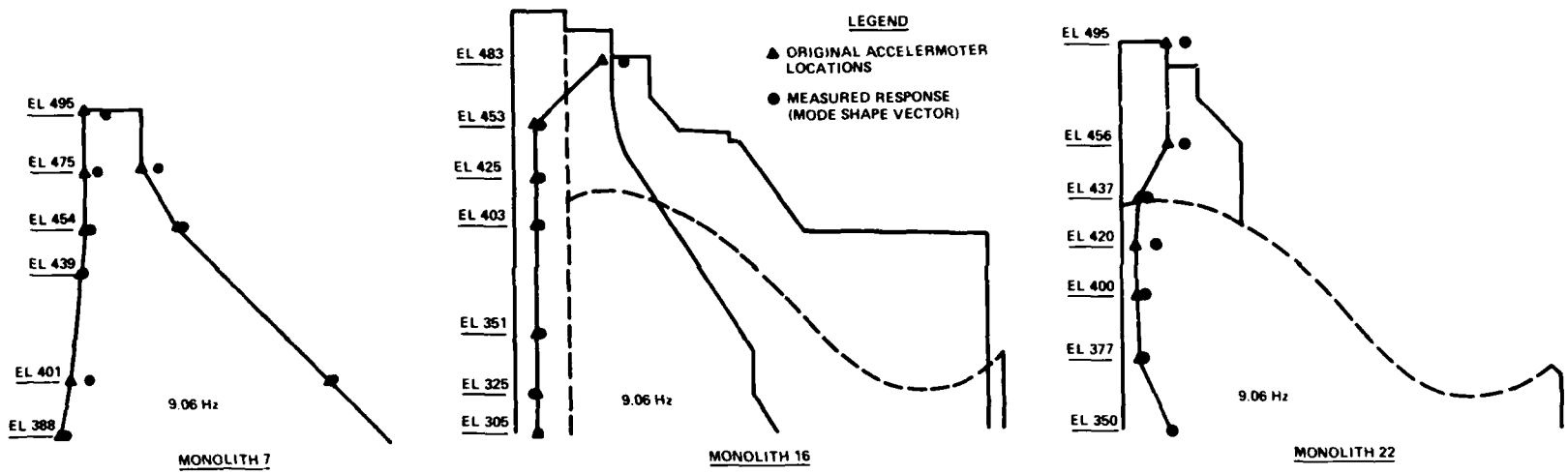

b. Cross sectional views

Figure 17. (Sheet 2 of 3)

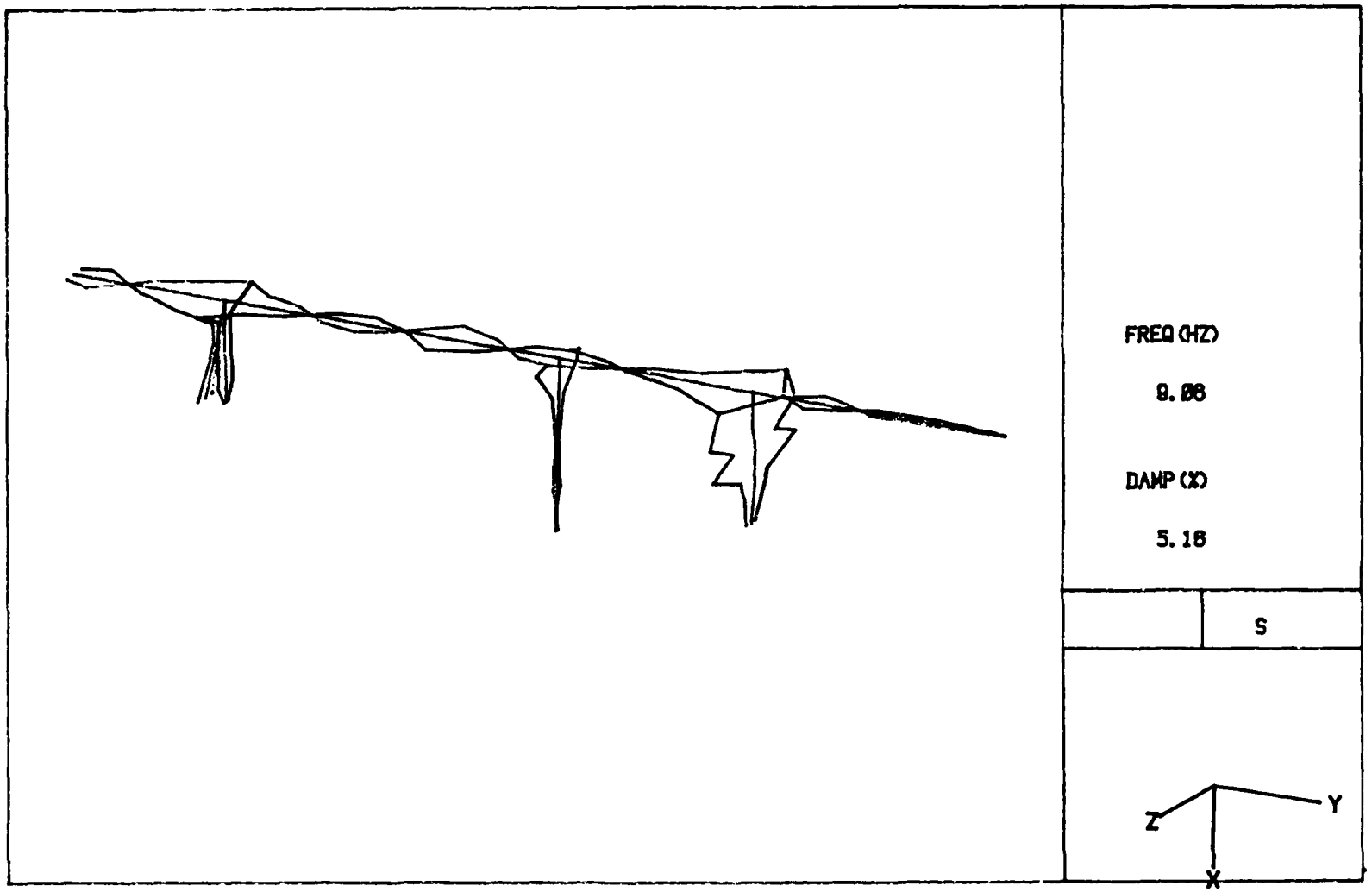

c. 3-D view

Figure 17. (Sheet 3 of 3)

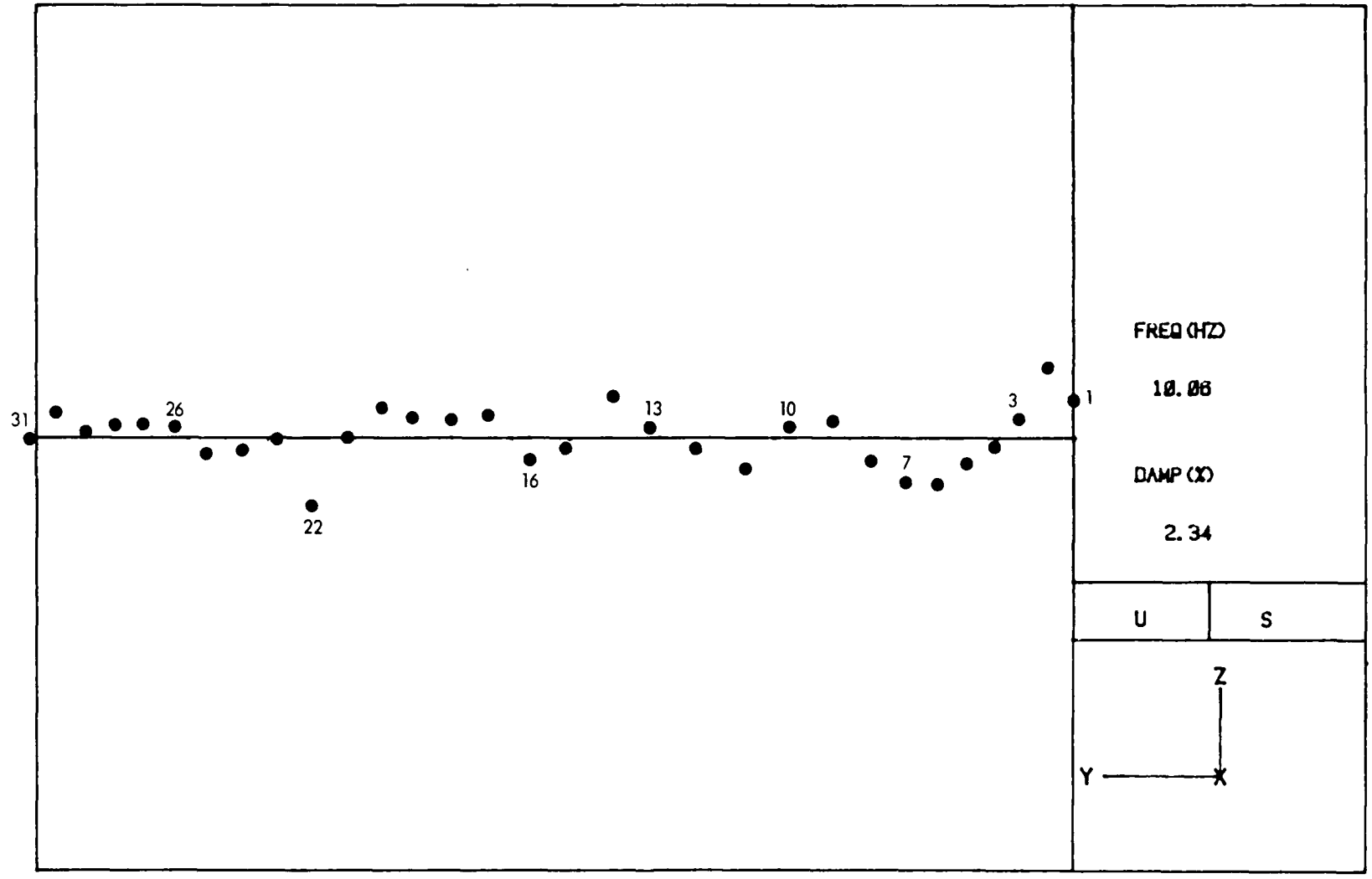

a. Plan view of crest

Figure 18. Mode shape 6 (Sheet 1 of 3)

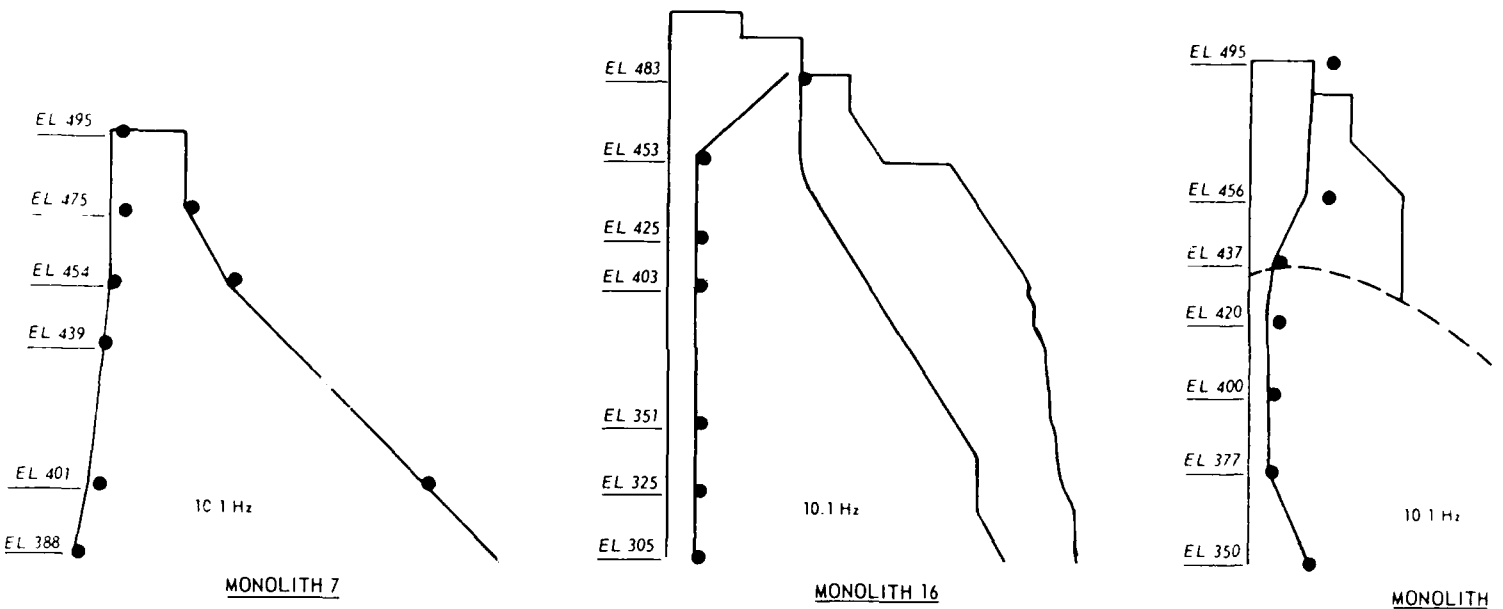

b. Cross sectional views

Figure 18. (Sheet 2 of 3)

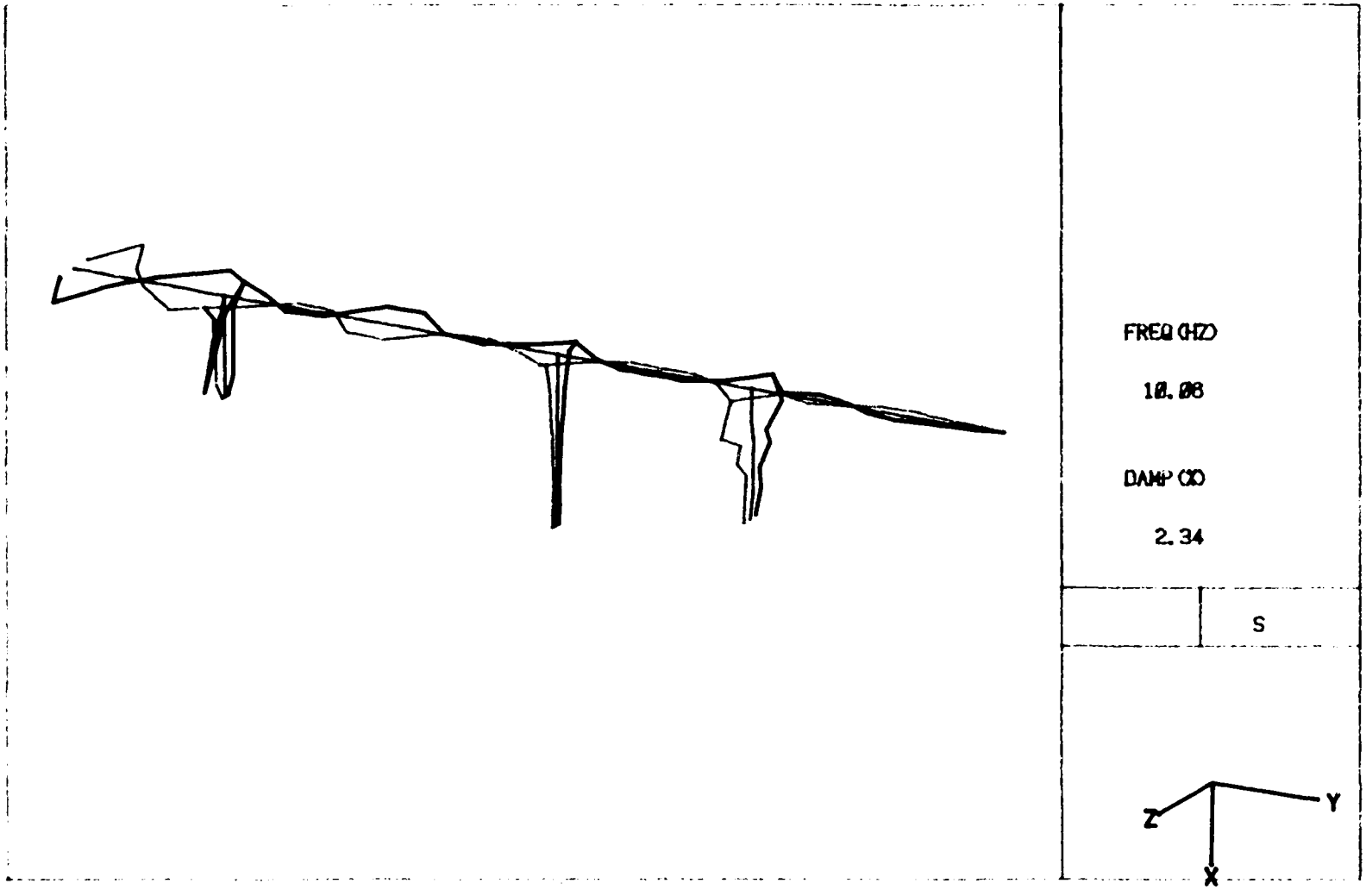

c. 3-D view

Figure 18. (Sheet 3 of 3)

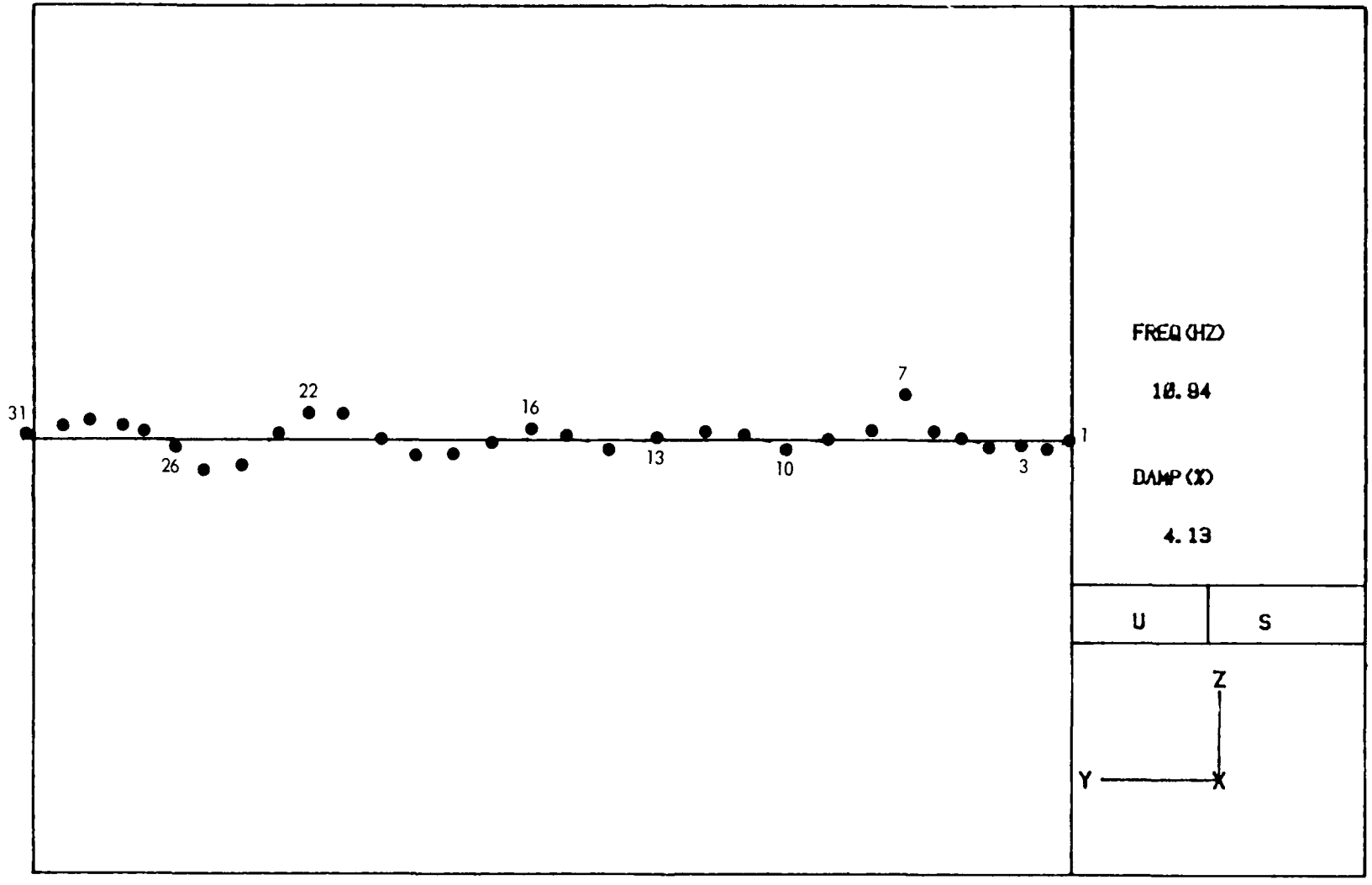

a. Plan view of crest

Figure 19. Mode shape 7 (Sheet 1 of 3)

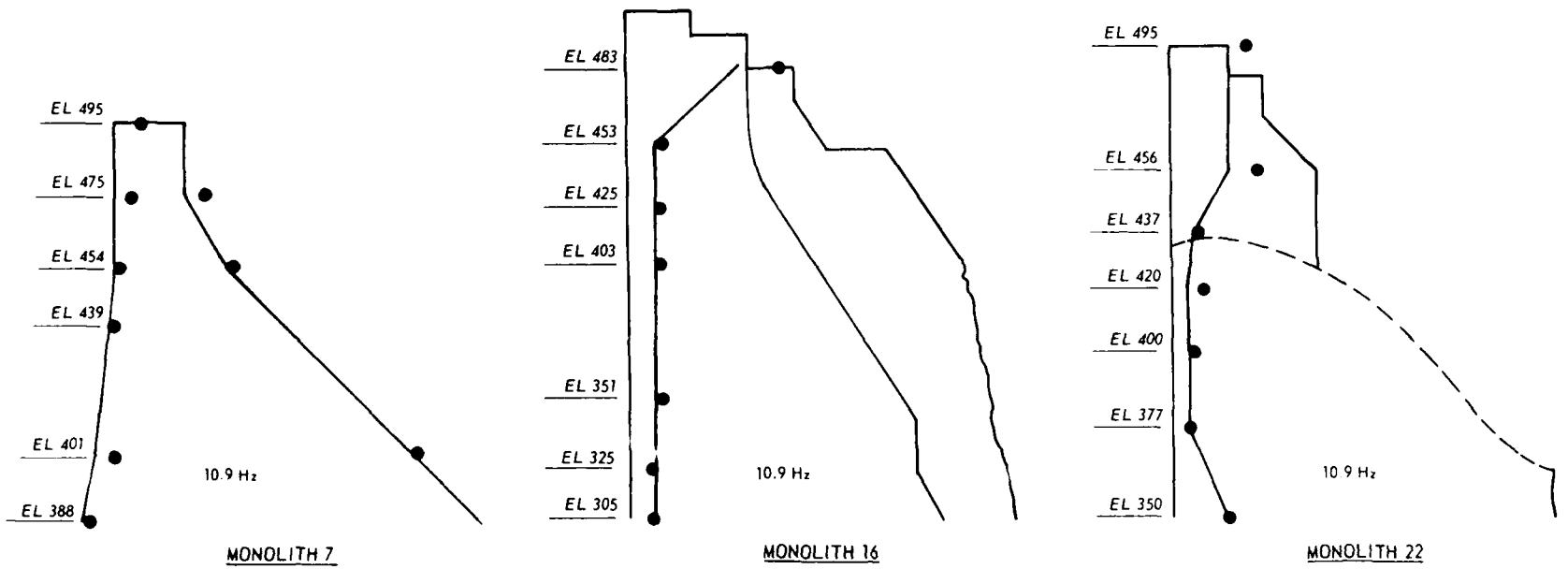

b. Cross sectional views

Figure 19. (Sheet 2 of 3)

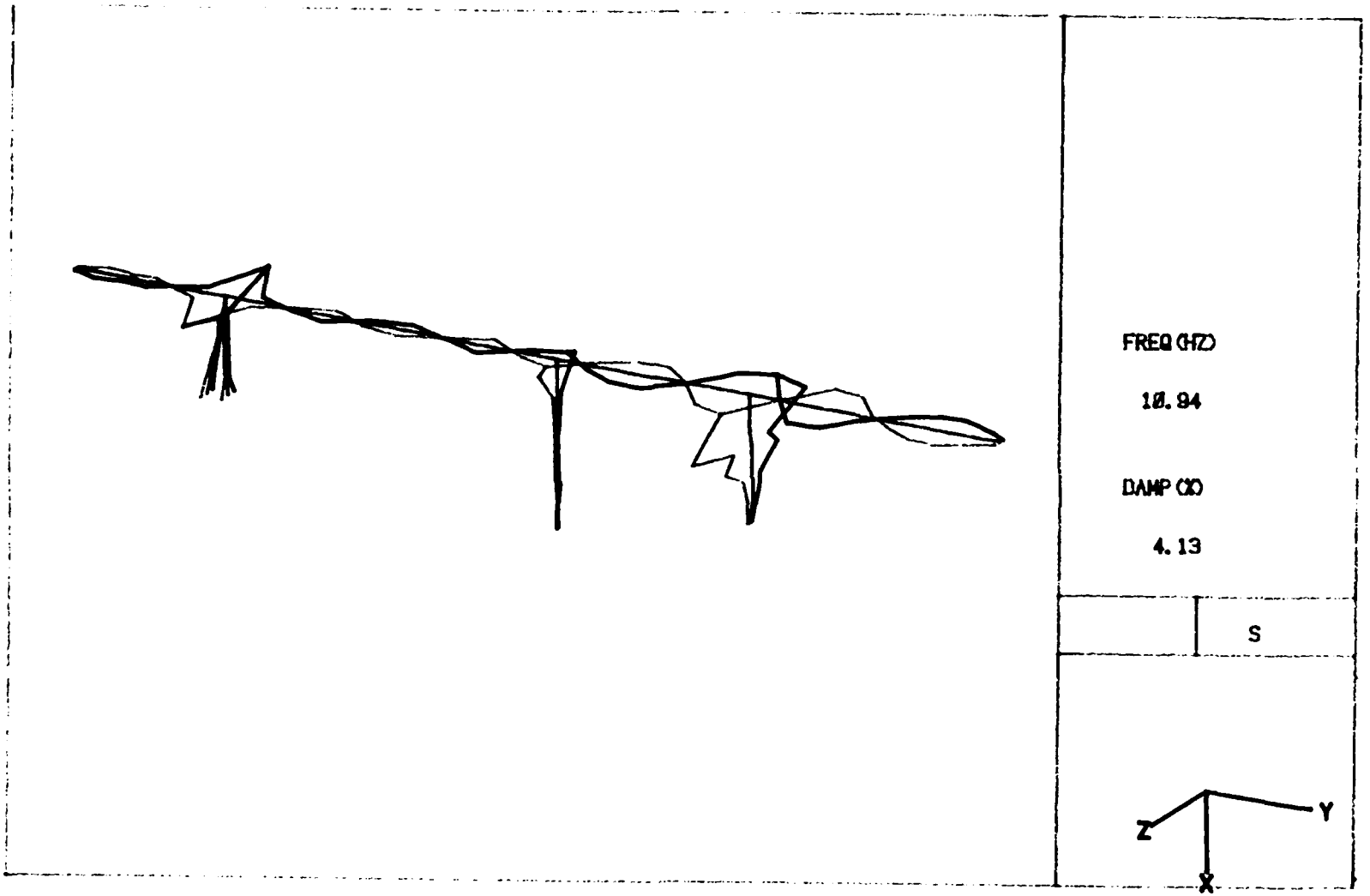

c. 3-D view

Figure 19. (Sheet 3 of 3)

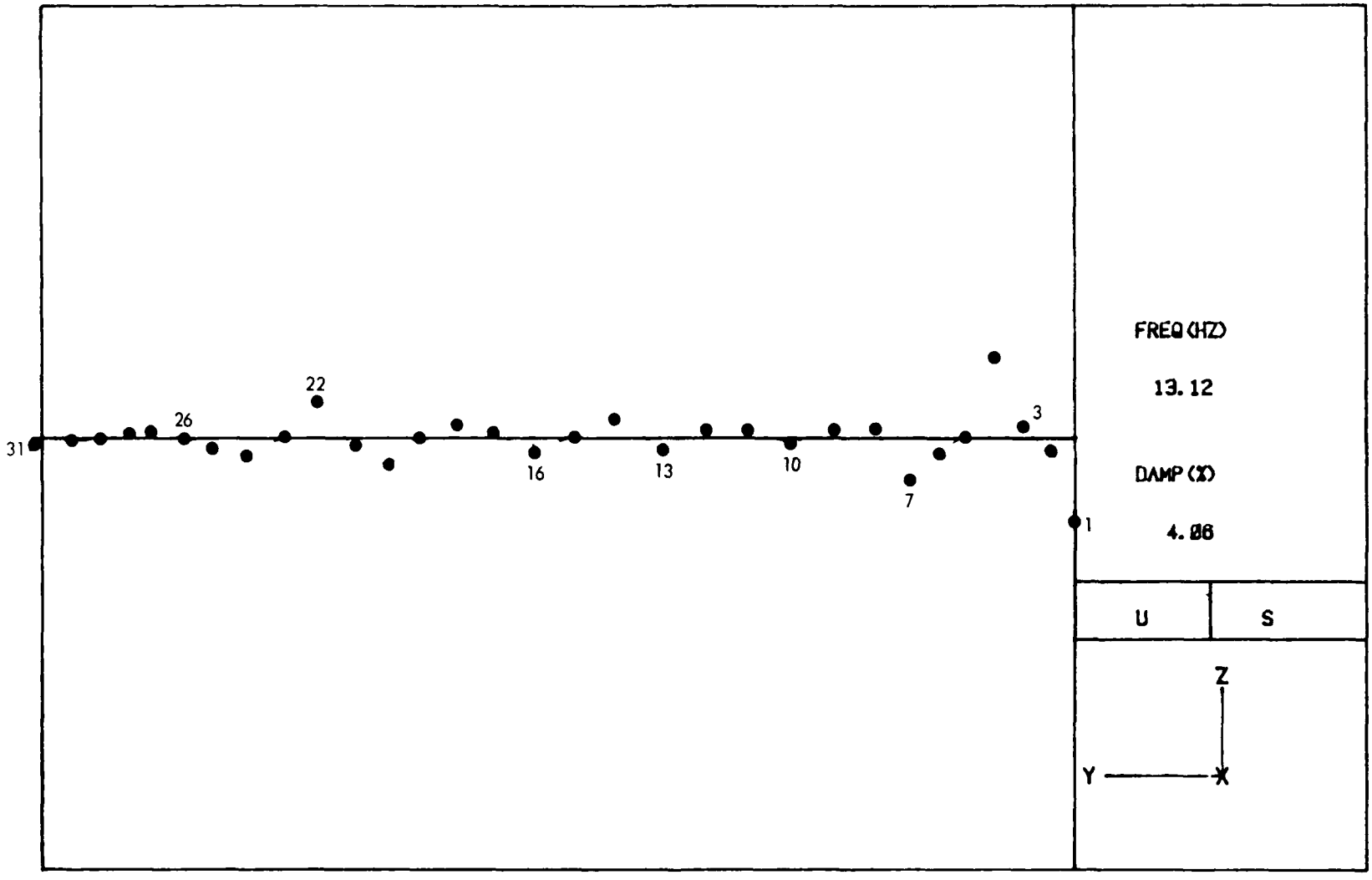

a. Plan view of crest

Figure 20. Mode shape 8 (Sheet 1 of 3)

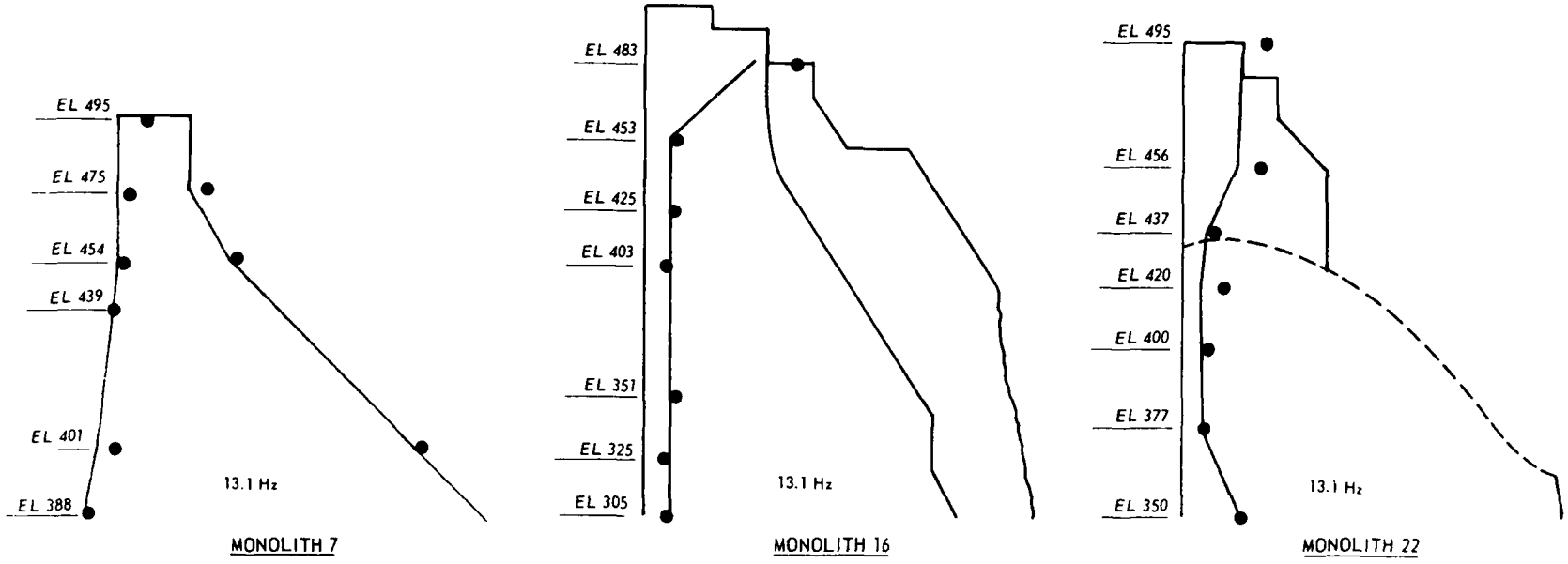

b. Cross sectional views

Figure 20. (Sheet 2 of 3)

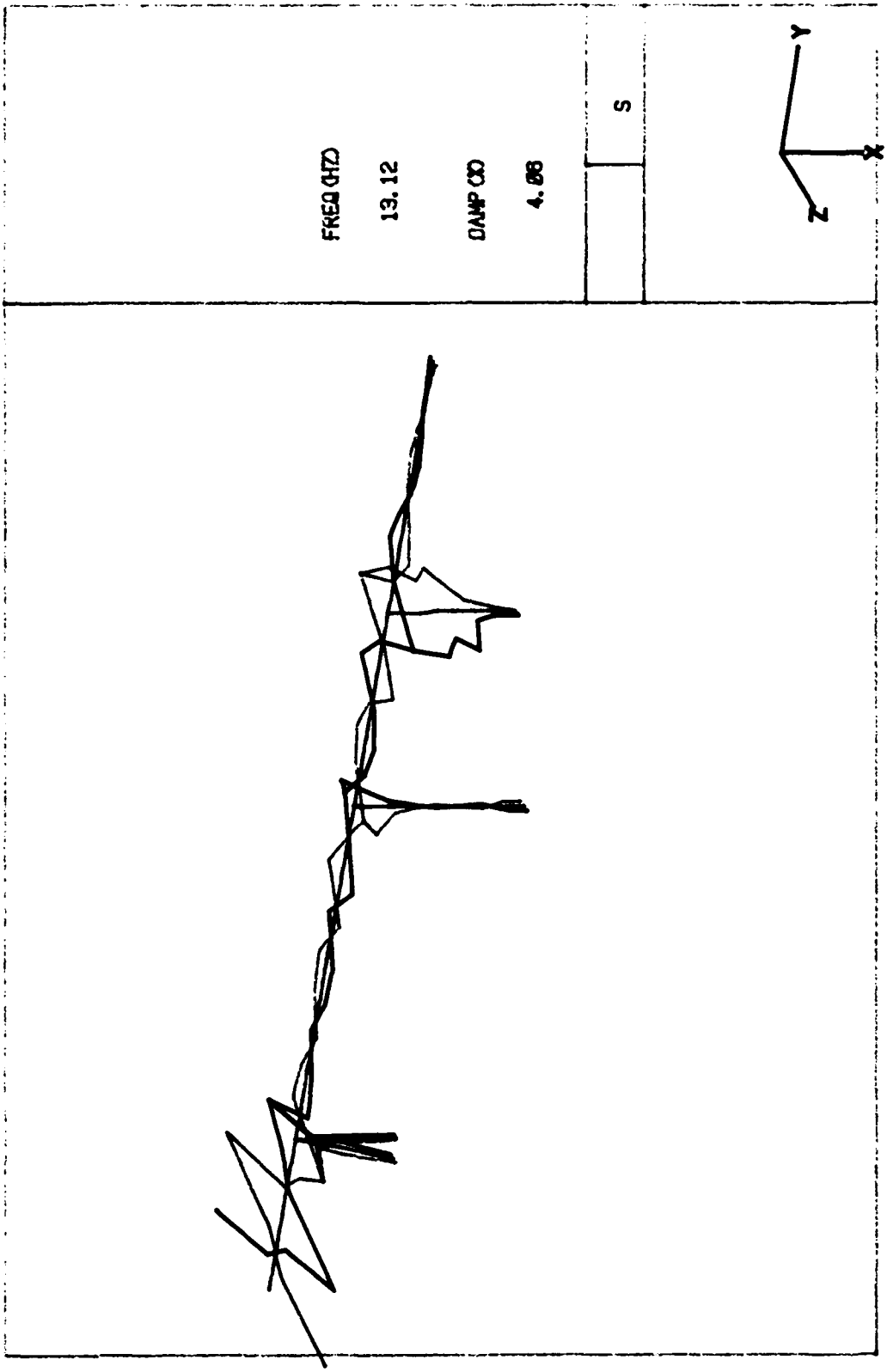

c. 3-D view

Figure 20. (Sheet 3 of 3)

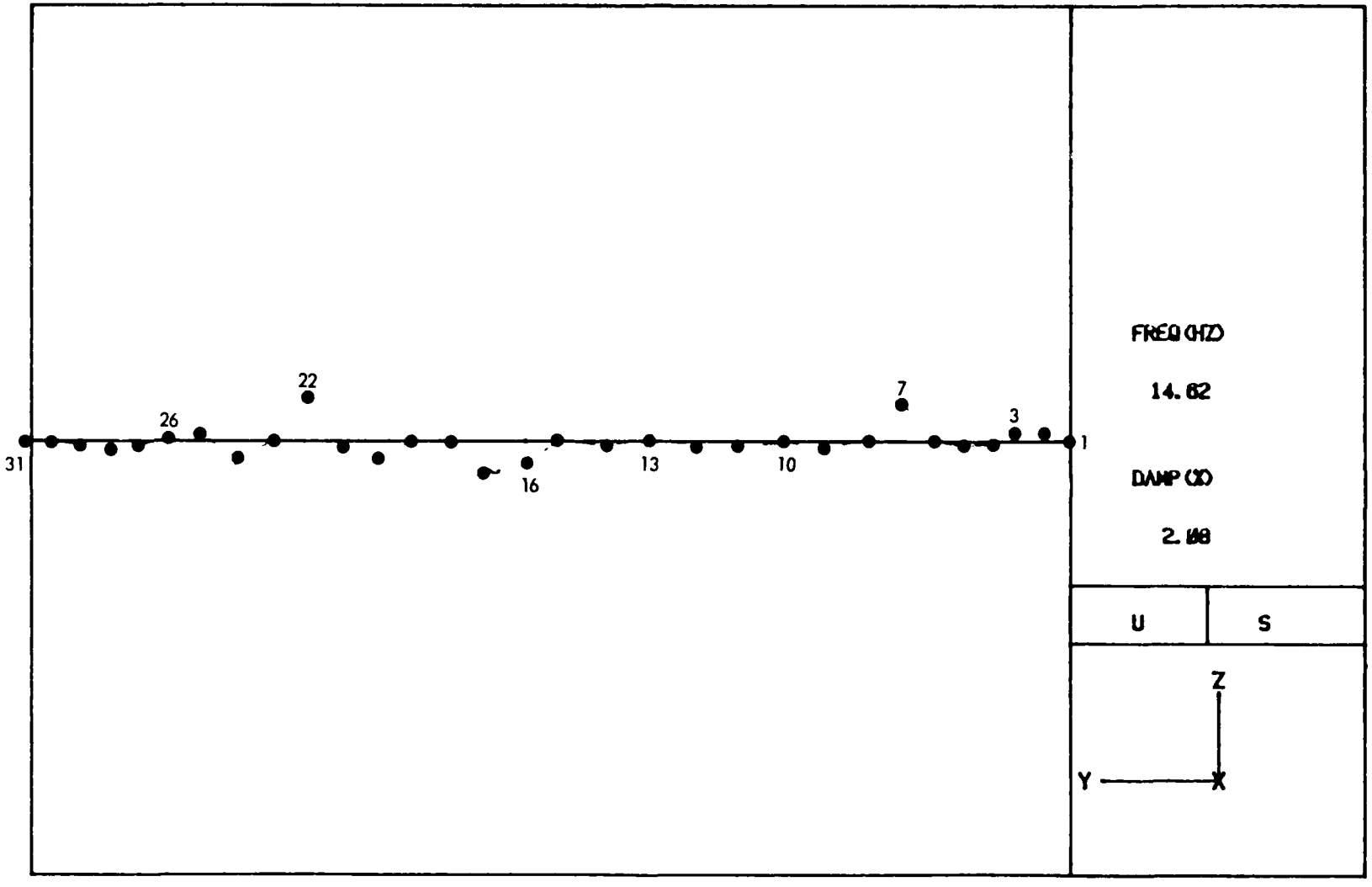

a. Plan view of crest

Figure 21. Mode shape 9 (Sheet 1 of 3)

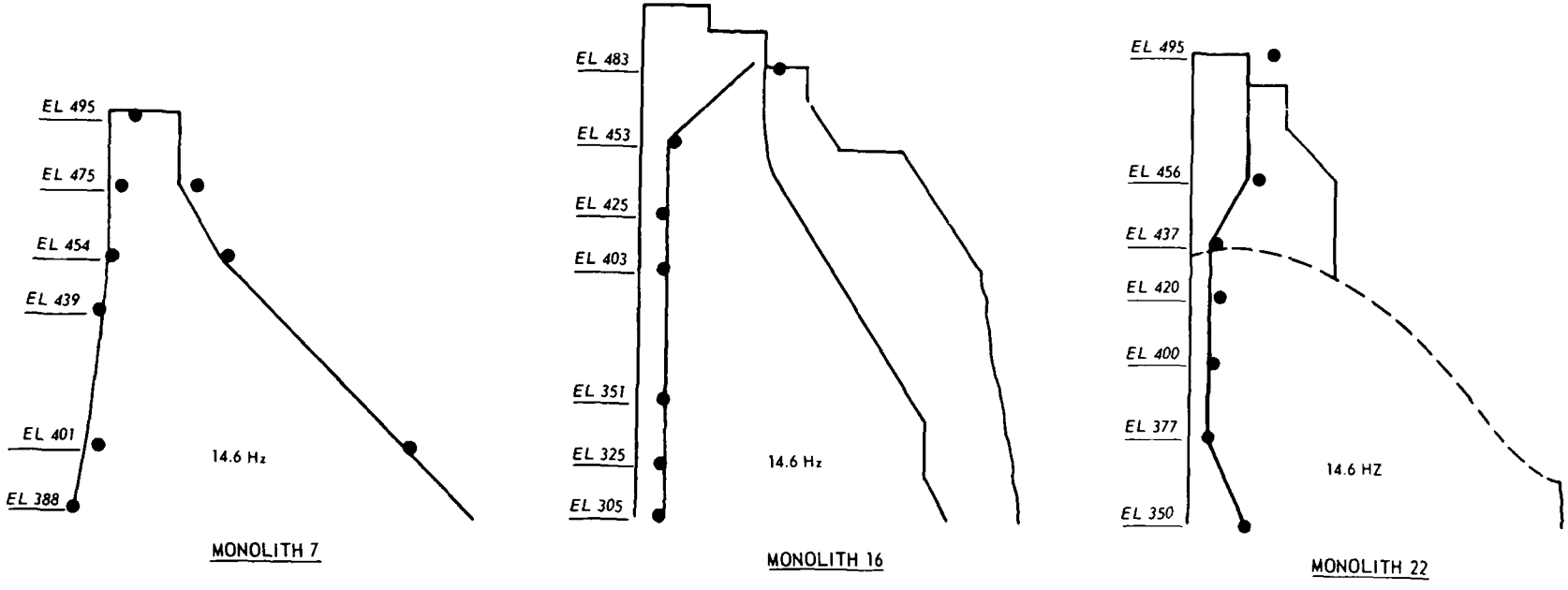

b. Cross sectional views

Figure 21. (Sheet 2 of 3)

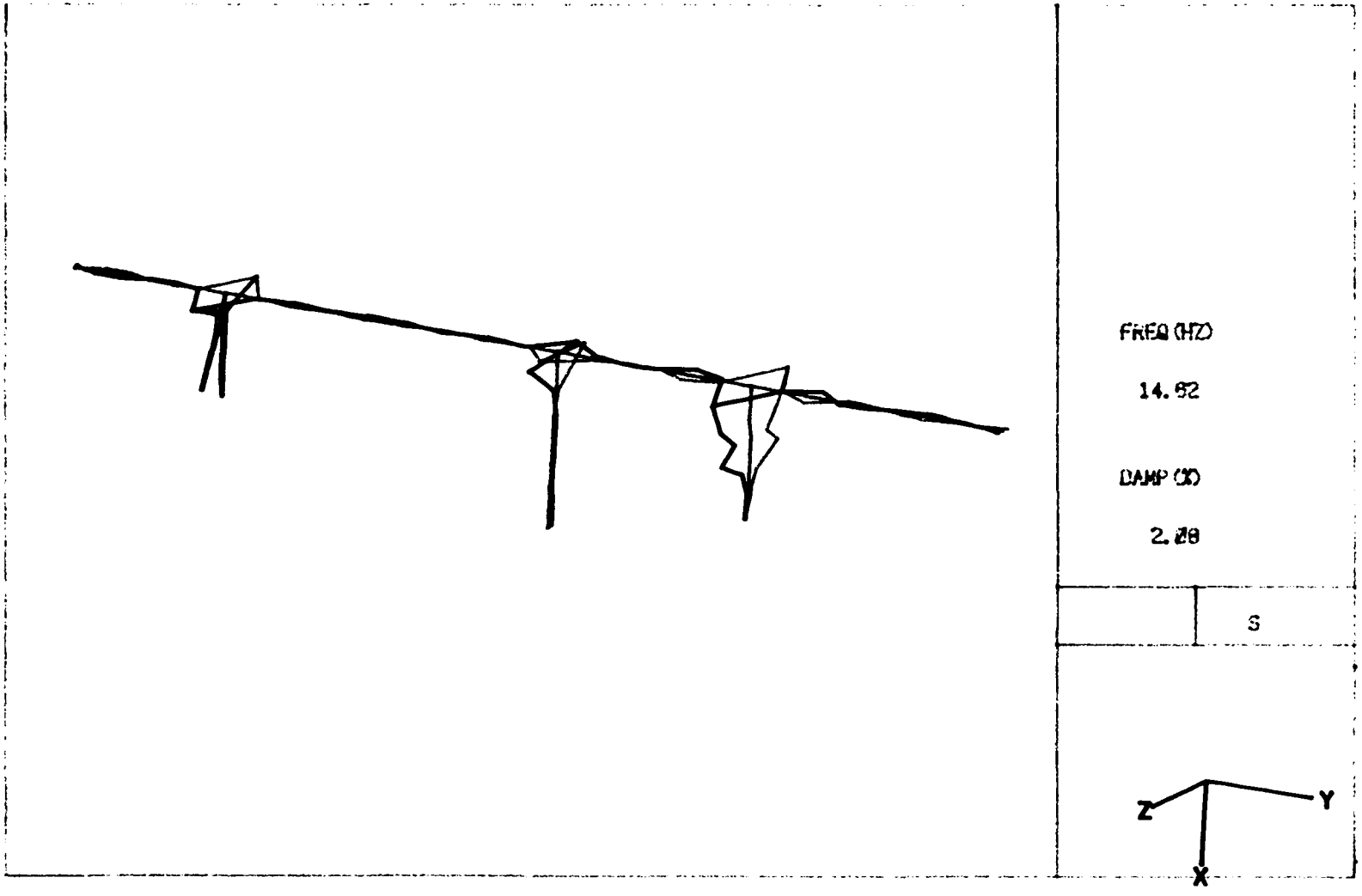

c. 3-D view

Figure 21. (Sheet 3 of 3)

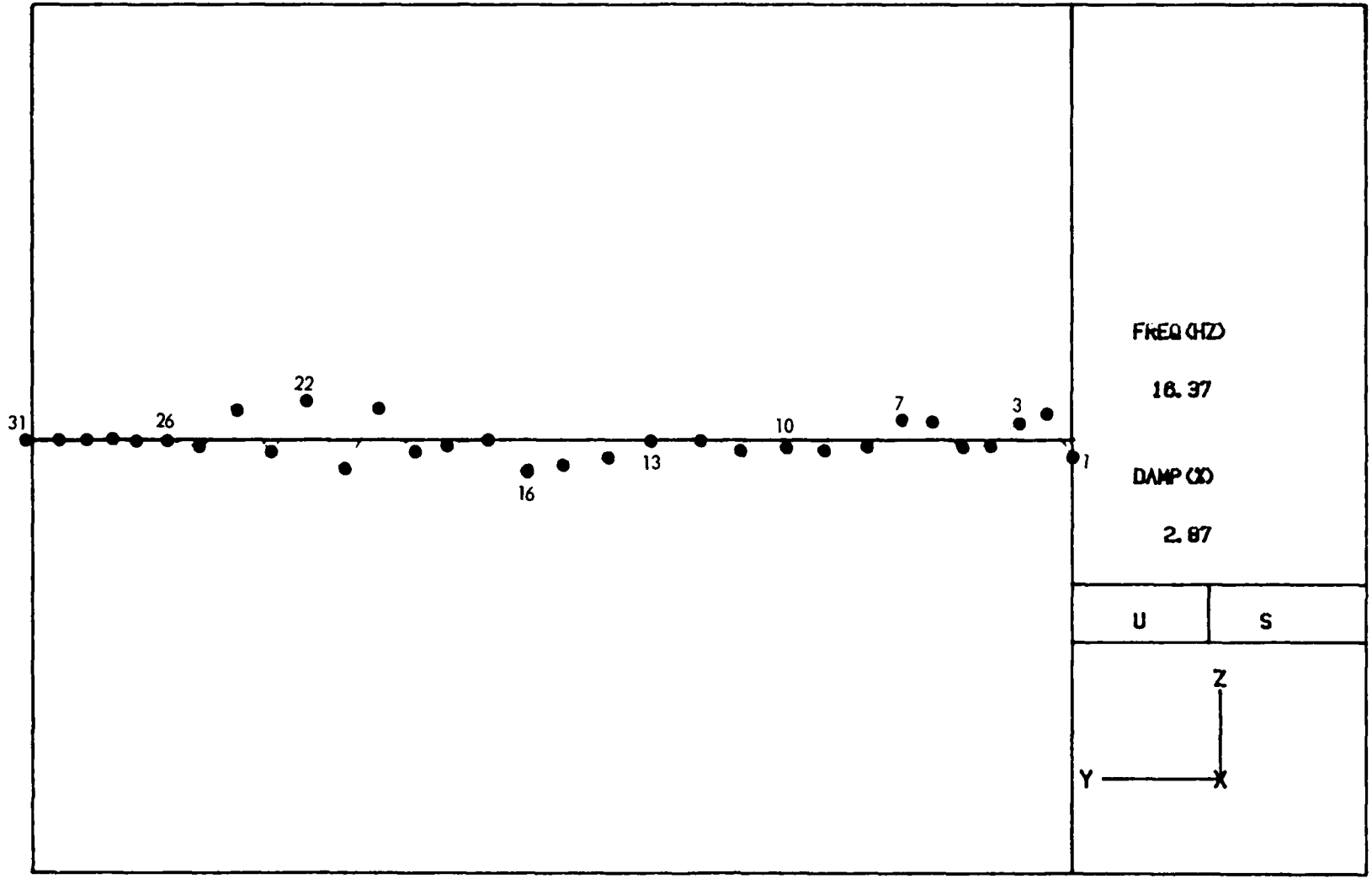

a. Plan view of crest

Figure 22. Mode shape 10 (Sheet 1 of 3)

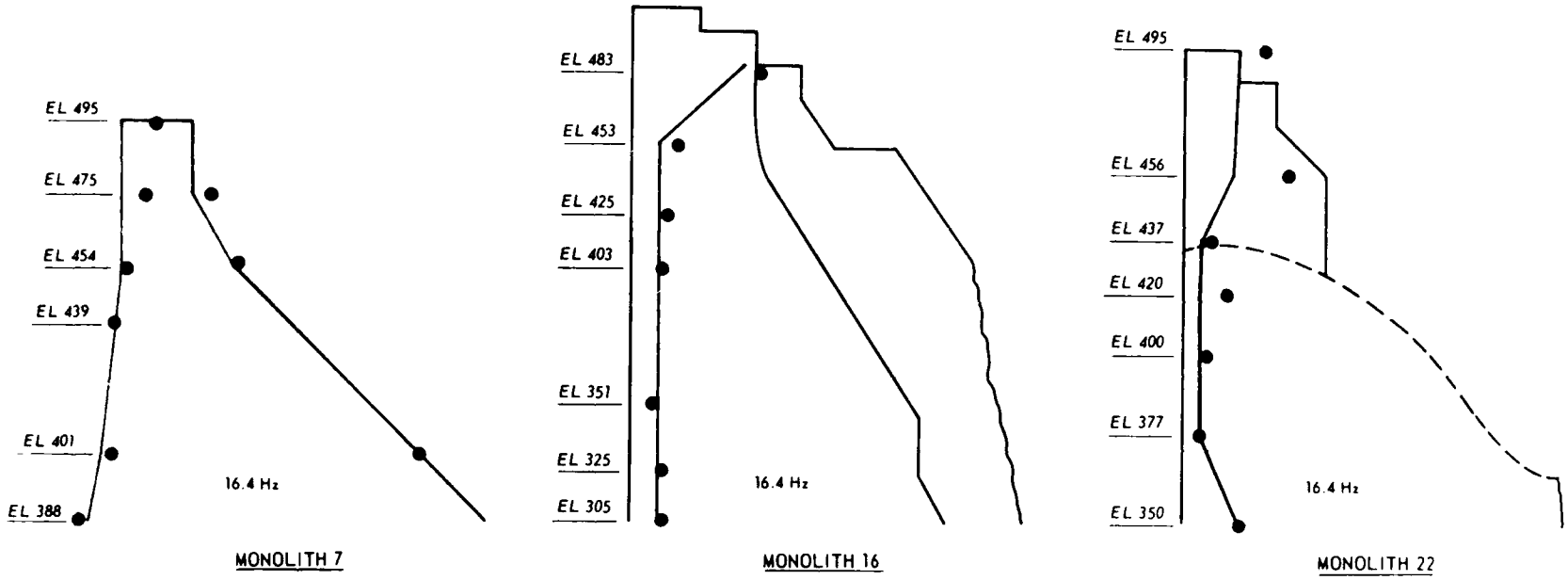

b. Cross sectional views

Figure 22. (Sheet 2 of 3)

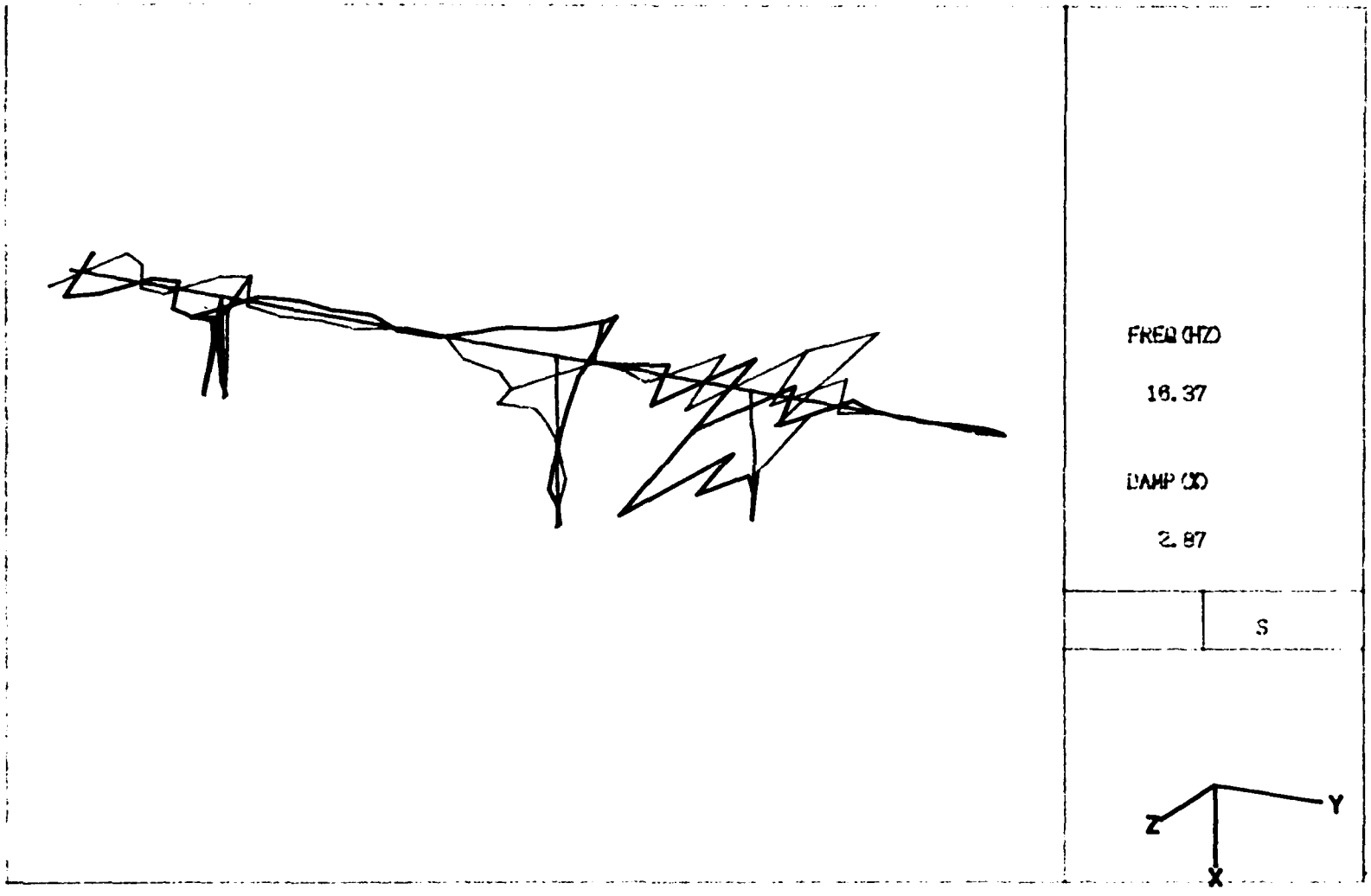

c. 3-D view

Figure 22. (Sheet 3 of 3)

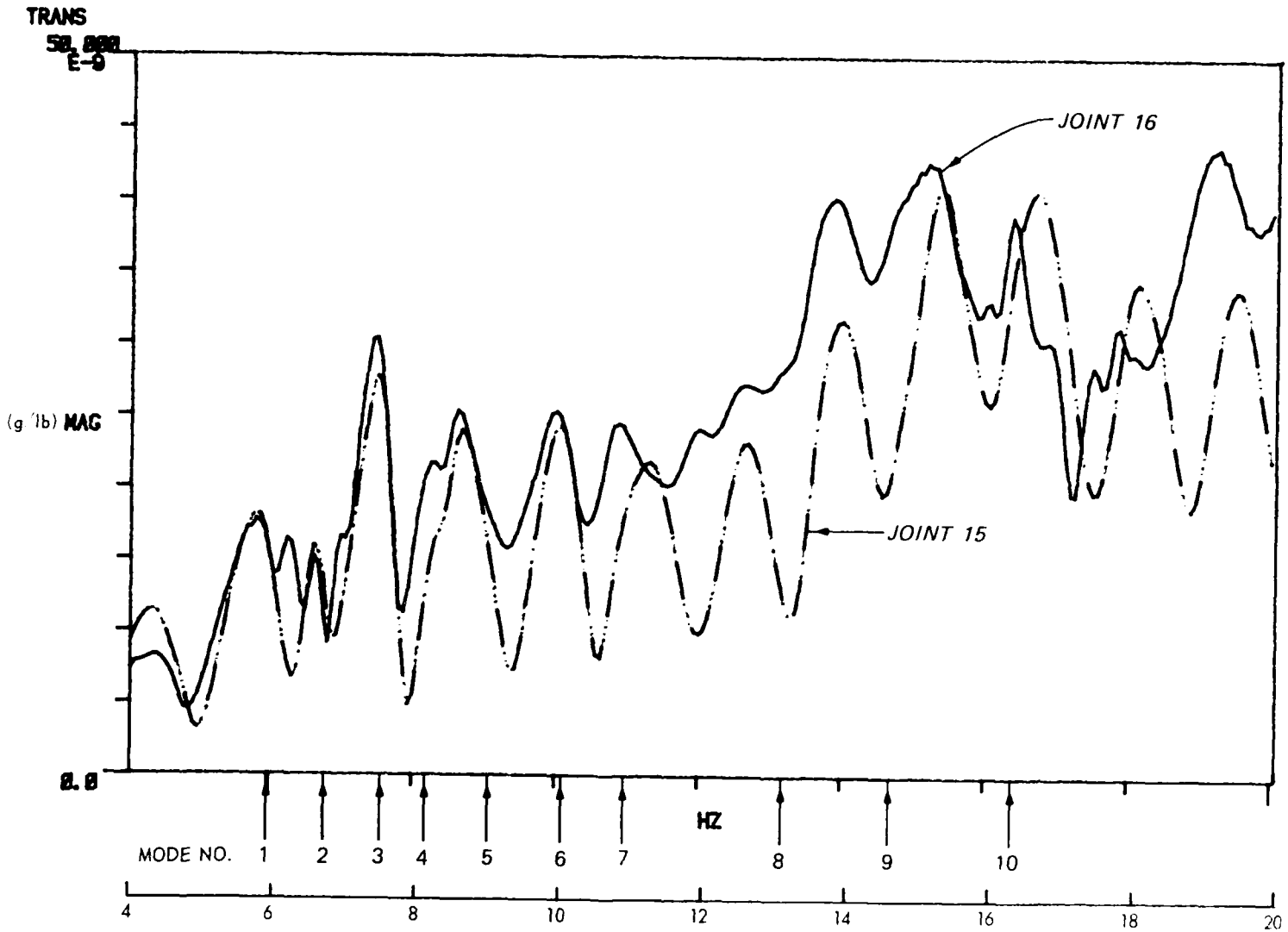

Figure 23. Magnitude of the transfer functions across joint 15-16

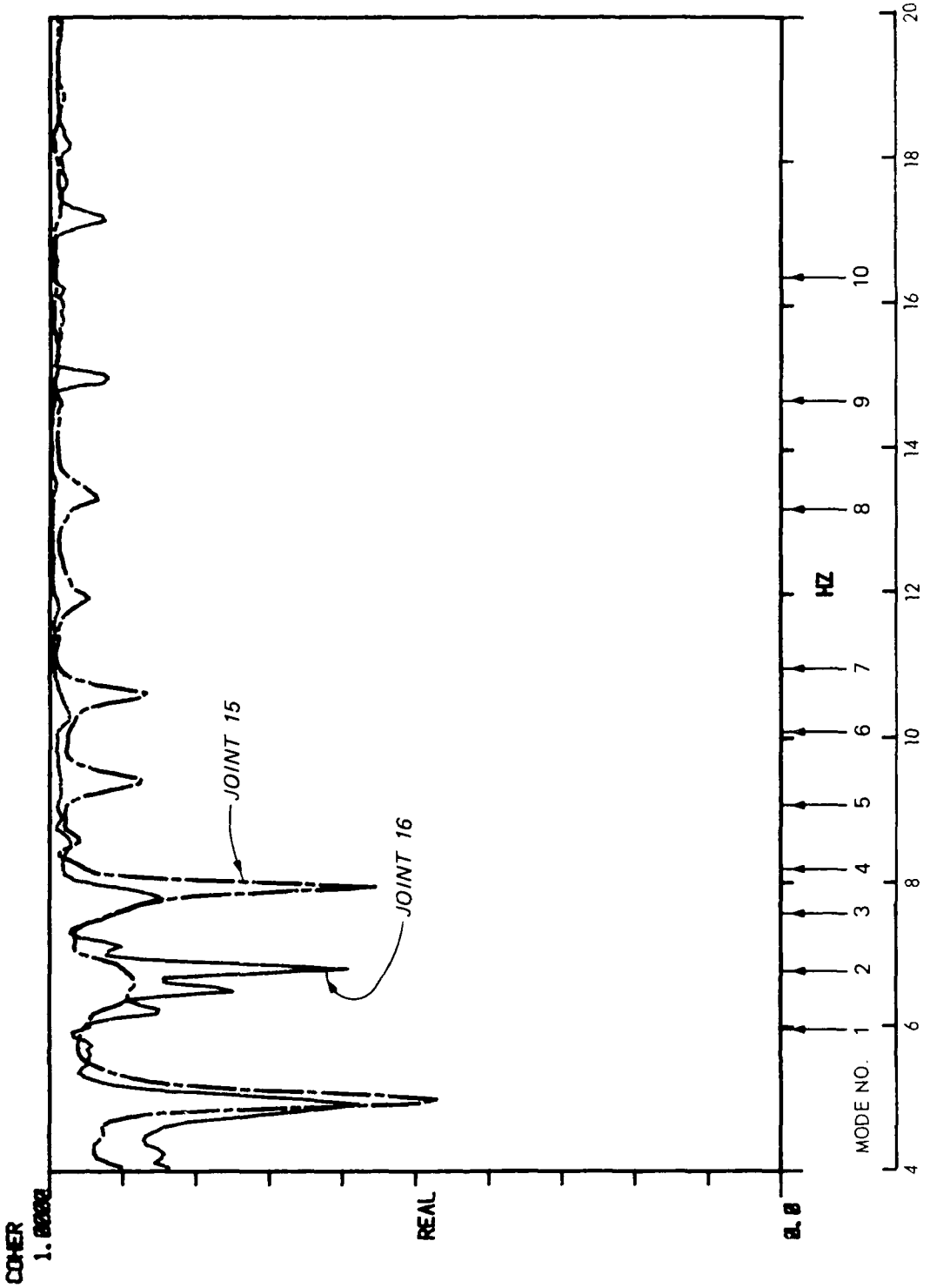

Figure 24. Coherence functions across joint 15-16

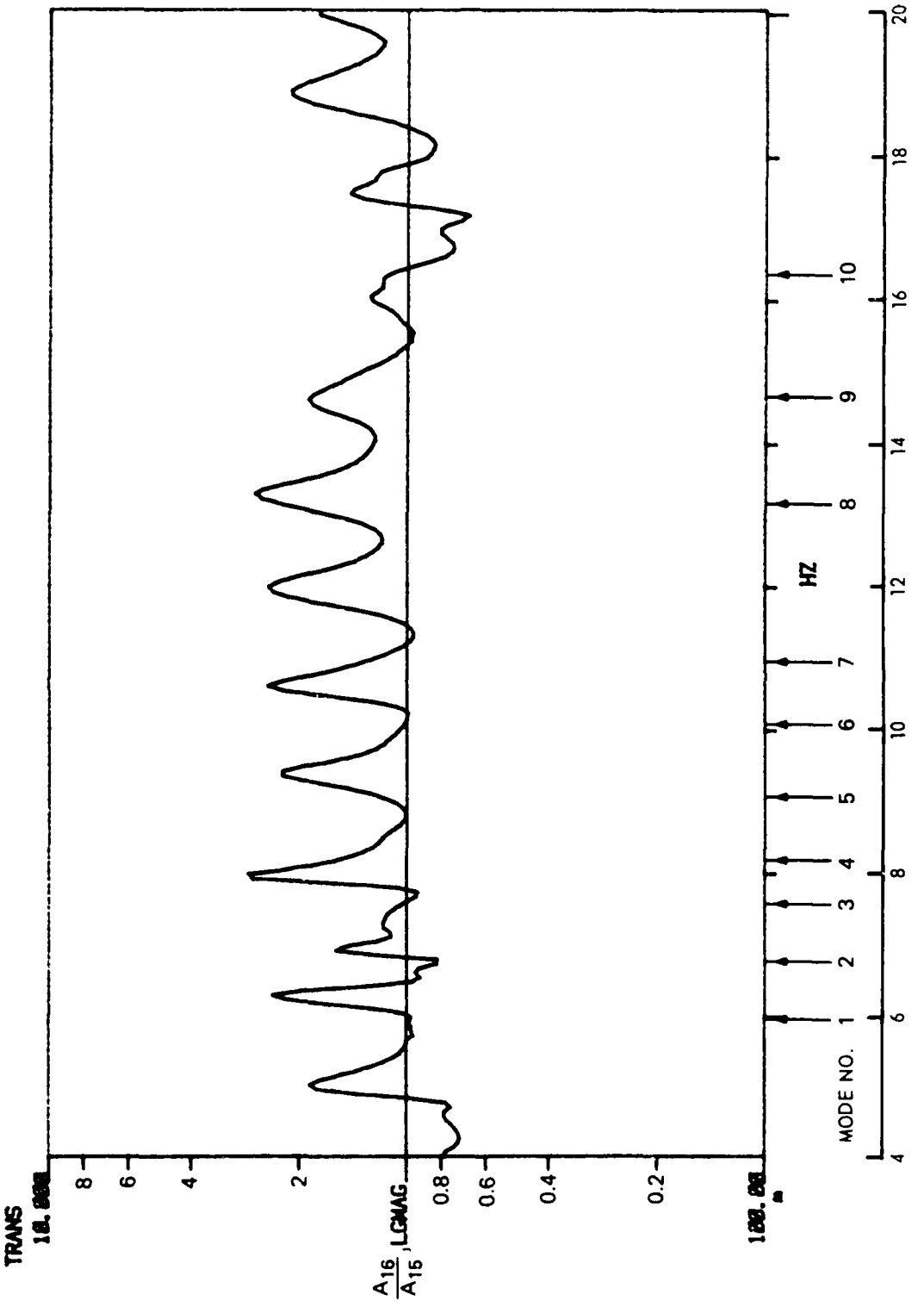

Figure 25. Ratio of acceleration of joint 16 to joint 15

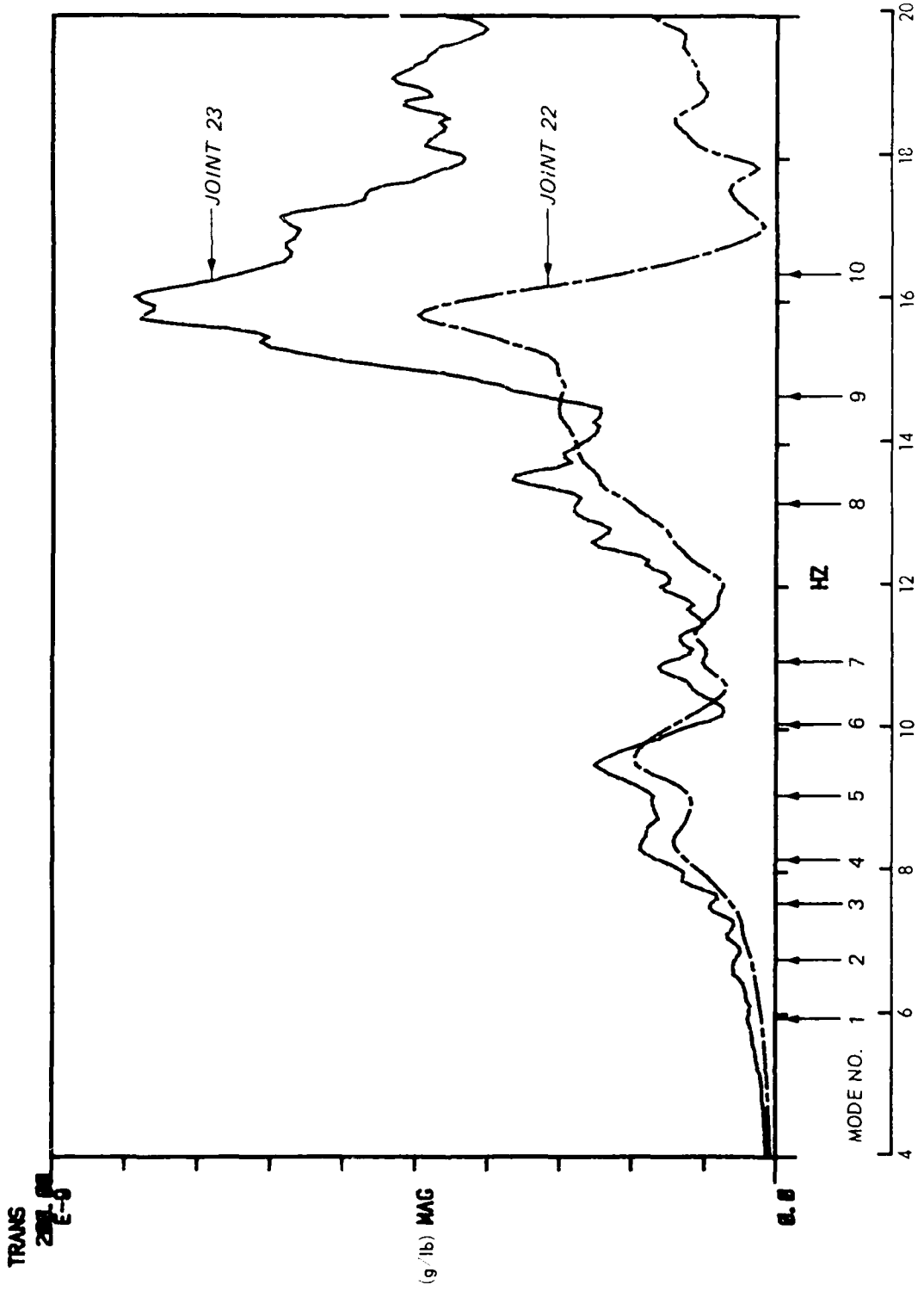

Figure 26. Magnitude of the transfer functions across joint 22-23

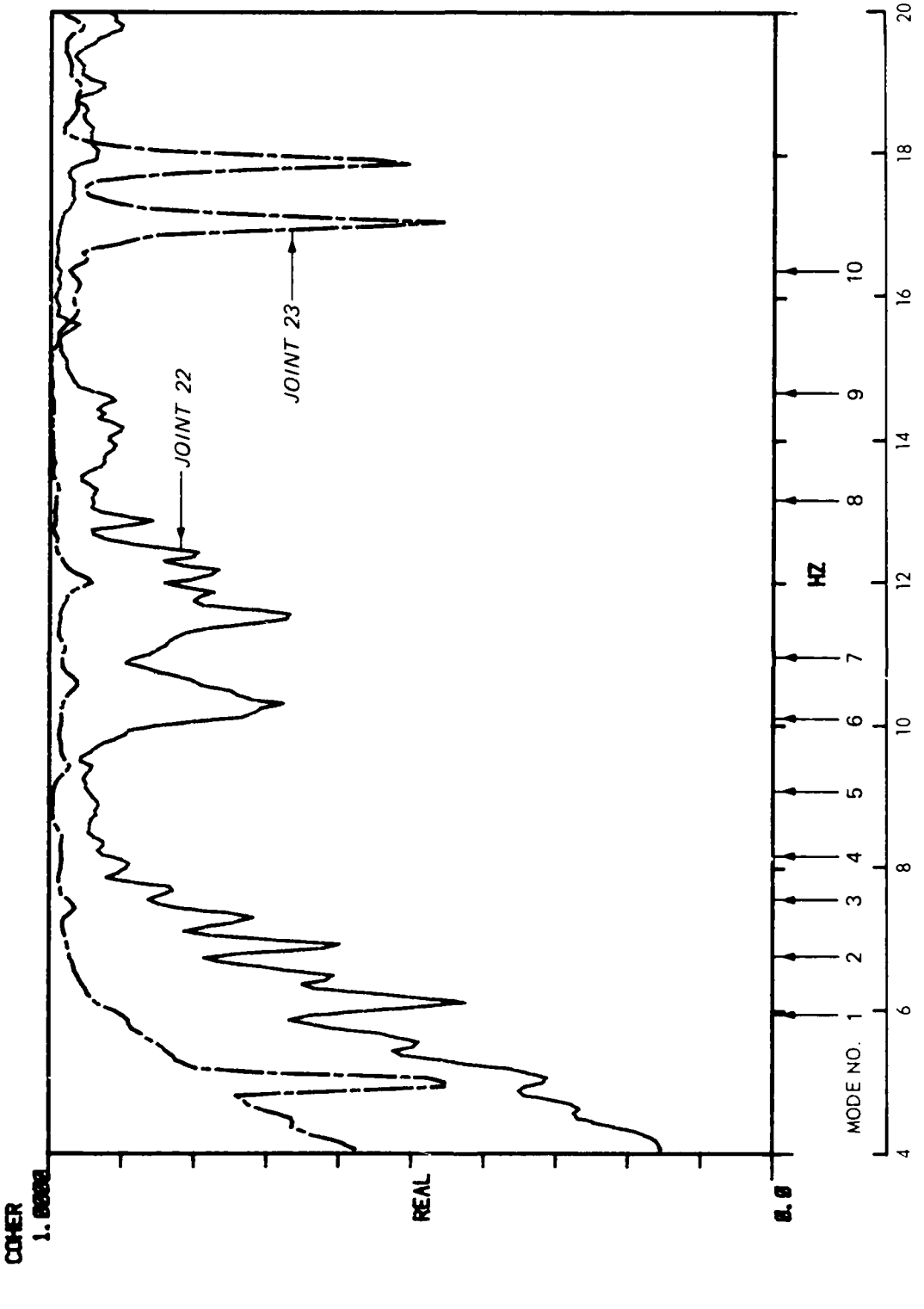

Figure 27. Coherence functions across joint 22-23

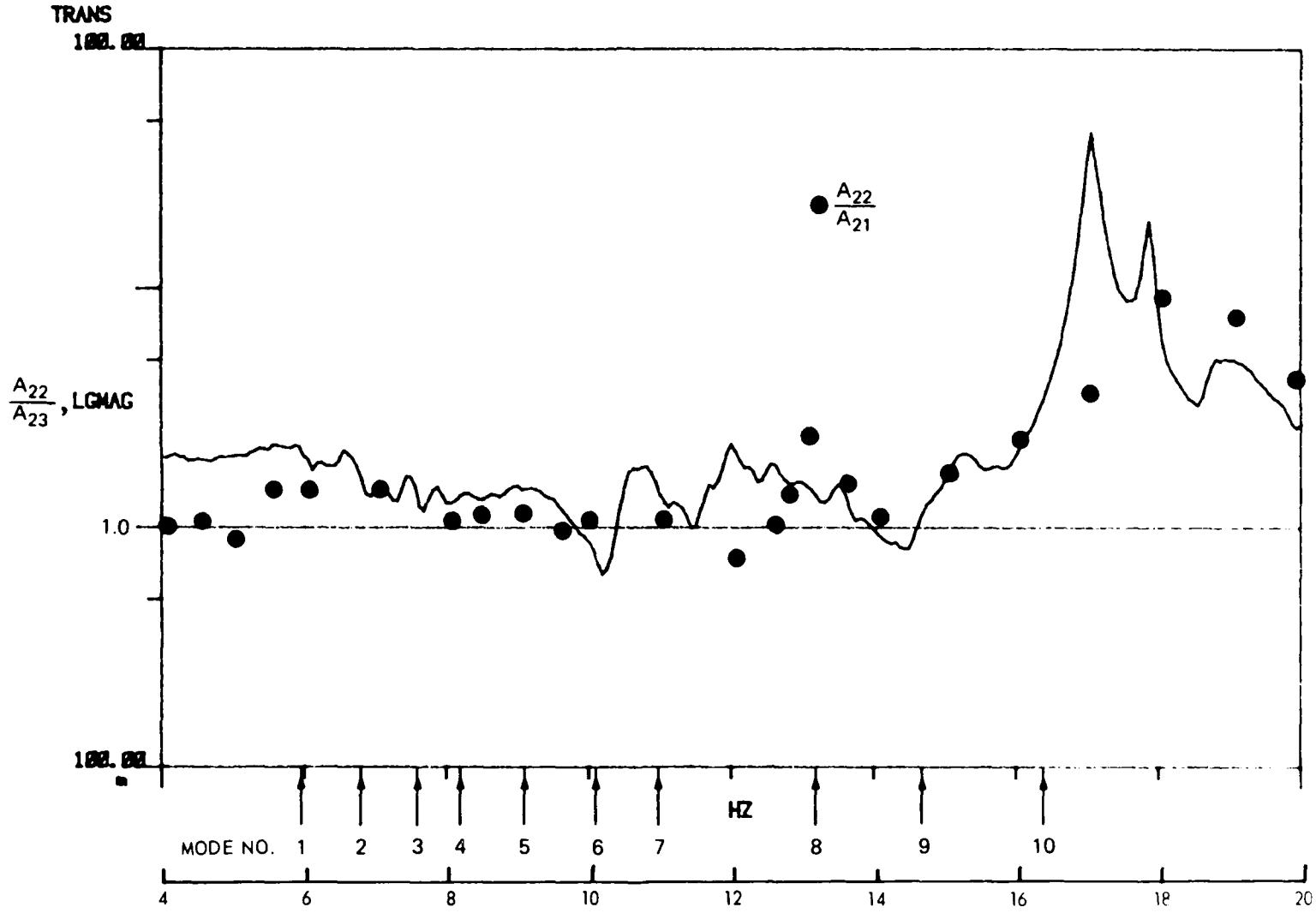

Figure 28. Ratio of acceleration of joints 22 to 23

PART IV: DISCUSSION OF RESULTS

19. In interpreting the foregoing results it should be recognized that the conditions of the dam deviated slightly from the experimentally optimal situation. Earth-moving equipment was being operated 24 hours a day, and there was water flowing through the sluices constantly even though there was no appreciable reservoir water impounded. Finally, there was on-going construction changing minutely the characteristics of certain sections of the dam between tests. However, the data were adequate to conduct a thorough modal analysis. In Table 2 the water levels (headwater and tailwater) are listed for certain tests. These three activities probably contributed some random excitation to the dam in addition to input from disturbances of nonstructural components caused by the controlled input to the dam during the tests. The abutment on the Georgia side was not completed which makes the west edge of the crest of monolith 1 a "free end." The existing grade of the earthen dam on Georgia's abutment monolith 1 was approximately 60 ft (18.3 m) below the crest elevation 495.00. South Carolina's abutment was finished, restraining monolith 32 with an expected degree of fixity.

20. The three mode shapes at 5.94, 6.75, and 7.56 Hz in Figures 13, 14, and 15 correspond to the first three natural modes of vibration found through test and analysis of the Pine Flat Dam (Rea, Liaw, and Chopra 1972). Some discontinuities appear in these lower mode shapes. In Figure 5 notice that the force rolls off at these frequencies. With a lower force input a lower signal-to-noise ratio (SNR) results. A low SNR implies the desired signal is more contaminated by noise than a measurement with a higher SNR. The SNR can be calculated from the coherence function for any frequency as

$$SNR = \frac{\gamma^2(f)}{1 - \gamma^2(f)}$$

where $\gamma^2(f)$ is the amplitude value of the coherence function at frequency f. For instance in Figure 13 the SNR at 10 Hz is only $(0.60)/(1 - 0.60) = 1.5:1$. Thus the apparent anomalies in the shapes could be attributed to noisy data. An undetected natural mode of vibration may exist between 7.6 and 8.1 Hz since mode No. 4 in Figure 16 identified at 8.19 Hz resembles in crest plan a fifth normal mode shape of vibration of a fixed-fixed beam (Shock and Vibration Handbook, ed. Harris and Crede, 1961). It is possible that this mode was not

picked up because the three vibrator locations were nodes of this vibrational shape, or very close mode coupling occurred with the third or fifth mode, such that the resonance for the fourth mode is overshadowed. This mode coupling (very closely spaced resonant frequencies) is prevalent above 8 Hz. The mode shapes at 9.06, 10.06, and 10.94 Hz seem to correspond to the sixth, eighth, and tenth normal mode shapes in crest plan as seen in Figures 17, 18, and 19 of a fixed-fixed beam. Above 11 Hz the spatial density of response points is too sparse to narratively characterize the natural mode shape for the entire dam. The response of the dam above 11 Hz appears to be characterized by resonances of the different monolith sections. For instance the spillway sections have large responses at 13.12, 14.62, and 16.37 Hz but the intake sections are not as responsive at these frequencies, as seen in Figures 20, 21, and 22. Similarly the intake and nonoverflow sections are responsive at some frequencies when the rest of the structure is not. Some nonlinear responses are attributed to the monoliths' joint behavior. The analysis of the relative joint motions reveals this nonlinear behavior. From observing the crest plan view of the mode shape at 5.94 Hz it appears that the spillway sections are the most stiff and the intake sections the most flexible. By observing the first three mode shapes (in Figures 13, 14, and 15) the estimated location of the center of stiffness is between monoliths 11 and 13. The structural damping ratios for the modes shown range from 1.43 to 5.16 percent. These values bound the damping ratios determined from the Pine Flat vibration tests (Rea, Liaw, and Chopra 1972).

21. For most of the frequencies the governing mode shape in cross section resembles the fundamental mode shape of a cantilever beam (Part b of Figures 14-22). Only for monolith 16 does an intermediate node exist above 13.13, as shown in Figures 20b, 21b, and 22b. Consistent with recent conclusions about dam-foundation interaction (Chopra, Chakrabarti, and Gupta 1980) there is motion detectable near the base of each monolith and as expected is less than the response at the crest. The measured mode shapes in the cross sectional views are also consistent with those from the Pine Flat vibration test (Rea, Liaw, and Chopra 1972).

22. The instrumented joints 16-15, 22-21, and 22-23 were monitored close to the input since these joints would have the most relative motion. At joint 16-15 in Figures 23 and 24 the transfer function and the coherence function help explain what physically occurs. The peaks (resonant frequencies)

correlate well in both transfer functions, and above 10 Hz the coherence function is mostly above 0.90. The comparison of the transfer functions reveals that there is some relative motion at resonant frequencies but the slip is very small. The larger relative motion indicated by the ratio of the accelerations of joint 16 to 15 (A_{16}/A_{15}) in Figure 25 generally occurs at nonresonant frequencies. The joint may be acting as a filter dissipating the energy at these frequencies. At frequencies where A_{16}/A_{15} is greater than 1.0 also defines the ratio of two very small motions compared to the resonant responses. Where the coherence function drops smoothly and clearly so as to indicate nonlinear behavior of the joint or the presence of errors small SNR as seen below 10 Hz. The value of A_{16}/A_{15} equal to 1.0 implies no relative joint motion.

23. The joints 22-21 and 22-23 should be expected to behave similarly as these joints are both at a spillway crest. In Figures 26 and 27 the transfer and coherence functions are, respectively, shown for joint 22-23. Again the peaks occur at the resonant frequencies. Below 10 Hz the coherence functions are decreasing indicating decreasing SNR. However, at 17.0 and 17.8 Hz there are two smooth drops in the coherence function for joint side 23, and the transfer functions reveal large differences in responses. This may indicate constant relative joint motion above 15 Hz. The two nulls in the coherence function at 17.0 and 17.8 Hz correlate with the indication of two frequencies where joint slippage is most excited. The ratio of A_{22}/A_{23} shows a similar plot in Figure 28 where above 15 Hz there is the greatest measure of relative joint motion.

Discussion of Dynamic Cylinder Tests

24. The dynamic testing of the standard 6- by 12-in. (152- by 305-mm) concrete cylinders provided a measure of the material damping of the dam's concrete. In Table 3 it is seen that the material damping ratios range from 0.315 to 0.537 percent. The damping ratios of the dam determined from the modal analysis represent the combined effects of boundary and material damping. Thus, the effects of the boundary conditions (the supports: foundation and abutments) are greater than the effects of material damping. This is consistent with a previous analytical study (MacBain 1972).

Comparison to Previous Analysis

25. Previously a 2-D dynamic finite element (FE) analysis was conducted on the modified geometry of the nonoverflow monolith to compute the fundamental frequency (Norman 1979). The analysis assumed no reservoir with the height of the monolith at 185 feet. A value of 7.63 Hz was obtained compared to 5.94 Hz identified as the fundamental frequency of the prototype structure. This difference is expected and the value of the 2-D FE analysis would differ for the following reasons: (1) Foundation interaction is not accounted for in the 2-D FE analysis. The foundation interaction decreases the frequency (Norman and Stone 1979). (2) The elastic modulus in the 2-D FE analysis was a static value. Under low level dynamic conditions the modulus increases, thus both the stiffness and the frequency increase. (3) The 3-D FE behavior is shown to be stiffer than the 2-D FE behavior of Pine Flat Dam for the fundamental frequency and the frequency increased (Rea, Liaw, and Chopra 1972). The 3-dimensional response is expected to differ from the 2-dimensional finite element analysis. In the case of Pine Flat Dam, the 3-D response was stiffer in the fundamental mode than the 2-D. The effect in Russell Dam is not necessarily the same since Pine Flat and Russell Dams do not have geometrically similar boundary conditions.

26. Other factors would also cause a difference. One factor also not accounted for in the 2-D model is the relative joint motion between monoliths. Relative joint motion is a nonlinear behavior and it may increase the flexibility of the system.

Structural Integrity of Richard B. Russell Dam

27. As discussed previously, the dam's natural frequencies, damping ratios, and the mode shapes are consistent with design analyses and the dynamic properties determined from the Pine Flat prototype vibration test. Therefore, the dam appears to be structurally sound as built.

PART V: CONCLUSIONS

28. The low level vibration test of Richard B. Russell Dam has shown that the electrohydraulic shaker is adequate to excite the structure with measurable vibrations. Also, the use of a structural dynamics analyzer is a very efficient tool to both digitize and analyze the data to compute the dynamic properties.

29. The natural frequencies, damping ratios, and mode shapes determined are reasonably consistent with design analyses. The natural frequencies for the 10 mode shapes investigated expectantly ranged from 5.97 to 16.4 Hz. The damping ratios ranged from 1.43 to 5.16 percent which bounds the values from the Pine Flat vibration tests (Rea, Liaw, and Chopra 1972).

30. The first seven shapes of the dam resemble in crest plan the first three, fifth, sixth, eighth, and tenth normal mode shapes of a fixed-fixed beam. The governing mode shape for monoliths 7 (tallest nonoverflow), 16 (spillway transition), and 22 (spillway) at the resonant frequencies investigated resembled the fundamental mode shape of a cantilever beam. The tallest section, monolith 16, also revealed a mode shape at 14.6 and 16.4 Hz resembling the second normal mode of a cantilever beam.

31. Relative joint motions exist and are a function of the excitation frequency. Similar behavior was observed between joints 16-15 and the spillway crest joints 22-21 and 22-23. There appears to be a filtering effect between resonant frequencies at joint 16-15 and little relative movement at the resonant frequencies below 15 Hz. However, above 15 Hz (actually 15-20 Hz) there is larger relative motion between monoliths 21, 22, and 23 at the spillway crest than at joint 16-15. The nonlinear behavior of the dam is attributed mostly to the monoliths' joint behavior.

32. Since the dynamic properties (natural frequencies, damping ratios, and mode shapes) determined are reasonable and contain no gross anomalies, the dam appears to be structurally sound as built.

PART VI: FUTURE WORK

FY 83

33. Dynamic finite element analyses are planned to study the 2-D and 3-D behavior of the dam. The "as tested" prototype structural conditions are to be modeled. These dynamic analyses will check their validity when compared to the prototype test results. The foundation interaction effects studied will be used also as a check and compared to the prototype test results.

34. The mode shapes that have been obtained will provide good comparisons to 2-D and 3-D and dynamic finite element modeling.

FY 84

35. The second vibration test of the dam will be conducted with a full reservoir. From Table 2 it seems also the temperatures during tests were moderate which implies there is no need to conduct comparison vibration tests only during the month of February. However, when a vibration test is conducted with the reservoir impounded it is more desirable to choose a period when the pool water elevations will not change significantly. At that time it may be possible to determine mode shapes of certain sections by just measuring the accelerations caused by the ambient noise.

FY 85

36. The second test will be analyzed with a dynamic FE model including the hydrodynamic interaction. Also, the second vibration test will provide another measure of the dam's dynamic properties after the reservoir is filled. Hence largely the effect of hydrodynamic interaction will be measured.

REFERENCES

Alexander, A. Michel. 1981. "Development of Procedures for Nondestructive Testing of Concrete Structures; Feasibility of Impact Technique for Making Resonant Frequency Measurements," Miscellaneous Paper C-77-11, Report 3, U. S. Army Engineer Waterways Experiment Station, CE, Vicksburg, Miss.

Bendat, Julius S., and Piersol, Allan G. 1980. Engineering Applications of Correlation and Spectral Analysis, A Wiley-Interscience publication.

Chopra, Anil K., Chakrabarti, P., and Gupta, Sunil. 1980. "Earthquake Response of Concrete Gravity Dams Including Hydrodynamic and Foundation Interaction Effects," Report No. UCB/EERC-80/01, University of California, Berkeley, Calif.

Hewlett-Packard Company. 1982. "Notes from HP5423A User's Training Course," Structural Dynamics, Measurement and Analysis, Linear Theory.

_____. 1981. 5423A Structural Dynamics Analyzer Users Guide.

MacBain, James Carter. 1972. "Response of Materially Damped Timoshenko Beams Condidering Damped Flexible Supports," A Thesis submitted to the Faculty of Purdue University in partial fulfillment of the requirements for the Degree of Doctor of Philosophy.

Norman, C. Dean. 1979. "Earthquake Analysis of the Modified Geometry of the Concrete Nonoverflow Section, Richard B. Russell Dam," Technical Report SL-79-14, U. S. Army Engineer Waterways Experiment Station, CE, Vicksburg, Miss.

Norman, C. Dean, and Stone, Harry E. 1979. "Earthquake Analysis of the Gravity Dam Monoliths of the Richard B. Russell Dam," Technical Report SL-79-8, U. S. Army Engineer Waterways Experiment Station, CE, Vicksburg, Miss.

Rea, D., Liaw, C. Y., and Chopra, A. K. 1972. "Dynamic Properties of Pine Flat Dam," Report No. EERC72-7, University of California, Berkeley, Calif.

Richardson, M. H. 1980. "Detection of Damage in Structures from Changes in Their Dynamic (Modal) Properties - A Survey," NUREG/CR-1431, UCRL-15103, RJ, RM, RN, RO, prepared by Lawrence Livermore Laboratory, Livermore, Calif., for Division of Reactor Safety Research, Office of Nuclear Regulatory Commission, Washington, D. C., NRC FIN No. A0128.

Shock and Vibration Handbook. 1961. C. N. Harris and C. E. Crede, eds, McGraw-Hill.

U. S. Army Engineer Waterways Experiment Station, CE. 1949. "Method of Test for Fundamental Transverse, Longitudinal, and Torsional Frequencies of Concrete Specimens," CRD-C 18-59, Handbook for Concrete and Cement (with quarterly supplements and revisions), Vicksburg, Miss.

Table 1

Equipment List

Accelerometer	SDC, Q-FLEX Model QA1000 sensitivity, volts/g....0.25
Amplifiers	Built by ISD, WES phase compensated
Tape recorder record playback	 Sangamo Sabre V Sangamo
Electrohydraulic vibrator (horizontal mode)	Zonic, ZTL electro hydraulic servo control Driving Mass....17,000 lb-mass (7,711 kg) Dynamic force (pk sinusoidal) lb- force used - 20,000 lb (88.96 kN) Frequency range, HZ 1 - 25 HZ total harmonic distortion 25% Operating pressure 3000 psi (20.67 MPa)
Hydraulic power supply	Pump capacity - 70 gpm driven by a 150 hp, 3 phase, 440 v motor
Generator	Diesel Caterpillar 3306T, 150 KW set, Ser. No. 66D41617
Digital processor and modal analyzer	HP 5423A Structural Dynamics Analyzer

Table 2

Recorded Temperatures and Water Levels During Tests

Test No.	Date	Temperature °F at Test Time	Exciter Monolith	Water Elevations, ft Headwater	Tailwater
1	1/30/82	67	7	--	--
2	1/30/82	60	7	--	--
3	2/1/82	50	7	--	--
5	2/7/82	50	7	349.8	330.8
6	2/7/82	52	7	349.8	330.8
7	2/10/82	43	16	342.0	332.0
8	2/13/82	60	16	340.9	331.9
9	2/15/82	60	16	340.9	332.0
11	2/19/82	55	22	352.5	332.5
12	2/20/82	69	22	--	--
15	2/21/82	71	22	333.0	332.7
16	2/21/82	71	22	333.0	332.7
			Average =	342.7	331.9
				±7.48	±0.76
			Coefficient of variation:	C_v = 0.02	0.002

Table 3

Frequency and Damping Measurements on 6" by 12" Concrete Cylinders from Richard B. Russell Dam

Design Strength ksi	Design Strength KPa	Cylinder No.	Position*	Frequency HZ	Dynamic Modulus $\times 10^6$ psi	Dynamic Modulus $\times 10^6$ KPa	Damping Ratio %
4.0	27.6	5037	1	4023	5.59	38.5	0.331
3.0	20.7	5464	1	3953	5.40	37.2	0.330
		5464	2	3978	5.46	37.6	0.315
3.0	20.7	5166	1	4167	5.82	40.1	0.537
		5166	2	4133	5.84	40.2	0.391
		5166	3	4088	5.77	39.8	0.339
2.0	13.8	4954	1	3643	4.58	31.6	0.366
		4954	2	3611	4.50	31.0	0.380
2.0	13.8	5833	1	3625	4.54	31.3	0.364

Results from Uniaxial Compression Test

Cylinder No.	Poisson's Ratio	Initial Elastic Concrete Modulus 10^6 psi	Initial Elastic Concrete Modulus 10^6 KPa	Uniaxial Compressive Strength ksi	Uniaxial Compressive Strength KPa	Date Cast	Date Tested
5037	0.21	4.67	32.2	6.36	43.8	5 Mar 81	6 May 82
5166	0.20	4.91	33.8	5.86	40.1	20 Mar 81	6 May 82
5464	0.18	4.51	31.1	5.68	39.1	8 May 81	6 May 82
4954	0.20	3.44	23.7	3.45	23.8	25 Feb 81	6 May 82
5833	0.19	3.50	24.1	3.40	23.4	17 Jul 81	6 May 82

Cylinder No.	Initial Concrete Elastic Modulus E_{static} ($\times 10^6$ psi)	Initial Concrete Elastic Modulus $E_{dynamic}$ ($\times 10^6$ psi)	% Increase
5037	4.67	5.59	20
5166	4.91	5.89	18
5464	4.51	5.43	20
4954	3.44	4.54	32
5833	3.50	4.54	29
		Total	119

119/5 = 23% average increase

$E_{dynamic}/E_{static} = 1.23$

Note: All cylinders were removed from fog room on 23 Feb 83.

* Rotating specimens produced some scatter in the frequency and damping values. Some of the specimens were slightly ovate.

Table 4

Frequency and Damping Values

for First 10 Mode Shapes

MODE NO.	FRE-QUENCY Hz	DAMPING %
1	5.937	4.286
2	6.750	2.068
3	7.562	3.114
4	8.187	1.430
5	9.062	5.158
6	10.062	2.344
7	10.937	4.132
8	13.125	4.064
9	14.625	2.078
10	16.375	2.870

APPENDIX A: TRANSFER AND COHERENCE FUNCTIONS

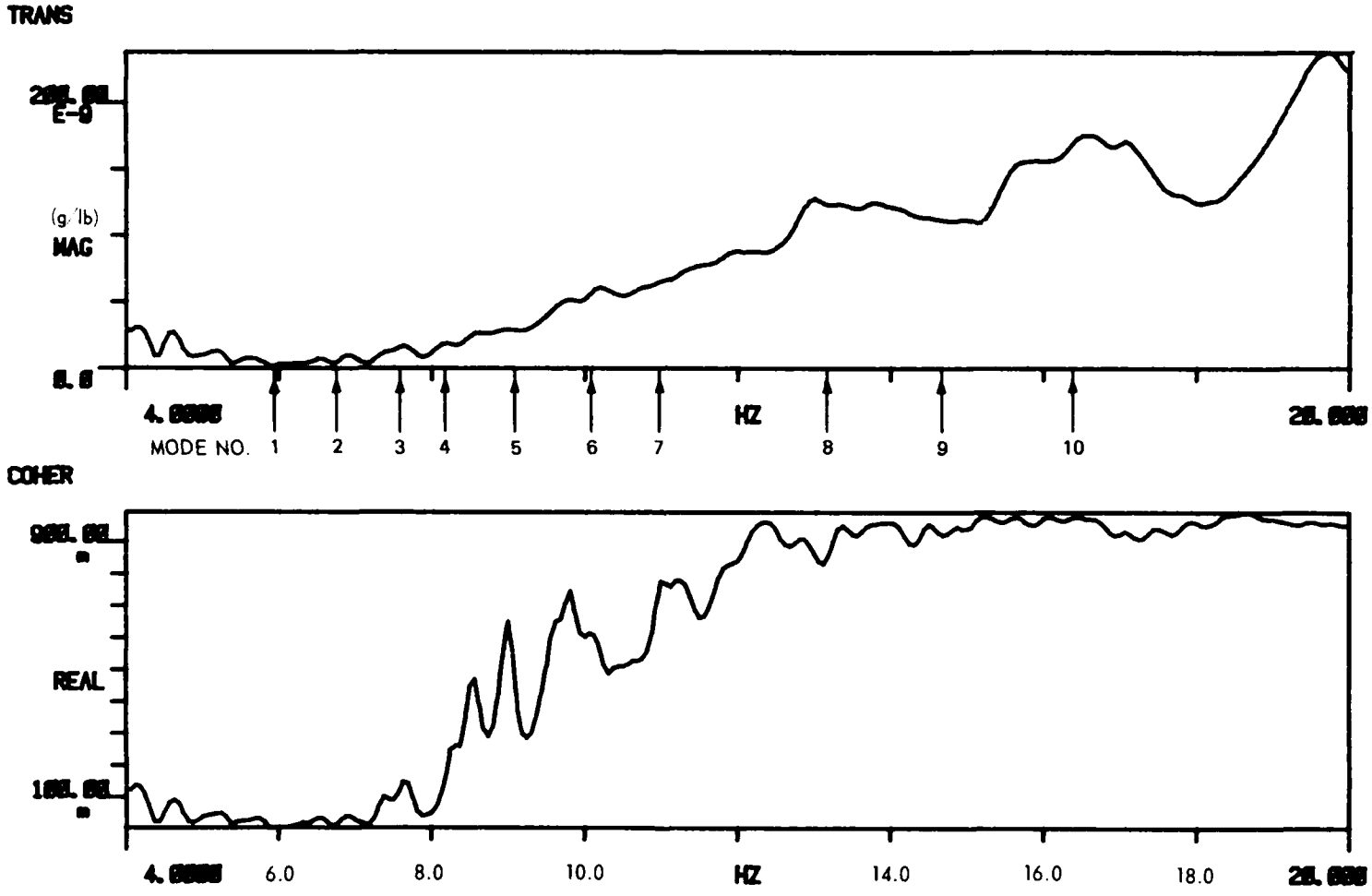

Transfer and coherence function: input-monolith 7(1-7), output-monolith 1(0-1); el 495

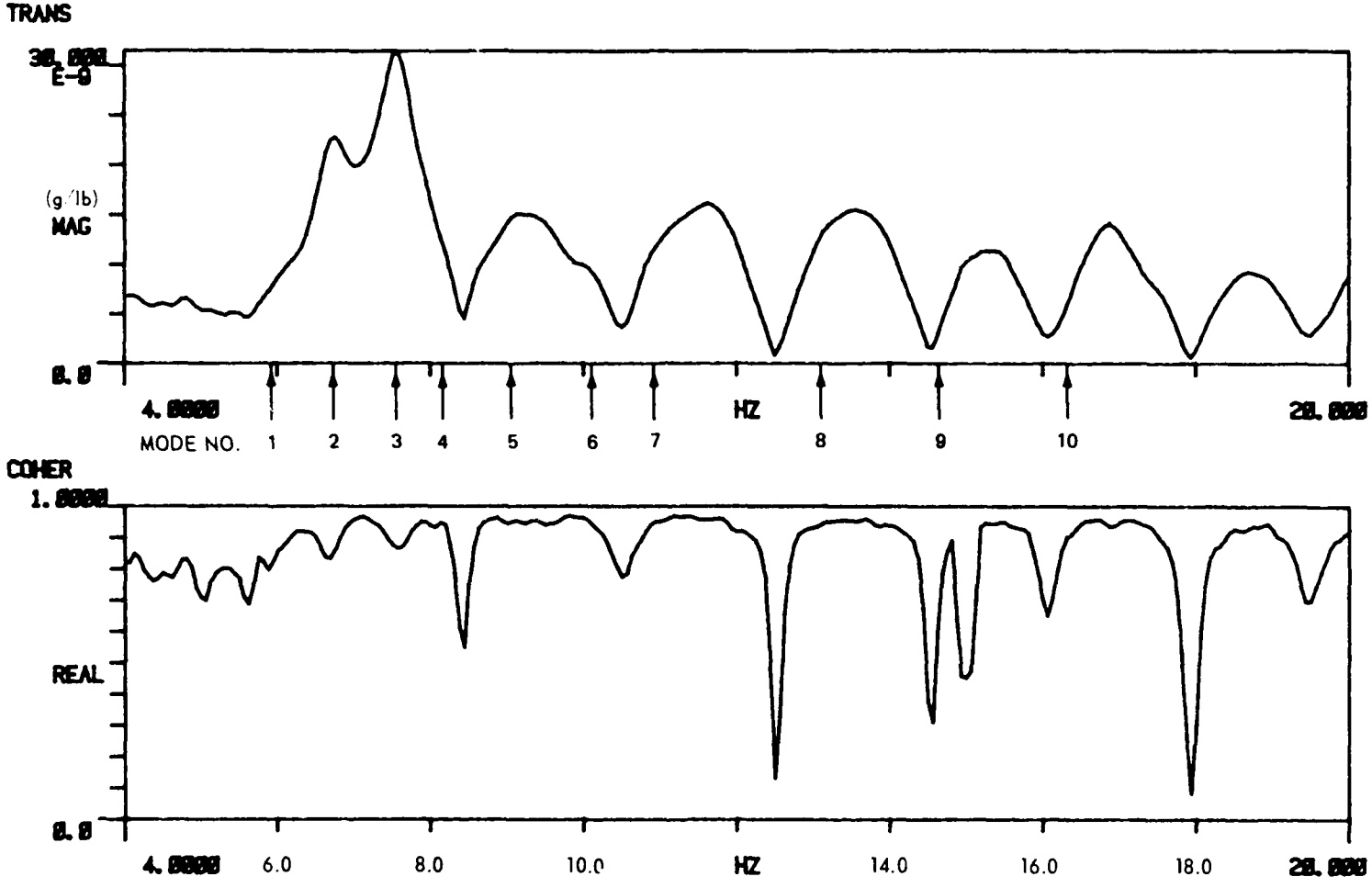

Transfer and coherence function: I-16, O-8; el 495

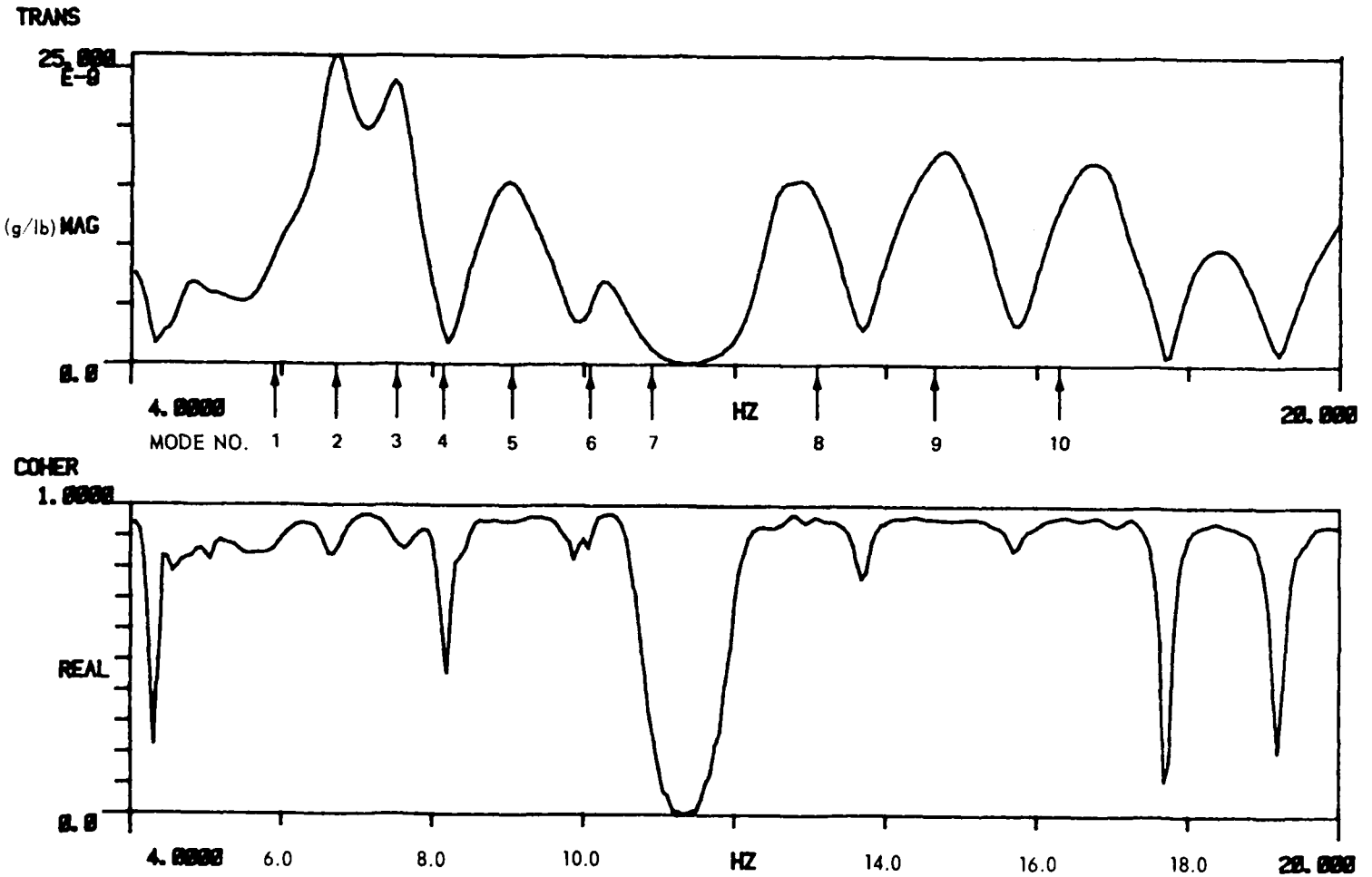

Transfer and coherence function: I-16, O-9; el 495

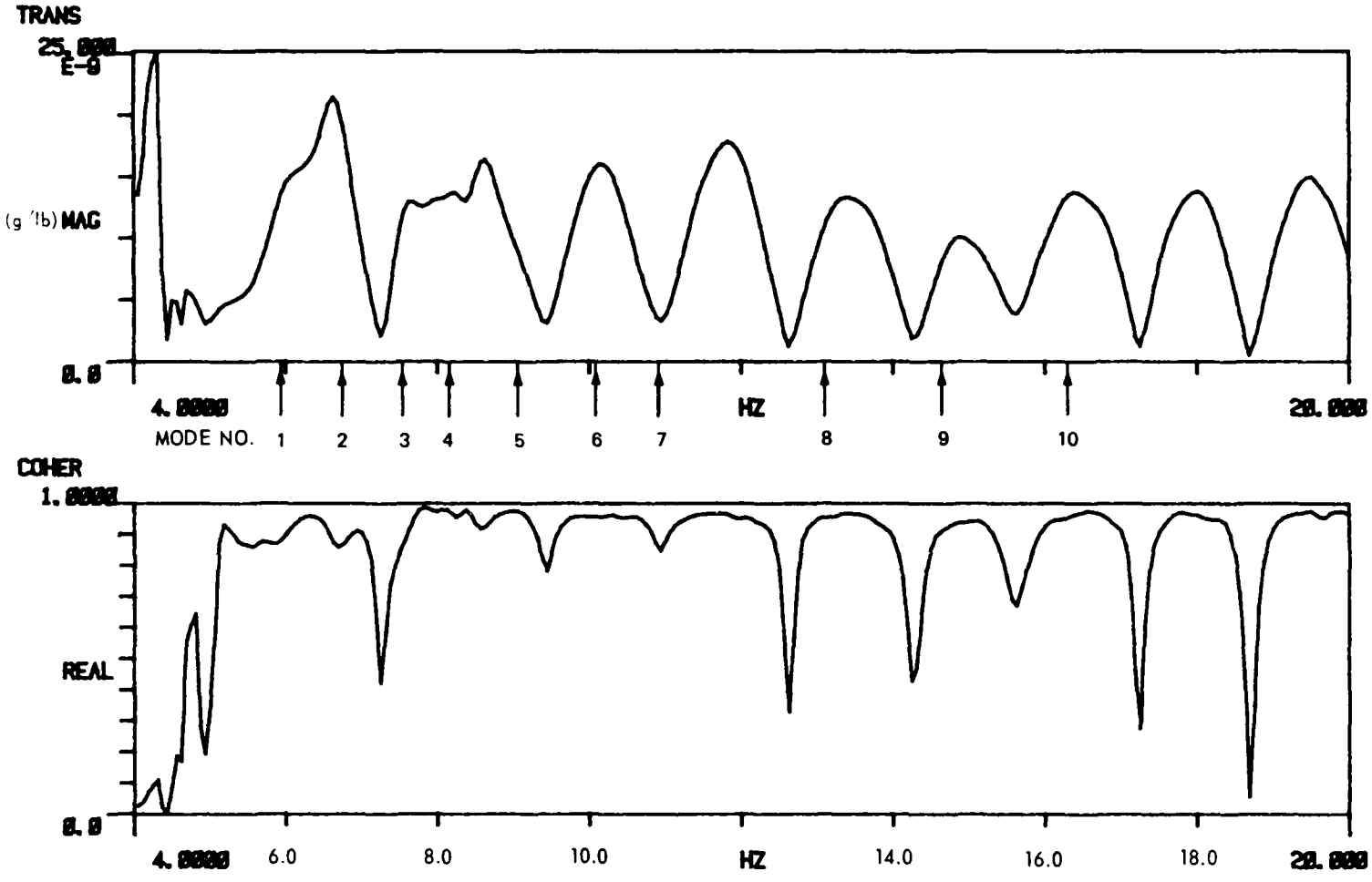

Transfer and coherence function: I-16, O-11; el 495

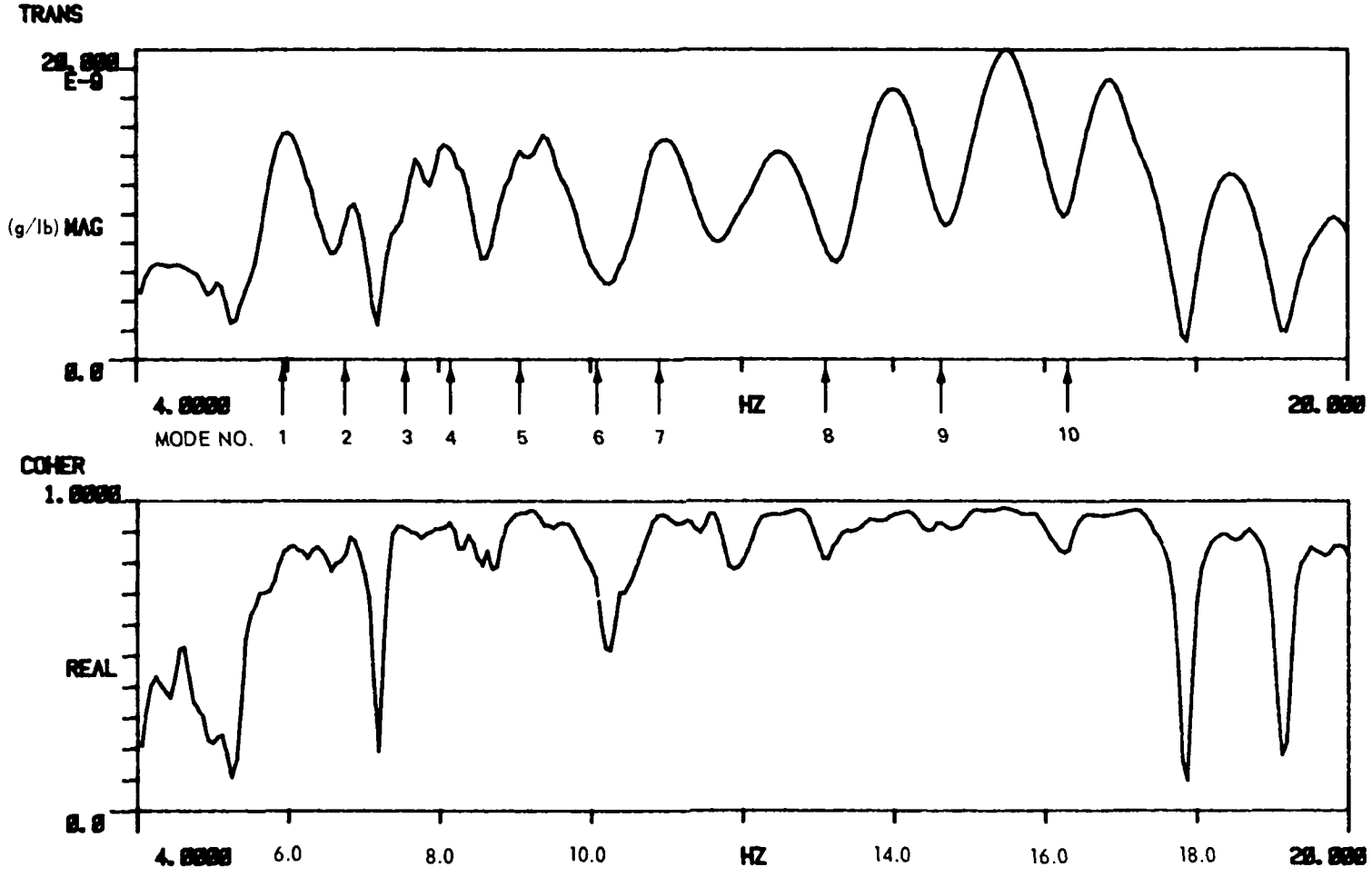

Transfer and coherence function: I-16, O-13; el 495

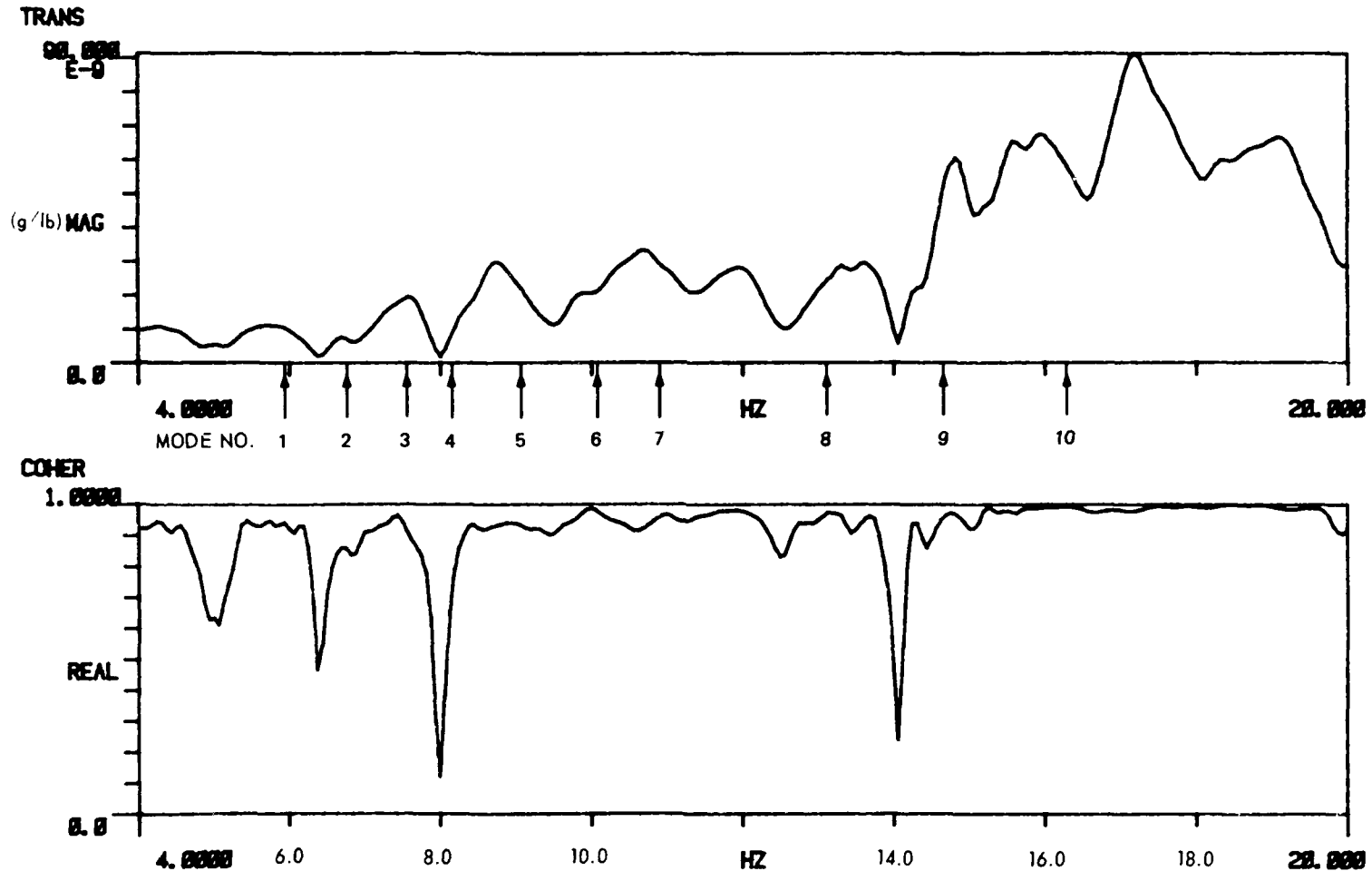

Transfer and coherence function: I-16, 0-17; el 495

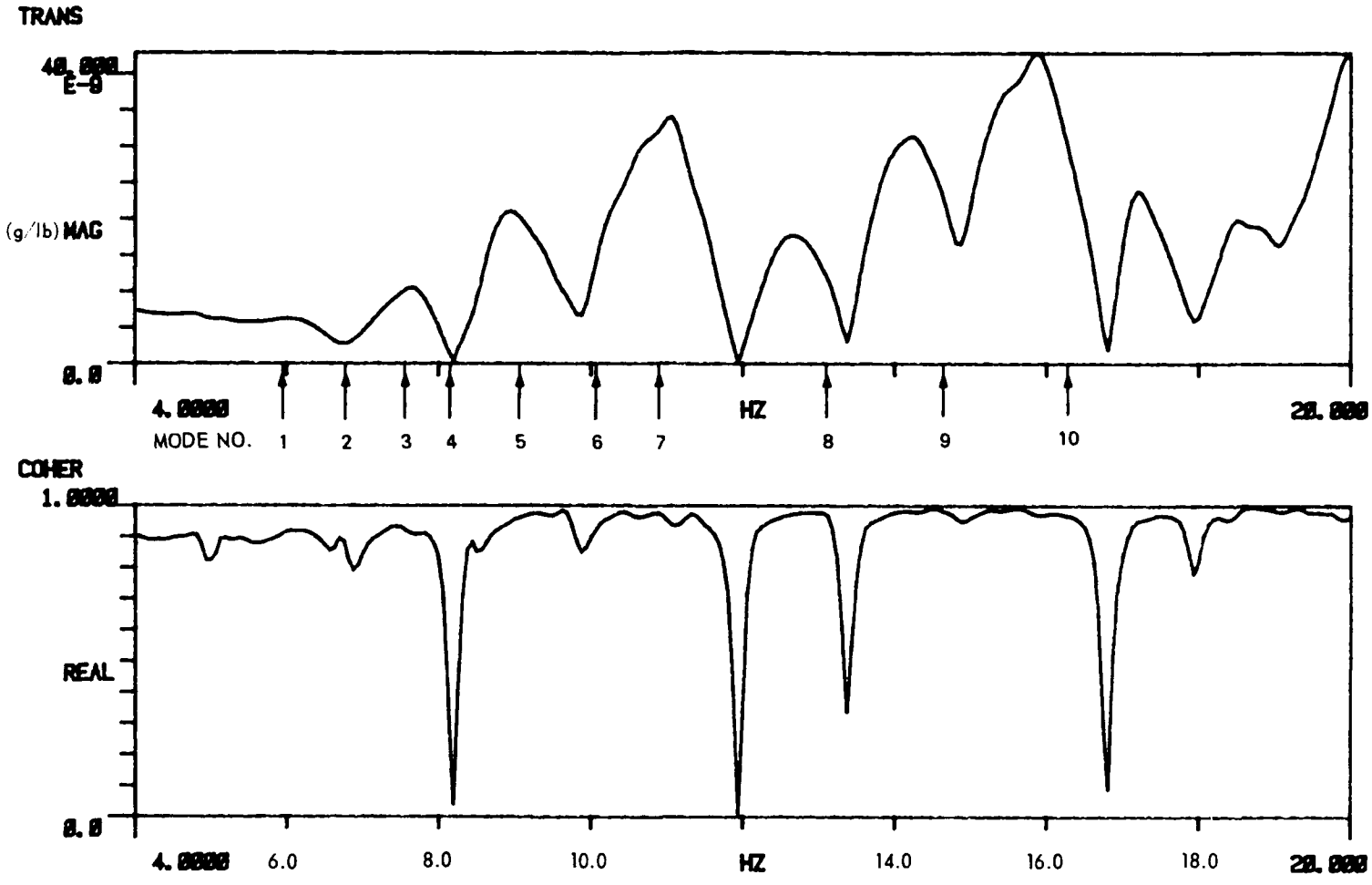

Transfer and coherence function: I-16, 0-20; el 495

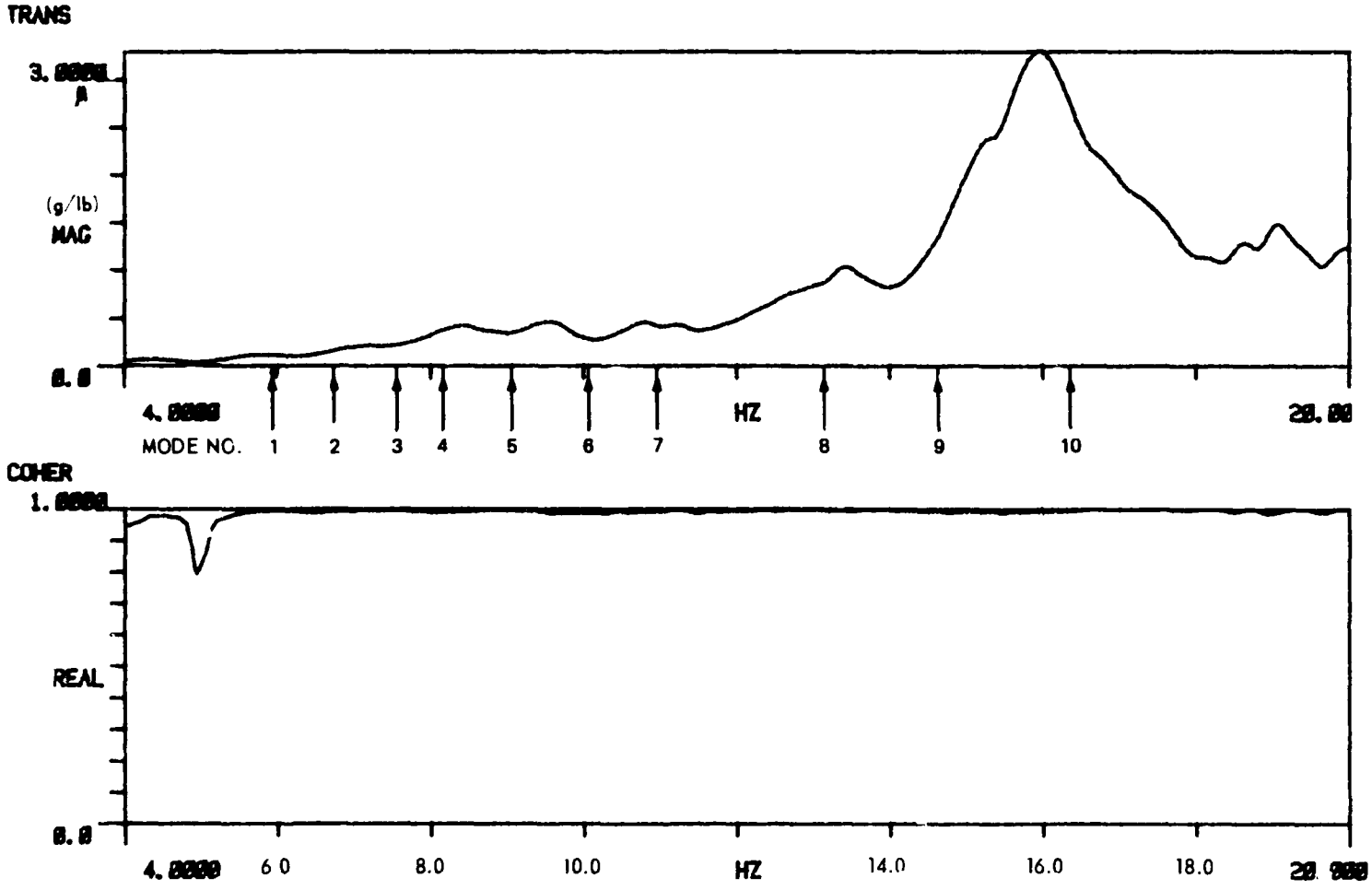

Transfer and coherence function: I-22, O-22; el 456

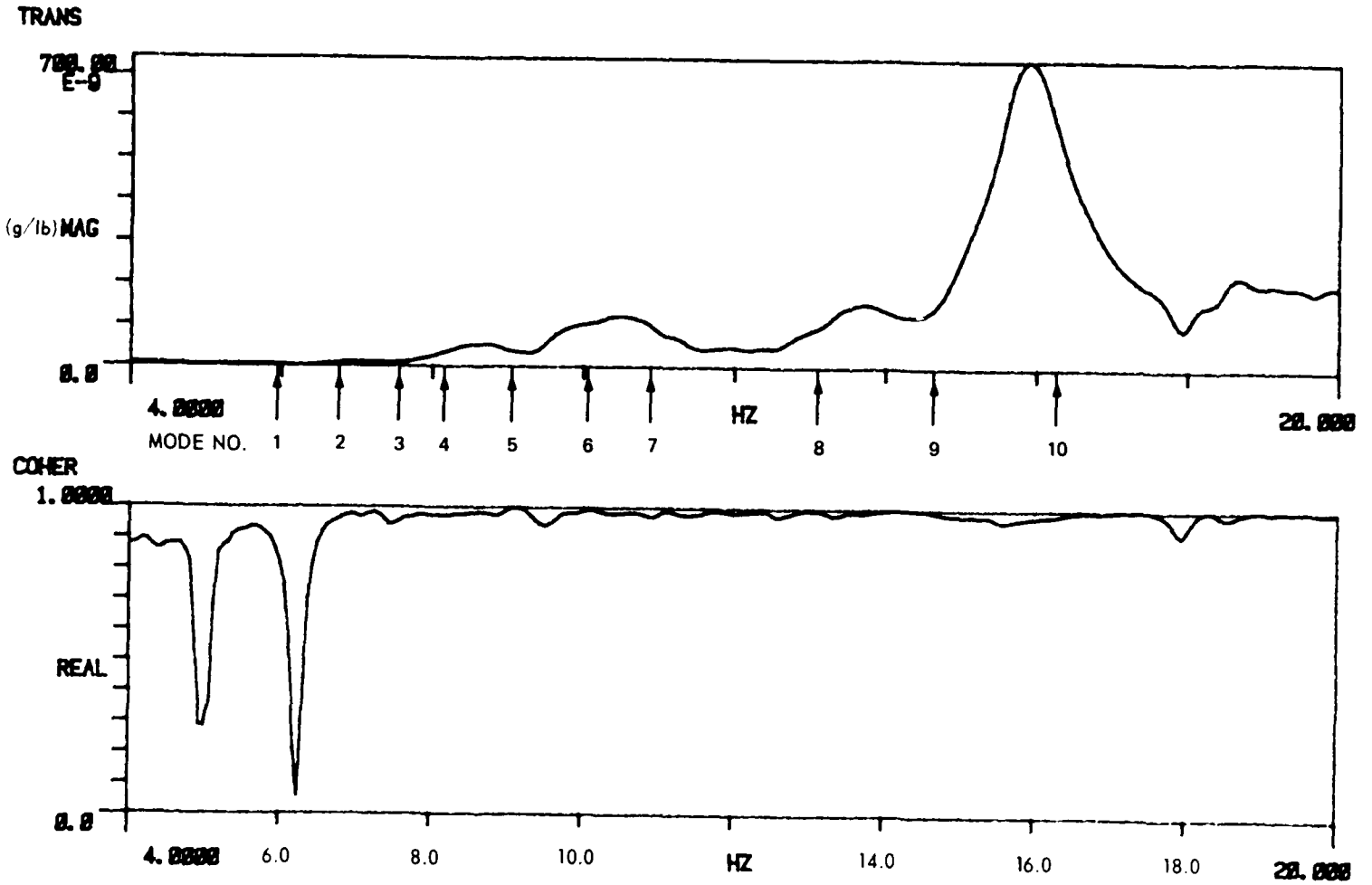

Transfer and coherence function: I-22, O-24; el 495

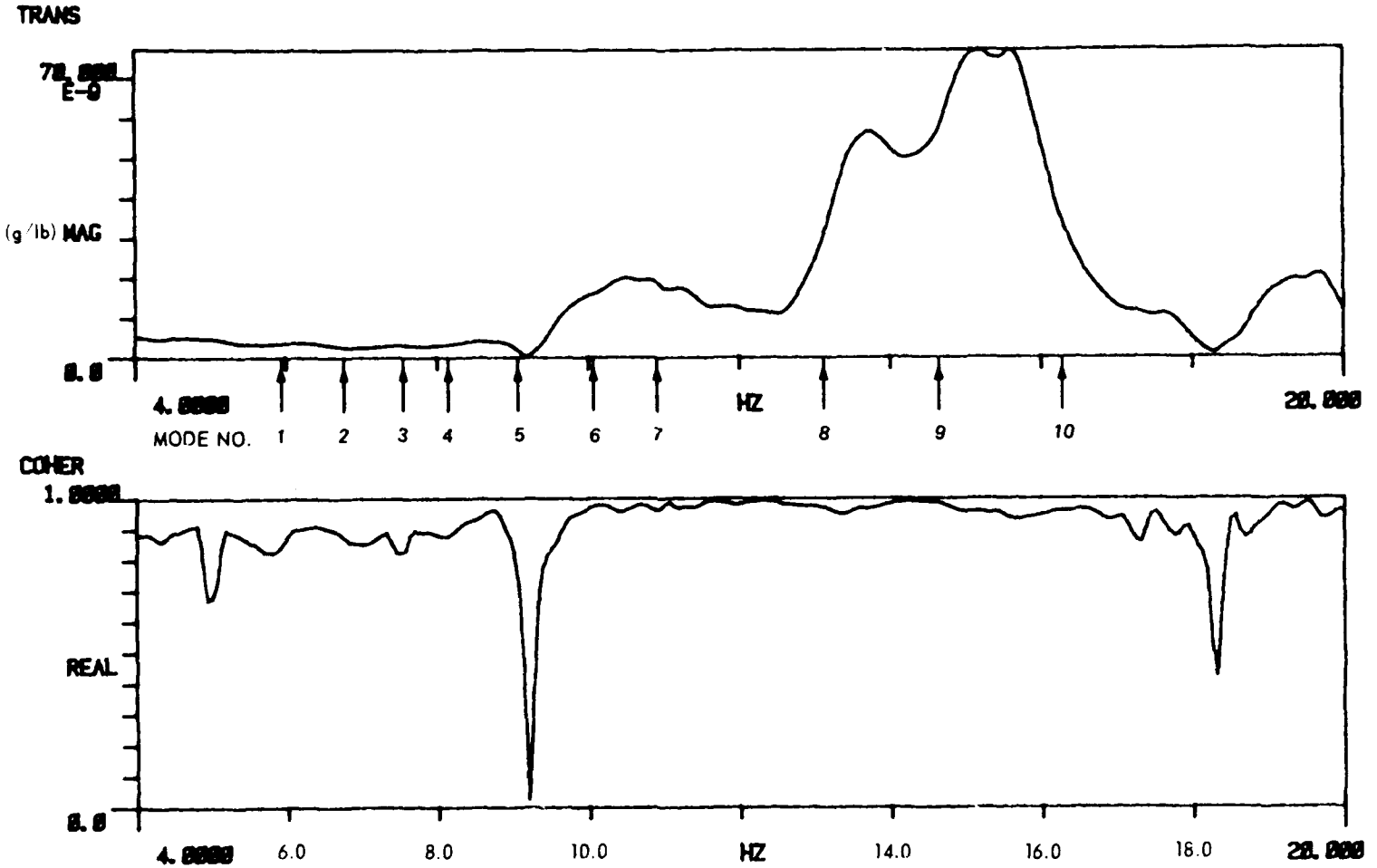

Transfer and coherence function: I-22, O-31; el 495

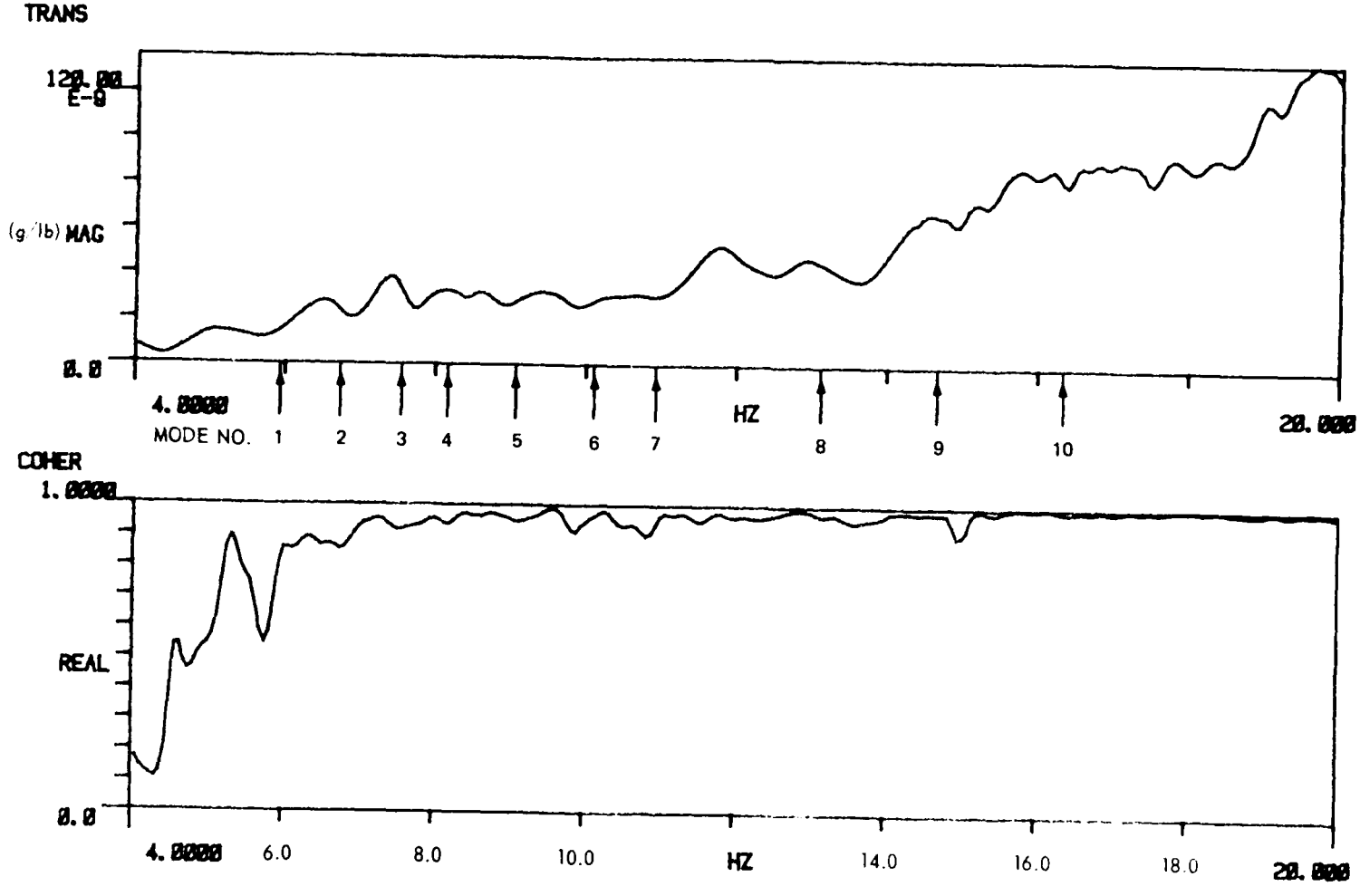

Transfer and coherence function: I-7, O-7, el 495

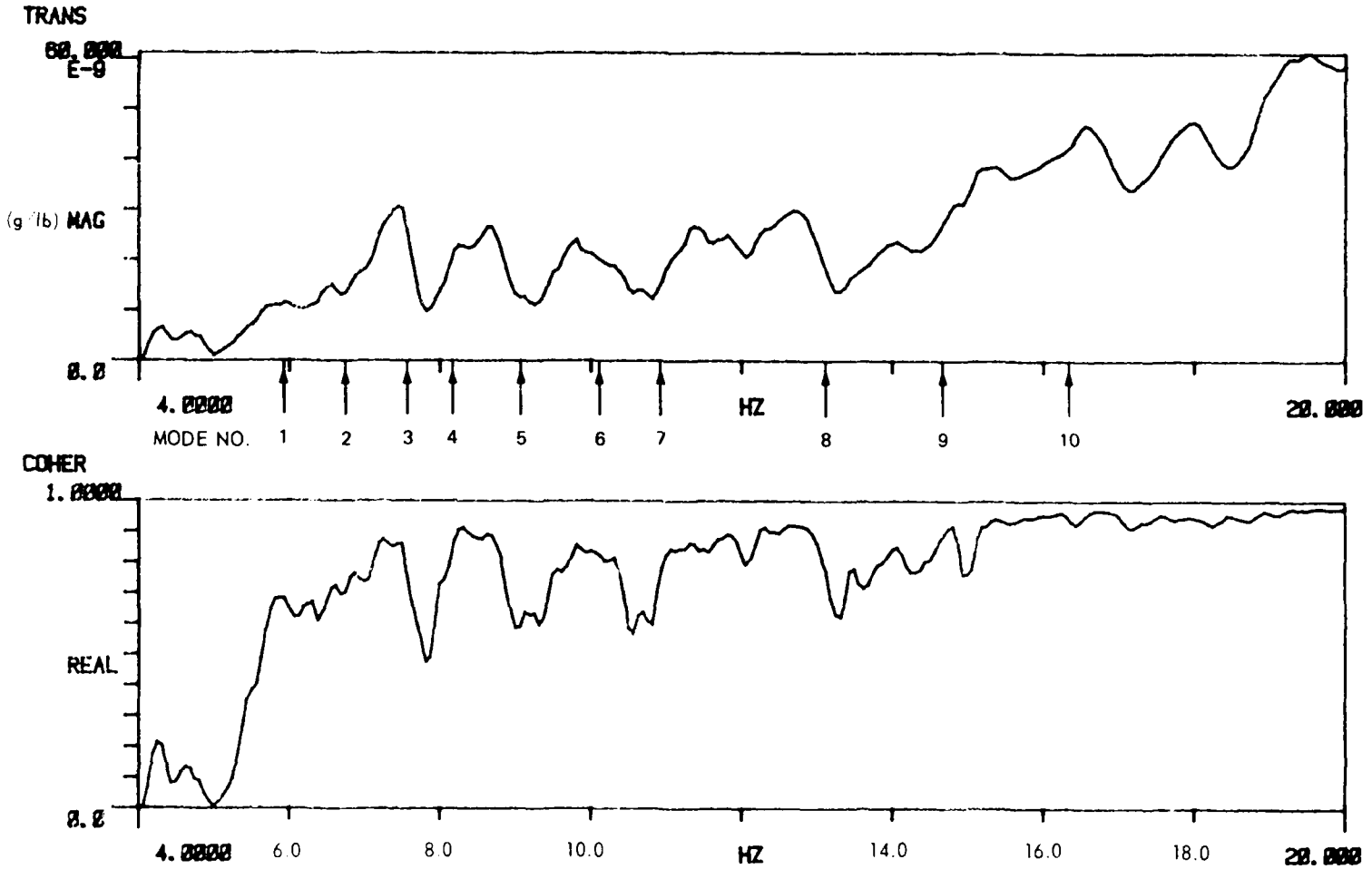

Transfer and coherence function: 1-7, 0-7; el 475 U.S.

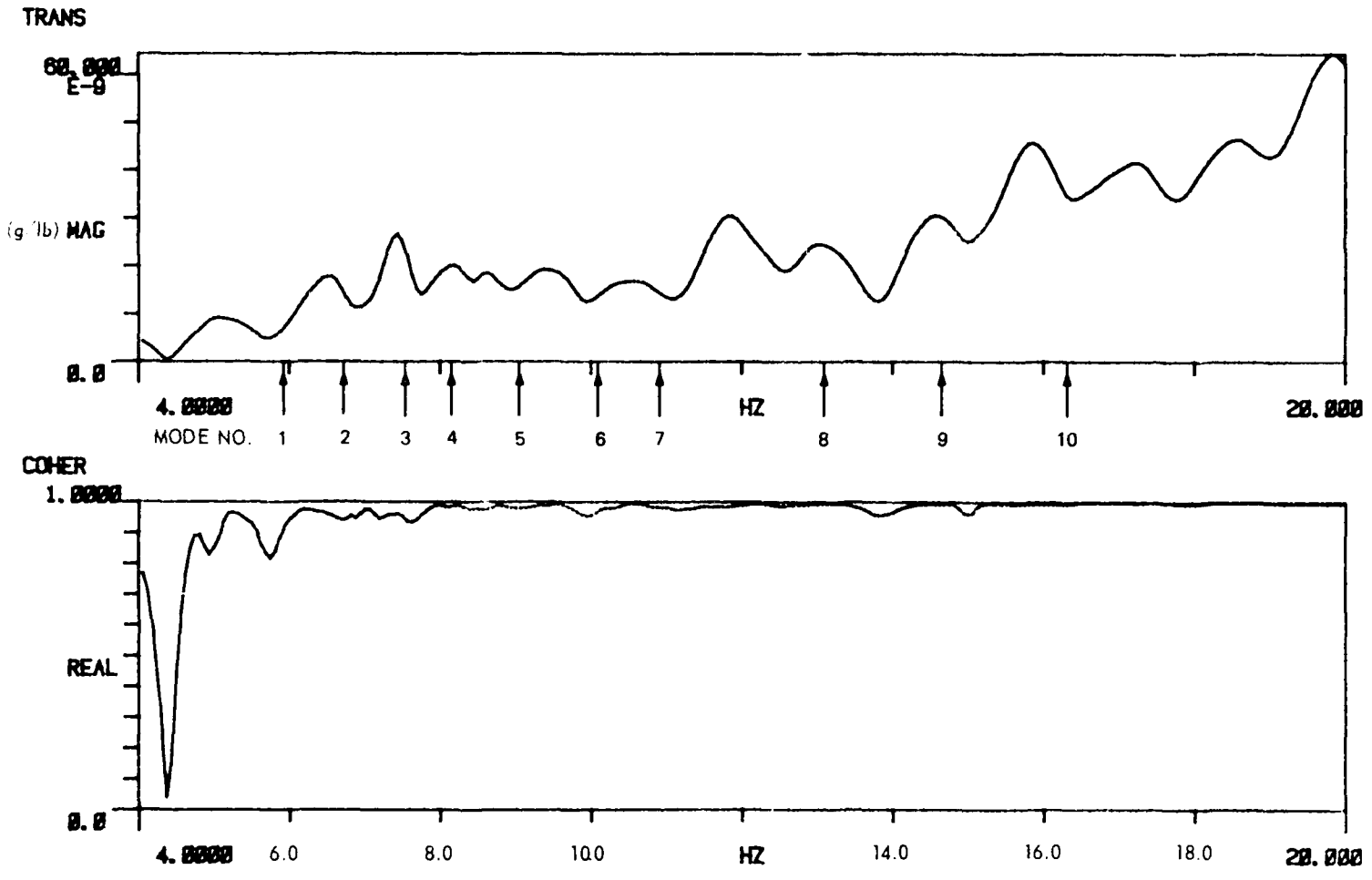

Transfer and coherence function: I-7, O-7; el 475 D.S.

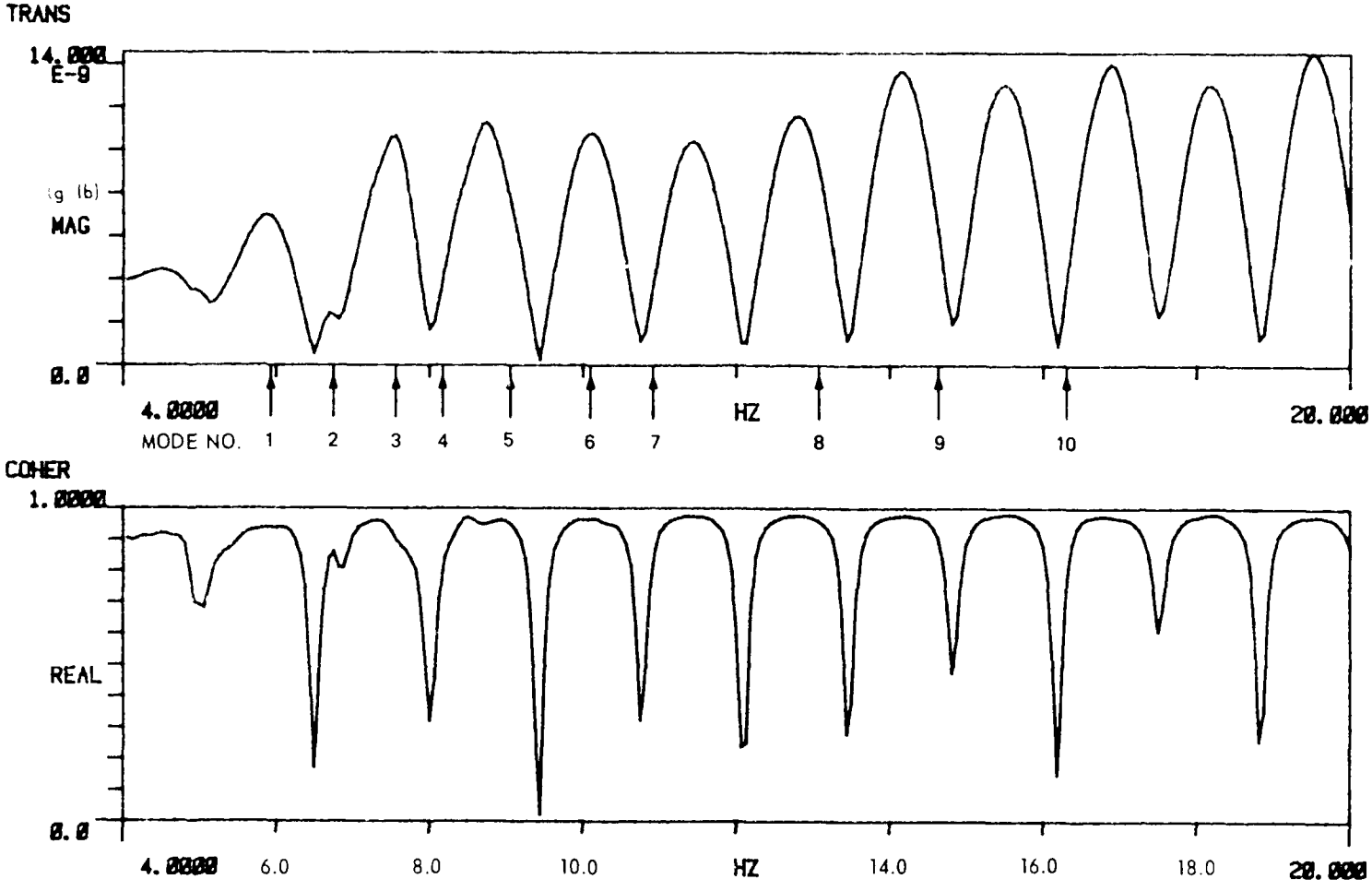

Transfer and coherence function: I-16, O-16; el 425

APPENDIX B: EXTRACTING MODAL PARAMETERS USING THE HP5423A

(Hewlett-Packard 1981 - See Measurement Overview)

1. Once the data stored on the 32 track analog system are digitized by the HP5423A the analyzer's modal analysis capabilities are used. From the data, transfer functions were computed representing the ratio of the measured output acceleration to the measured input force. A total of 70 transfer functions were computed from the available data. The transfer functions (complex functions, i.e., composed of both real and imaginary components) are used to identify the resonant frequencies. The resonant frequencies are distinguished by peaks in the transfer functions. Once the resonant frequencies are determined data points about the peak are curve fitted using a least squares criterion. Once parameters of the curve fitting function are determined an estimate of the damping ratio is possible. A single degree of freedom (SDOF) function is used to fit the data for the damping ratio.

2. For transfer measurements of acceleration to force peaks occurring in the imaginary part and zero crossings in the real part of the transfer function mark resonant frequencies. Also the phase angle between the real and imaginary parts equals ±90 degrees at a resonant frequency.

3. The functions shown in Figure B-1 will be used to illustrate how the analyzer is used to compute resonant frequencies, damping ratios, and mode shapes. The transfer function from the response point on monolith 13 is used to identify the resonance at 5.94 Hz. Looking at Figure B-1a, a peak is observed between 5.70 and 6.38 Hz in the magnitude of transfer function--indicating a possible resonant frequency. Next any of the three remaining functions can be studied. Secondly, the phase function (phase angle of the transfer function versus frequency) is -90 degrees at about 5.9 Hz. Thirdly, the real part of the transfer function has a zero crossing at about 5.9 Hz. And, finally in the imaginary part of the transfer function a peak is observed at 5.94 Hz. Therefore, from studying the four functions using each as a criterion a resonant frequency is found. If other transfer functions are observed peaks are found at 5.94 Hz also. The transfer function shown was

chosen because it represents a point on the dam crest with the largest response recorded at 5.94 Hz.

4. Once the resonant frequency is found 11 data points in the transfer function are curve fitted using a least squares criterion. The data used in the curve fit include 5 points to each side of and the resonant frequency points. The equation is in the following form:

$$H(S) = \frac{r_i\,(S + 2\pi\gamma_o) + r_r\,2\pi f_o}{S^2 + 4\pi\gamma_o S + (2\pi\gamma_o)^2 + (2\pi f_o)^2}$$

where the unknown parameters f_o , γ_o , r_i , and, r_r are determined from the least squares criterion and:

f_o = damped natural frequency (Hz)

γ_o = damping coefficient (Hz)

r_i = imaginary part of the residue

r_r = real part of the residue

$H(S)$ = transfer function evaluated at $S = j2\pi f$, where f is frequency in Hz

$j = \sqrt{-1}$

The damping ratio, γ_d , is determined by $\gamma_d = \gamma_o / \sqrt{\gamma_o^2 + f_o^2}$. For instance at $f_o = 5.937$ Hz , $\gamma_o = 0.2534$ Hz , therefore $\gamma_d = (0.2534) / \sqrt{(0.2534)^2 + (5.937)^2} = 0.04262$ or 4.262 percent of critical damping as shown in Table 4.

5. When the natural frequency and the damping ratio are computed residue values from the other transfer functions are determined. The residue values are proportional to the magnitude of the modal shape vectors. For acceleration measurements the imaginary, or quadrature, part of the transfer function is used to compute the residues for the other response points as:

$$r = r_i + r_r = 2j(2\pi\gamma_o)\left\{I_m[H(s)]\right\}$$

(remember r is a complex function) where

$I_m[H(S)]$ = imaginary part of the transfer function evaluated at $S = j2\pi f_o$

(Hence, the name "quadrature peak picking method.")

6. The residues and the mode shape vectors are related by the expression:

$$r_k = (A_k)\ (U_k)\ (U_k)^t$$

where

r_k = $[r_{11}(k)\ r_{12}(k)\ \ldots]$
$[r_{21}(k)]$
$[\cdot]$
$[\cdot]$
$[\cdot]$
(where $r_{12}(k)$ is the residue at response point 1 due to input at response point 2)

U_k = n dimensional vector

A_k = scaling constant

t = denotes transpose (refer to matrix operations)

7. Hence, when all the residues are calculated the analyzer uses a routine to compute and scale mode shape vectors for each response point. The mode shape vectors are combined and define the mode shape for the portion of the structure marked by the response points. The views of the mode shapes in Figures 13 to 22 are the resulting shapes from the combined mode shape vectors (one vector per point having both magnitude and direction).

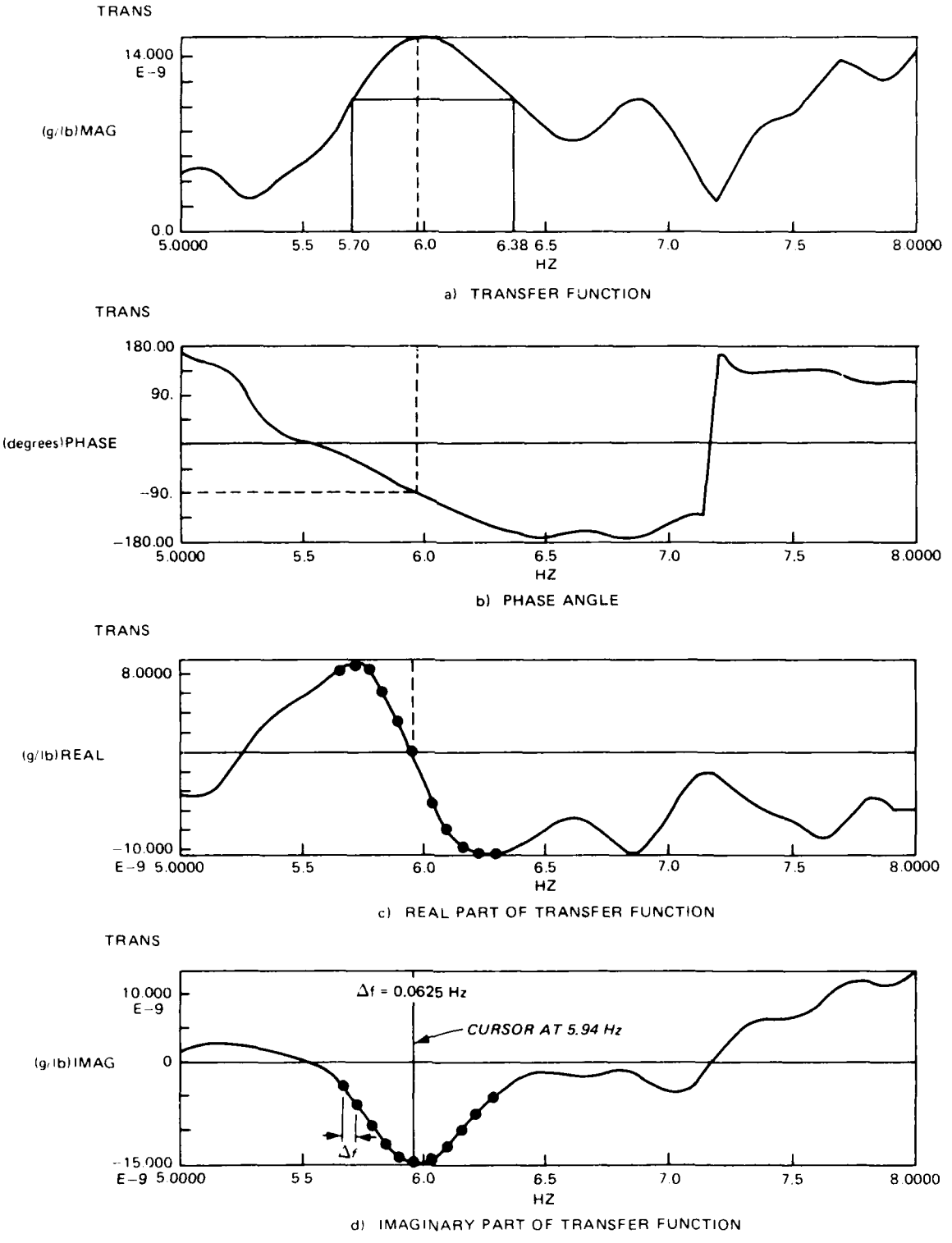

Figure B1. Transfer function: input monolith 16, output monolith 13, el 495

In accordance with letter from DAEN-RDC, DAEN-ASI dated 22 July 1977, Subject: Facsimile Catalog Cards for Laboratory Technical Publications, a facsimile catalog card in Library of Congress MARC format is reproduced below.

Chiarito, Vincent P.
Vibration test of Richard B. Russell Concrete Dam before reservoir impoundment / by Vincent P. Chiarito, Paul F. Mlaker (Structures Laboratory, U.S. Army Engineer Waterways Experiment Station). -- Vicksburg, Miss. : The Station ; Springfield, Va. : available from NTIS, 1983.
84 p. in various pagings : ill. ; 27 cm. -- (Technical report ; SL-83-2)
Cover title.
"May 1983."
Final report.
"Prepared for Office, Chief of Engineers, U.S. Army and U.S. Army Engineer District, Savannah."
Bibliography: p. 61.

1. Concrete dams. 2. Vibration tests. I. Mlaker, Paul F. II. United States. Army. Corps of Engineers.

Chiarito, Vincent P.
Vibration test of Richard B. Russell Concrete : ... 1983.
(Card 2)

Office of the Chief of Engineers. III. United States. Army. Corps of Engineers. Savannah District. IV. U.S. Army Engineer Waterways Experiment Station. Structures Laboratory. V. Title VI. Series: Technical report (U.S. Army Engineer Waterways Experiment Station) ; SL-83-2.
TA7.W34 no.SL-83-2